Sludge Particle Separation Efficiencies During Settler Tank Retrieval Into SCS-CON-230

Prepared for the U.S. Department of Energy
Assistant Secretary for Environmental Management

Contractor for the U.S. Department of Energy
under Contract DE-AC06-08RL14788

CH2MHILL
Plateau Remediation Company

P.O. Box 1600
Richland, Washington 99352

Sludge Particle Separation Efficiencies During Settler Tank Retrieval Into SCS-CON-230

Project No: A21C   Document Type: RPT   Program/Project: STP

J. I. Dearing
CH2M HILL Plateau Remediation Company
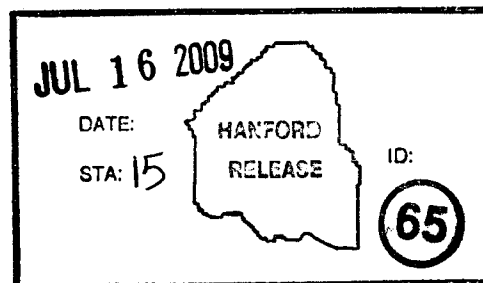
M. Epstein
M. G. Plys
Fauske & Associates, LLC

Date Published
July 2009

Prepared for the U.S. Department of Energy
Assistant Secretary for Environmental Management

Contractor for the U.S. Department of Energy
under Contract DE-AC06-08RL14788

CH2MHILL
Plateau Remediation Company

P.O. Box 1600
Richland, Washington

JUL 16 2009
DATE:
STA: 15
HANFORD
RELEASE
ID:
65

Nancy A Fouad   7-16-09
Release Approval   Date   Release Stamp

TRADEMARK DISCLAIMER

Reference herein to any specific commercial product, process,
or service by trade name, trademark, manufacturer, or
otherwise, does not necessarily constitute or imply its
endorsement, recommendation, or favoring by the United
States Government or any agency thereof or its contractors or
subcontractors.

This report has been reproduced from the best available copy.

Printed in the United States of America

Total Pages: ___156___

Sludge Particle Separation Efficiencies
During Settler Tank Retrieval
Into SCS-CON-230

Table of Contents

Attachments

Attachment A, FAI/09-091, *Sludge particle Separation Efficiencies for the Rectangular SCS-CON-230 Container*

Attachment B, Review and Verification Files

    Attachment B1, *Review of FAI/09-91 Portions Modeled in MathCAD*

    Attachment B2, MGP062609, *Review of FAI/09-91 Portions Authored by Michael Epstein*

    Attachment B3, MGP062909A, *MathCAD Files for FAI/09-91* (listing of file names only)

**Sludge Particle Separation Efficiencies
During Settler Tank Retrieval
Into SCS-CON-230**

1.0 INTRODUCTION

The purpose of this document is to release, into the Hanford Document Control System, FAI/09-91, *Sludge Particle Separation Efficiencies for the Rectangular SCS-CON-230 Container*, by M. Epstein and M. G. Plys, Fauske & Associates, LLC, June 2009.

The Sludge Treatment Project (STP) will retrieve sludge from the 105-K West Integrated Water Treatment System (IWTS) Settler Tanks and transfer it to container SCS-CON-230 using the Settler Tank Retrieval System (STRS). The sludge will enter the container through two distributors. The container will have a filtration system that is designed to minimize the overflow of sludge fines from the container to the basin. FAI/09-91 was performed to quantify the effect of the STRS on sludge distribution inside of and overflow out of SCS-CON-230.

Selected results of the analysis and a system description are discussed below.

2.0 ANALYSIS RESULTS

The principal result of the analysis is that the STRS filtration system reduces the overflow of sludge from SCS-CON-230 to the basin by roughly a factor of 10. Some turbidity can be expected in the center bay where the container is located. The exact amount of overflow and subsequent turbidity is dependent on the density of the sludge (which will vary with location in the Settler Tanks) and the thermal gradient between the SCS-CON-230 and the basin.

Attachment A presents the full analytical results. These results are applicable specifically to SCS-CON-230 and the STRS filtration system's expected operating duty cycles. Some important results are:

1. The analysis ran several sensitivity cases for varying particle densities and temperature differences. The results are presented in Table 5-2 of Attachment A. The conclusion states "The escape fraction for particles of average expected density (6 g/cc) is between about 1% and 2% depending on the inlet water temperature (Cases 2A and 3A). The escape fraction for particles of less than average expected density (4 g/cc) is between about 2% and 6% (Cases 2B and 3B). The escape fraction for extremely light particles could range from about 8% to 13% (Cases 2C and 3C)."
2. The analysis estimates that 3.4% of the sludge transferred to the container will escape for a typical sludge composition of 60% at 6 g/cc, 30% at 4 g/cc, and 10% at 2 g/cc with an inlet temperature difference of 2°C (Using cases 1A, 1B, and 1C of Table 5-2 of FAI/09-091).

However this is only an example and the actual value will vary with sludge density and temperature difference.

3. The analysis estimates that up to 38% of the total sludge transferred would flow out of the container if there were no filtration system.

4. The most important sludge property governing potential particle escape is density. The less dense particles have the most potential of escaping.

5. The most important environmental factor governing potential particle escape is the thermal gradient between the inside of the container and the basin. The potential for particle escape increases as the temperature difference increases.

6. The most important overall factor in preventing potential particle escape is maintaining adequate inflow of basin water through the gap between the lid and the upper flange of SCS-CON-230.

7. Sludge will not escape from SCS-CON-230 when all four filter assemblies are operating under credible thermal gradients.

8. Sludge can only flow out of SCS-CON-230 when the following conditions exist
   a. The filters are being back flushed and a thermal gradient exists between the container and the basin water (even 0.1 C is sufficient to induce flow).
   b. The flow into and out of the container is stopped and thermal gradients cause convection currents.

9. The bounding inlet temperature of sludge pumped into SCS-CON-230 by the STRS is 4°C above the basin temperature (based on accounting for the power added by all pumps in the system). This equates to a bulk thermal gradient of 1.2 °C between SCS-CON-230 and the basin. Under this bounding condition, sludge particle loss from the container can be prevented by maintaining a net container suction flow of 8 gpm. In other words, the filters must remove at least 8 gpm more fluid than is being pumped into the container by the STRS.

10. Continuing to run the filter system after shutdown of the retrieval system is beneficial to reduce thermal gradient induced release of sludge to the basin. However, running the filters too long could cause the finest particles to imbed in the filters in such a way that they cannot be removed by back flushing. The report recommends running the filters for 30 minutes after shutting down the retrieval system.

3.0 SYSTEM DESCRIPTION

Sludge from washing spent nuclear fuel has accumulated in the KW basin Settler Tanks. This sludge will be pumped from the Settler Tanks to SCS-CON-230 at a rate of approximately 15 to 18 gpm. The sludge will flow into the container through two distributors. Sludge flow into SCS-CON-230 will vary depending on the instantaneous concentration of the sludge water mixture.

SCS-CON-230 is 60" wide by 142" long (inside dimensions) with an "egg crate" shaped bottom. The top of the egg crate bottom is 128" below the top of the tank. The egg crate bottom is 26" tall. The container has a polycarbonate cover that is raised above the top flange of the container by approximately 1". The short ends and part of the adjoining long sides are open to

the basin. The majority of each long side is closed. See Figures 1-1 through 1-6 in Attachment A for additional tank details.

Four filter assemblies containing three filter cartridges each are installed in the top of container SCS-CON-230. Each filter assembly has a flow of 7 gpm. The combined filtration system has a net flow of 28 gpm when all four filters are operating or 21 gpm when one of the filters is back flushing. The hydraulic analysis for the filter system is provided in KBC-39812, *K Basin Settler Tank Retrieval System (STRS) Hydraulic Calculations.*

The back flush sequence is initiated when the filter system reaches a preset differential pressure. Each of the four assemblies is first pulsed with back flush water briefly (3 seconds) to dislodge a large part of the filter cake. This helps ensure that the 21 gpm flow rate through the system is maintained during the full back flush. The filtration control system then starts the sequence of injecting low volume (0.083 gallon), "high" pressure (80 psig) water pulses through each isolated filter assembly in turn. This sequence introduces pulsed flow for approximately 15 seconds at an approximate rate of 1 pulse per second. It provides an average flow rate of less than 5 gpm (1.25 gallons is injected during the flush of each filter assembly). This is followed by a 2 to 3 minute wait period to allow material to fall away from the filter element before placing the element back online. The total volume of back flush water introduced into SCS-CON-230 during each backwash cycle will be approximately 5 gallons. The analysis demonstrates that, while the retrieval system is operating, sludge can only escape from the container during these brief back flushes. Sludge can also escape due to thermal gradients after the filtration system is stopped.

Attachment A

FAI/09-091, *Sludge particle Separation Efficiencies for the Rectangular SCS-CON-230*
Container

FAI FAUSKE
& ASSOCIATES, LLC

WORLD LEADER IN NUCLEAR AND CHEMICAL PROCESS SAFETY

Report No.: FAI/09-091

Sludge Particle Separation Efficiencies

for the Rectangular SCS-CON-230 Container

Submitted To:

CH2M Hill Plateau Remediation

Richland, Washington

Prepared By:

Michael Epstein and Martin G. Plys

Fauske & Associates, LLC

16W070 83rd Street

Burr Ridge, Illinois 60527

June, 2009

TABLE OF CONTENTS

TABLE OF CONTENTS – (Cont'd)

LIST OF FIGURES

LIST OF FIGURES – (Cont'd)

LIST OF TABLES

1.0   *INTRODUCTION AND SUMMARY*

Sludge is to be supplied to the central region of the rectangular SCS-CON-230 container through two downward facing ports (distributors). Water is withdrawn from the tank through four vertical-cylindrical filters located in the upper region of the tank. The tank is open to the K-Basin pool through a 1.0" gap along the periphery of the short sides of the tank at the top of the tank. Figures 1-1 through 1-3 provide drawings and dimensions of SCS-CON-230. Figures 1-4 through 1-6 provide useful cutaway elevation and isometric views illustrating the placement of inlet ports, filters, and the egg crate section.

When all the filters are operating the flow through the gap should be from the K-Basin pool into the tank; however, it is possible that a segment of the gap may experience outflow from the tank to the K-Basin pool, if a significant water current moves through the basin and/or if there is a temperature difference between the container water and the surrounding basin water.

The goals of the analysis described below are to quantify the fraction of the sludge particles that do not settle to the bottom of the tank but instead are intercepted by the filters and the fraction of the sludge particles that escape the tank and enter the basin due to outflow through the gap. Two cases are considered: all four filters are operating or only three filters are operating and one is backwashing.

The stated goals were accomplished as follows:

(1)   An analysis of the sludge particle-laden plumes that form as a result of continuous sludge injection was made.

(2)   The plume analysis was combined with a stability analysis of the particle-laden lower layer that initially forms at the bottom of the container, from which it is concluded that the container environment is in a transition zone between a stably stratified environment (particle-laden layer at the bottom and clear water above) and a well-mixed container with

a spatially uniform particle concentration. To err on the conservative side a well-mixed container was assumed.

(3)   A number of physical processes that could potentially result in an outflow were examined. Only one process was identified that could result in container outflow, namely thermal convection. A thermal analysis of the container was performed which clearly indicated that the thermal convection mechanism of sludge particle escape is operative only during back washing.

(4)   A uniform particle concentration model was developed in which the fraction of particles that separate at the bottom of the container depends on the relative rates of particle removal by coagulation and by sedimentation at the container bottom, by flow into the filters and by outflow through the gap. A realistic log-normal particle size distribution was incorporated into the model.

From the theoretical studies listed above, the following conclusions are drawn:

(1)   The effect of a one-way flow through the basin on flow out of the container was examined and found not to be significant. The reason is that the pressure drop induced by the basin flow velocity on the downstream side of the container is less than the pressure difference required to drive inlet flow across the gap.

(2)   Small temperature differences between the container water and the surrounding basin water will generate significant buoyancy-driven countercurrent flows and, therefore, container outflows, but only during back washing. During normal operation, there is no countercurrent flow unless the container water is about 3.0°C above the basin water temperature. A thermal analysis of the container was performed that showed that a sludge inlet temperature of slightly over 11.0°C relative to the basin temperature is required for the container water temperature to be 3°C above the basin water temperature. Therefore sludge particles can only escape the container during back flushing.

From numerical simulations of particle behavior to simulate particle settling, particle escape, and the impact of filters, the following conclusions may be drawn:

(1)   Results for long-term suspended particle volume demonstrate that daily retrieval campaigns are independent of one another with respect to the potential for particle escape. Also, results are not very sensitive to assumed idealizations of operations.

(2)   Particles can only escape from the container during a filter back flush and when the water supply and suction from the container are shut off after daily operations. Most particle escape seen in simulated operations occurred after water is shut off.

(3)   The most important sludge property that governs the potential for particle escape is particle density. The escape fraction for particles of average expected density (6 g/cc) is between about 1% and 2% depending on the inlet water temperature, the escape fraction for particles of less than average expected density (4 g/cc) is between about 2% and 6%, and the escape fraction for extremely light particles (2 g/cc) could range from about 8% to 13%. The parameter of second interest to results is the temperature of water entering the container.

(4)   It is recommended that filters be operated for at least 30 minutes after the last particle retrieval of a daily operation. Filter operation for about two hours after the last particle retrieval is also beneficial.

(5)   The impact of filters is substantial; without them, about 1/3 of added particles would escape.
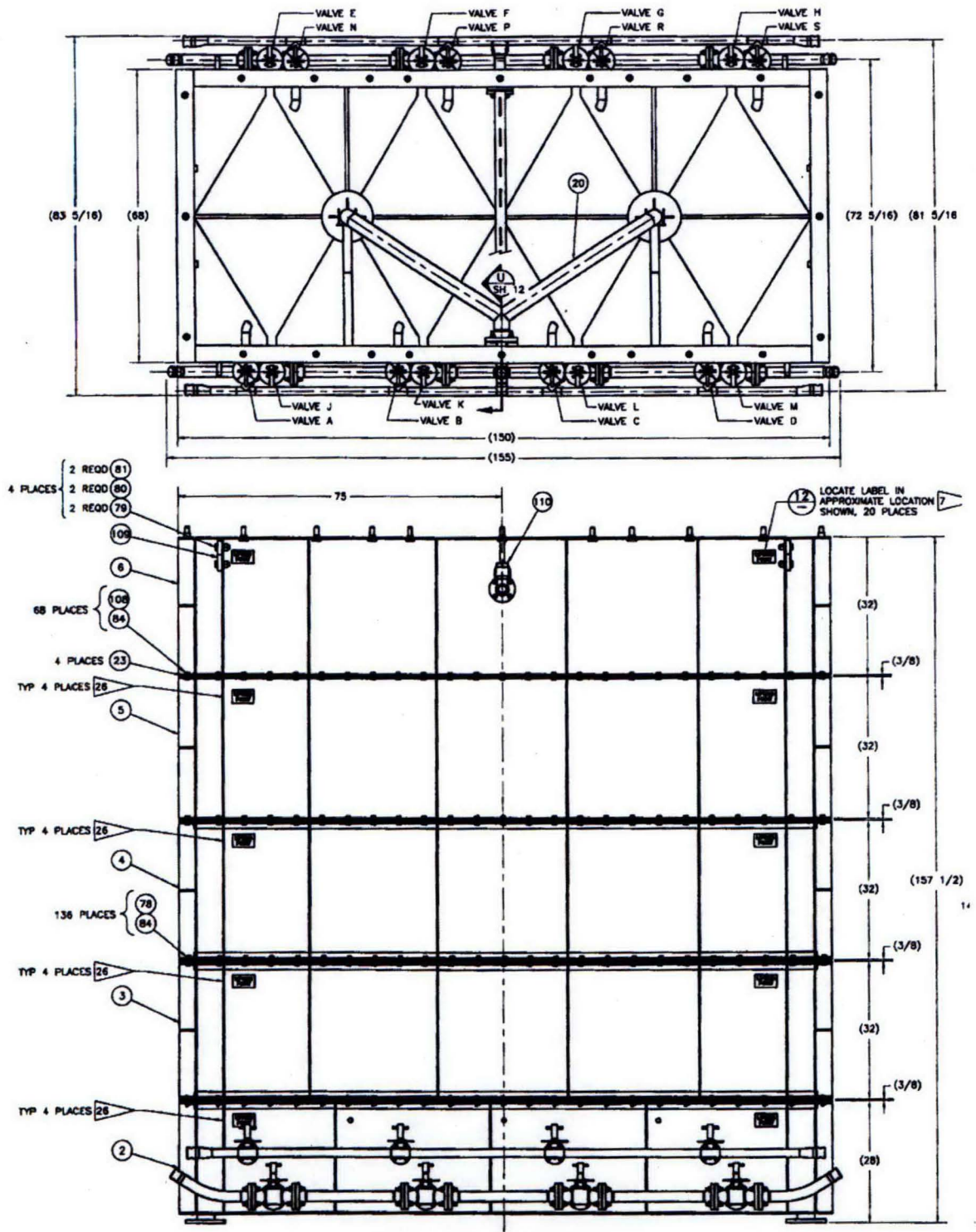
Figure 1-1 SCS-CON-230 lengthwise elevation and top plan
views from drawing H-1-88419-03, Rev. 4.
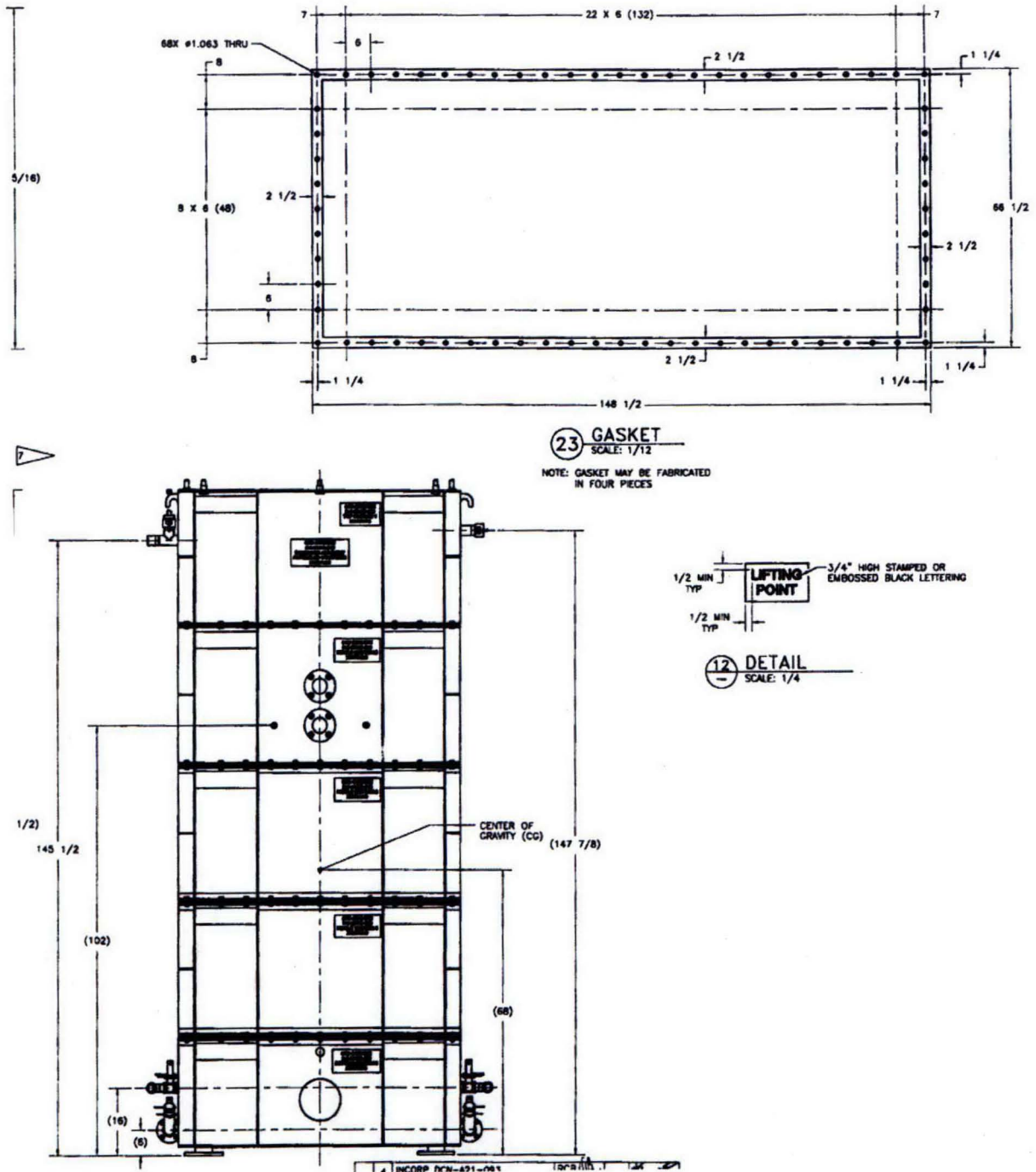
Figure 1-2   SCS-CON-230 widthwise elevation and gaslet plan
views from drawing H-1-88419-03, Rev. 4.
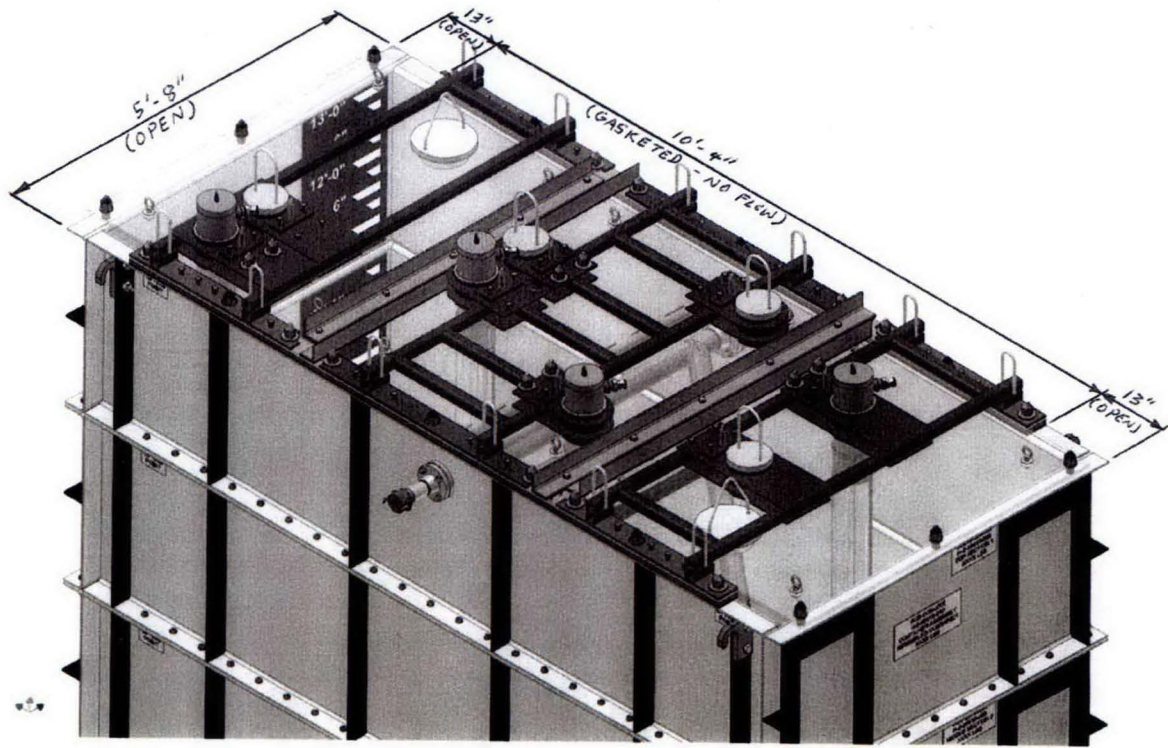
Figure 1-3   SCS-CON-230 top lid and gasket detail.
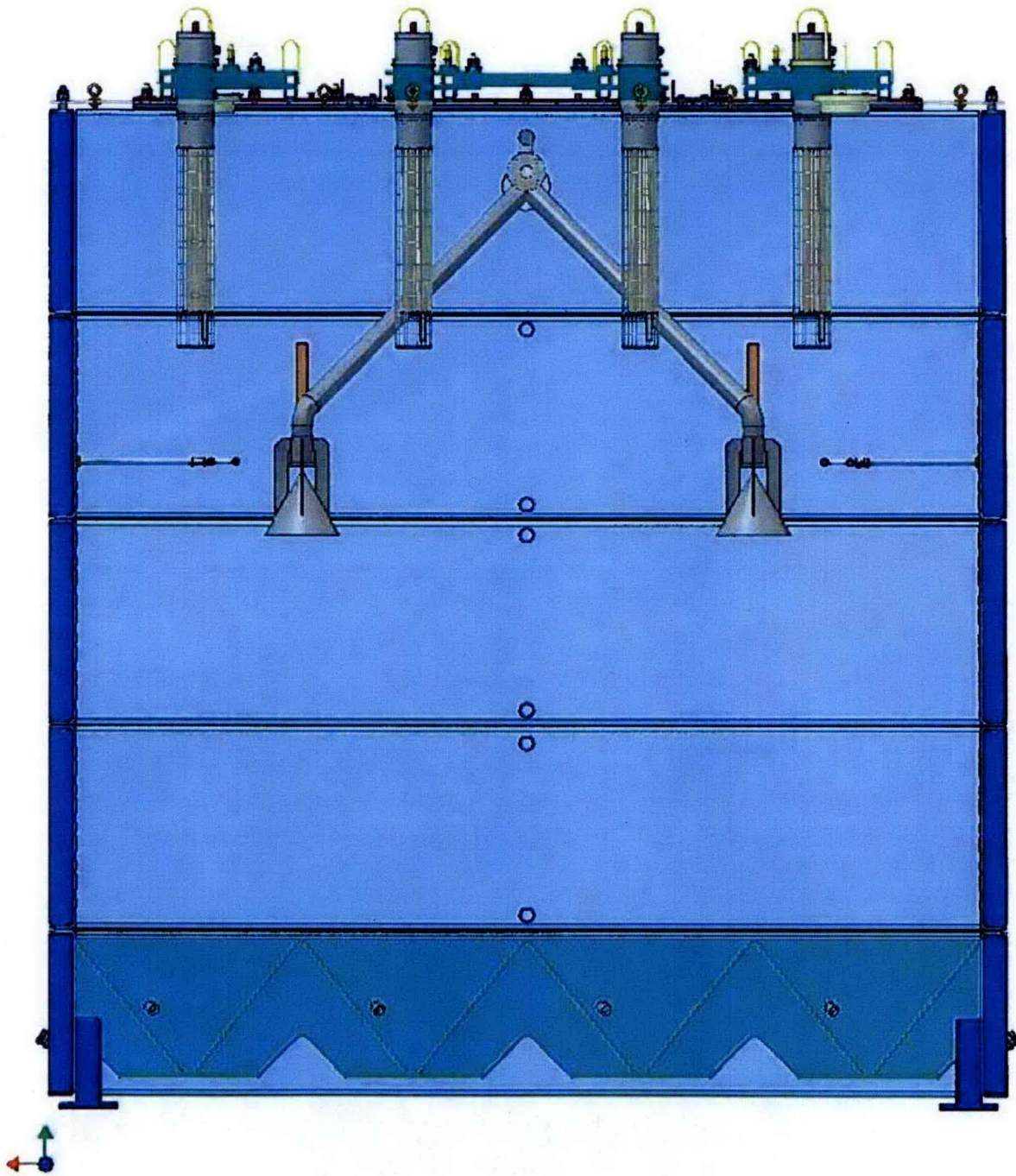
Figure 1-4   SCS-CON-230 lengthwise cutaway view.
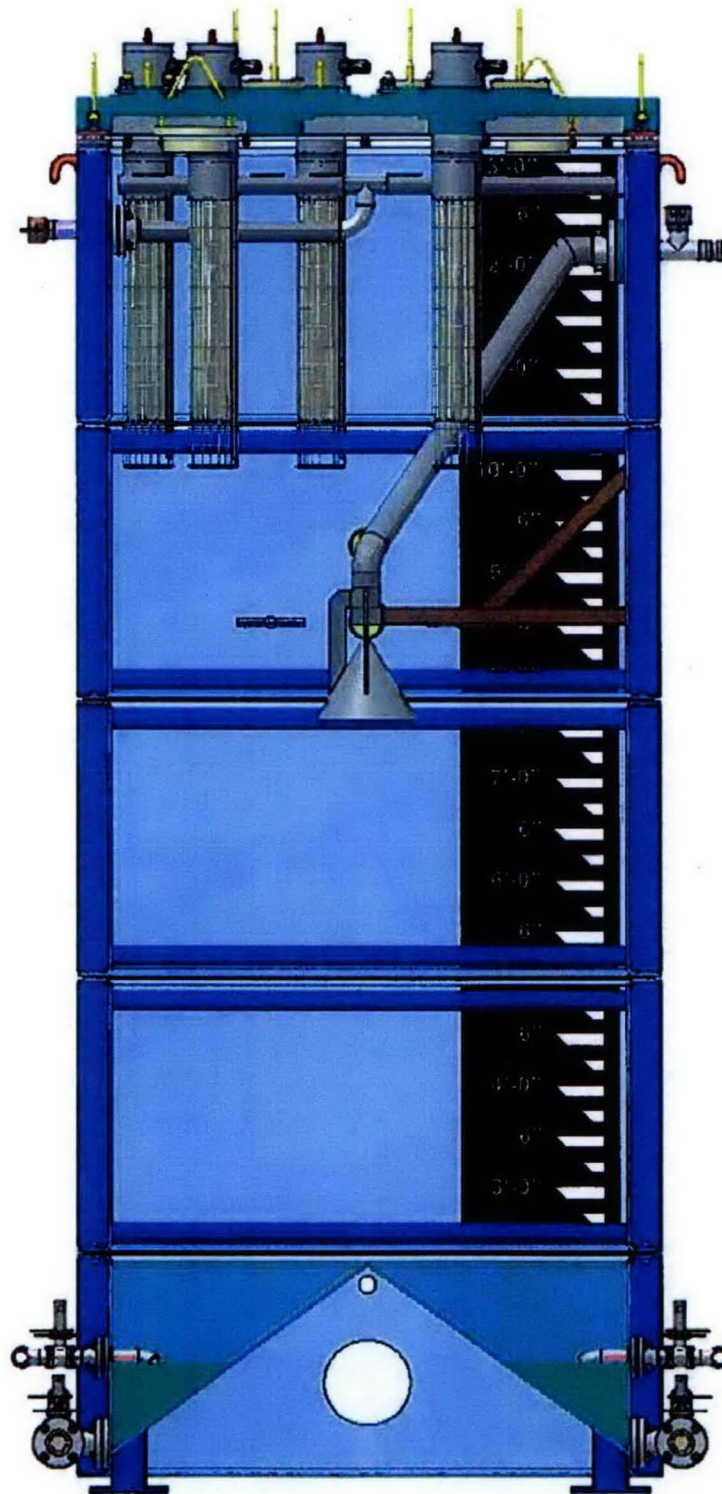
Figure 1-5   SCS-CON-230 widthwise cutaway view.
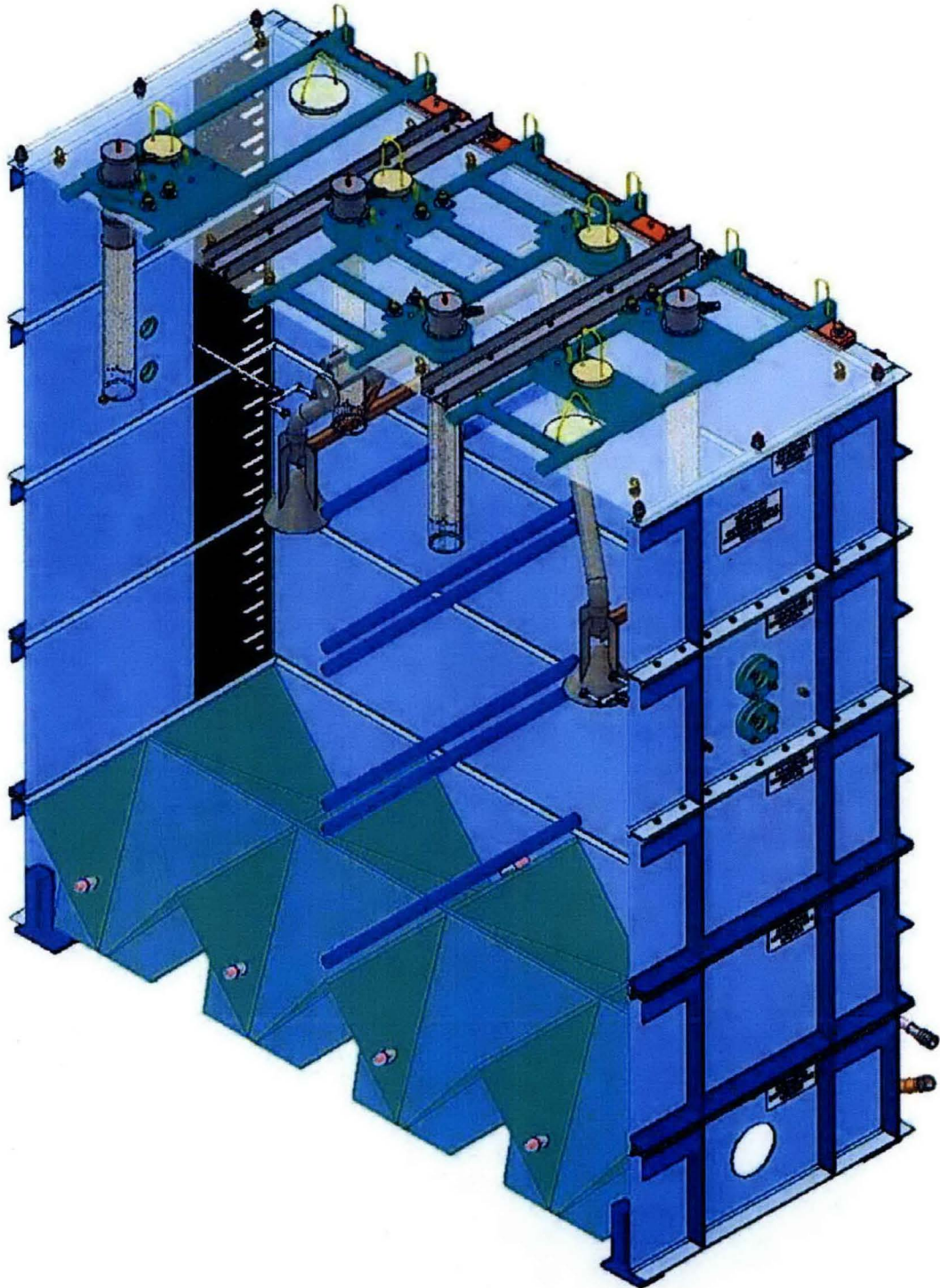
Figure 1-6   SCS-CON-230 isometric cutaway view.

2.0 SLUDGE-PARTICLE-LADEN PLUME DISCHARGES AND THE EVOLUTION OF THE PARTICLE CONCENTRATION IN THE CONTAINER

2.1 Description of Sludge-Plume-Filling-Container Problem

If the sludge discharge time is long, a plume of sludge particles and water is formed below each of the two sludge distributor ports. The plume may be regarded as a continuum of particles and water (Cary et al., 1988). The presence of the heavy sludge particles increases the bulk density of the continuum plume in comparison to the surrounding container water. Thus the emerging sludge flow has a significant downward buoyancy flux which can potentially stir the container fluid and mix the sludge particles from top to bottom of the container.

When the dense particle-laden plume discharged from one of the distributors reaches the egg crate bottom of the container, the two-phase mixture will displace the lighter water from the pockets that comprise the egg crate design and lie within the plume's impingement zone. Once the pockets are full of particle-laden water, the two phase mixture will spread out and fill the pockets that are located outside the plume's impingement zone, and will ultimately merge with the spreading two-phase mixture produced by the discharge from the other sludge distributor on the opposite of the container. The result is the formation of one coherent layer of particles and water beneath a deep layer of overlying pure container water.

The stability of the heavy layer of particles and water becomes very important in the subsequent development of the vertical distribution of sludge particles. The stable layer is defined by a distinctive interface which separates the lower particle-containing water form the upper clear water. In the stable layer there is a significant vertical variation in particle concentration, with the location of maximum particle concentration at the bottom of the layer, that is at the bottom of the container. This vertical particle concentration profile tends to enhance the particle settling rate at the bottom of the container. On the other hand, if the layer is unstable, a large scale vertical circulation is set up in the container which quickly mixes the particle/water mixture from the bottom of the container to the elevation of the sludge

distributors. As a result of continued addition of water through the distributors and water withdrawal at the filters, the well-mixed layer will ultimately fill the entire container from top to bottom.

The stability of the lower layer of particle-laden water is examined below. The examination begins with a model of the sludge plume.

2.2 Sludge-Particle-Laden Plume

Consider a turbulent, axisymmetric particle-laden plume created by the downward release of a negatively buoyant (heavier than water) sludge suspension from a sludge distributor. Owing to the presence of the cone-shaped sludge deflector just below the distributor orifice, it is assumed that the plume has no initial momentum and, therefore, that the distributor acts as a point source of negative buoyancy. On leaving the source the turbulent plume entrains surrounding container water as it descends and, hence, its bulk density decreases as it descends (Figure 2-1). On the other hand, due to entrainment, the plume radius increases as it descends. With respect to plume buoyancy (negative), plume growth wins out over plume dilution and the plume gains buoyancy as it descends.

Therefore, even in the absence of the sludge particle deflector at the source, at some distance below the source the plume begins to behave as a purely buoyant plume with no initial momentum. It can be shown that the vertical distance below the sludge distributor at which the plume transitions to a point source buoyant plume is less than the distance to the settled particle layer (see, e.g., Epstein and Fauske, 2001 for a general discussion of the behavior of fluid releases with initial momentum and buoyancy). The justifiable assumption is made that the particle and water phases move with the same velocity at any point within the plume.

The plume is modeled in the usual way (Morton, Taylor and Turner, 1956). Top-hat profiles for the lateral (radial) velocity and particle concentrations distributions in the plume are assumed. The Boussinesq approximation is made which states that the plume density is constant and equal to the density of the surrounding water except in the buoyancy term of the momentum

equation. The lateral inflow (entrainment) velocity u_e into the plume is proportional to the vertical velocity v in the plume:

$$u_e = E_0 v \tag{2-1}$$

where the empirical coefficient $E_0 \cong 0.12$ for buoyant (or negatively buoyant) plumes.

The equations expressing the conservation of volume, momentum and sludge-particle mass for an axisymmetric plume are

$$\frac{d}{dz}(vR^2) = 2\,E_0 vR \tag{2-2}$$

$$\frac{d}{dz}(v^2R^2) = \frac{g(\rho_s - \rho_f)}{\rho_f}\,\alpha R^2 \tag{2-3}$$

$$\dot{m}_s = \pi\rho_s \alpha vR^2 \tag{2-4}$$

where α is the local volume fraction of the sludge particles within the plume (at vertical location z measured downward from the sludge distributor), v is the local downward plume velocity at location z, R is the plume radius at location z, g is the gravitational constant, $\dot{m}_s$ is the mass flow (in kg s^{-1}) of the sludge-solid-particles supplied to the plume at the distributor orifice, and ρ_s and ρ_f are the constant material densities of the sludge solid and the water, respectively.

It is well known that the asymptotic (point source) solutions of Eqs. (2-2) to (2-4) are expressed in terms of fractional power functions of z. Substituting these mathematical forms into Eqs. (2-2) to (2-4) and solving for the unknown coefficients and exponents gives

$$v = \left(\frac{25}{48\pi}\right)^{1/3}\left(\frac{b}{z}\right)^{1/3} \tag{2-5}$$

$$\alpha = \frac{4}{3}\left(\frac{25}{48\pi}\right)^{2/3}\frac{b^{2/3}}{g(\rho_s/\rho_f - 1)\, z^{5/3}} \tag{2-6}$$

$$R = \frac{6}{5}E_0 z \tag{2-7}$$

where

$$b = \frac{g(\rho_s/\rho_f - 1)\,\dot{m}_s}{\rho_s E_0^2} = \frac{g(\rho_s/\rho_f - 1)\,\alpha_0 Q_0}{E_0^2} \tag{2-8}$$

In the definition of b above α_0 is the volume fraction of particles in the sludge at the sludge release orifice (distributor) and Q_0 is the volumetric rate of sludge flow through the distributor.

In deriving Eqs. (2-5) to (2-7) it was implicitly assumed that the cross-sectional area in a horizontal plane of the container occupied by plumes is a small fraction of the total cross-sectional area of the container. That is, it was assumed that (see Eq. 2-7)

$$\frac{2\pi(6/5)^2\, E_0^2\, H_d^2}{A_c} \ll 1.0 \tag{2-9}$$

where the factor 2 accounts for two sludge distributor plumes, H_d is the elevation of the sludge distributors above the egg crate (1.9 m) and A_c is the cross-sectional area of the sludge container (5.5 m^2). The left-hand side of Eq. (2-9) is 0.086. This result ensures that the plume flow is uncoupled from the container wide upward displacement of water due to sludge injection and/or filter flow.

2.3   Particle/Water Layer Stability

The stability condition derived in this section was apparently first suggested by Baines and Turner (1969).

The force that stabilizes the lower particle-laden layer of water of thickness of the order of the plume radius at the bottom of the container (top of the egg crate pattern) is the buoyancy force

$$F_B = A_c R(H_d) \, g \, (\rho_s - \rho_f) \, \alpha \tag{2-10}$$

The vertically (downward) directed momentum (or inertial force F_M) due to two discharge sludge plumes entering the lower particle-laden water layer, namely,

$$F_M = 2\pi \, [R(H_d)]^2 \, [v(H_d)^2] \, \rho_f \tag{2-11}$$

is the destabilizing force. Forming the ratio F_M/F_B and using Eqs. (2-5) to (2-7), all evaluated at $z = H_d$, yields after some algebra

$$\frac{F_M}{F_B} = \frac{(9/5) \, \pi \, E_0 H_d^2}{A_c} \tag{2-12}$$

The ratio F_M/F_B turns out to be strictly a function of container geometry and the location of the sludge discharge ports. The rate at which the sludge is discharged does not influence the stability of the heavy lower-layer. This is because an increase in the sludge discharge rate (or discharge momentum) is neutralized by a corresponding increase in the buoyancy (negative) of the lower particle-laden layer. The experimental work of Baines and Turner (1969) and Kumagai (1984) indicate that a transition from a stably stratified container to a vertically well-mixed container occurs as F_M/F_B increases from about 0.25 to 0.7. For the container SCS-CON-230 the ratio $F_M/F_B = 0.45$. The conclusion to be drawn from this result is that the container is partially mixed, in the sense that a semi-stably stratified layer exists at the bottom of the container, but waves grow at the interface at the top of the layer and overturn to release particles to the upper portion of the container. To err on the conservative side, a well-mixed container with a spatially uniform particle concentration distribution is assumed.

20090604-4ME
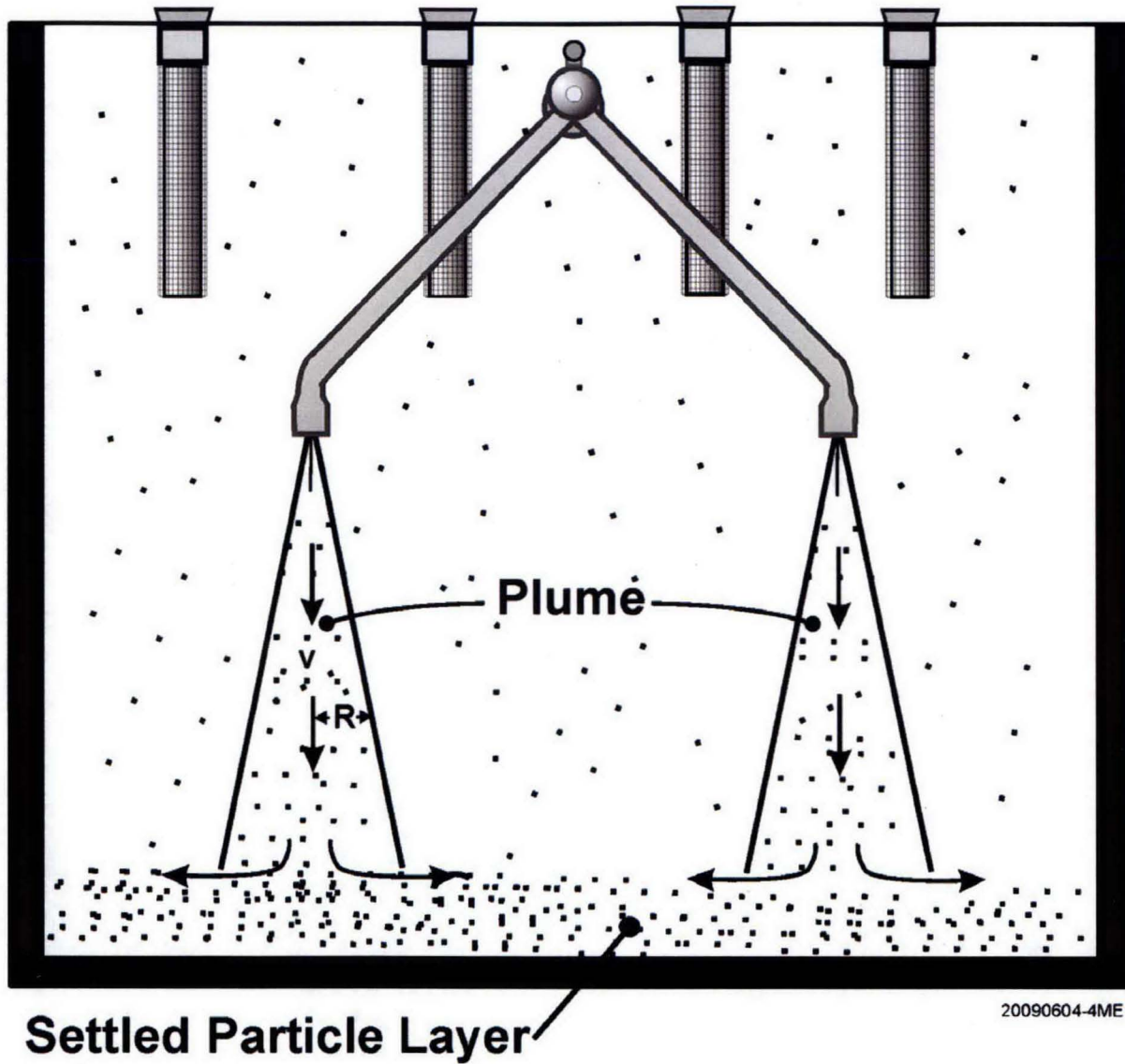
Figure 2-1   Model of particle plume in the container.

3.0   *CONTAINER OUTFLOW*

3.1   Discussion of Container Outflow Mechanisms

Suppose all four filters are operating and the flow through the gap is everywhere inward. Denoting the sink flow into each filter by the symbol Q_{fl} (in m^3 s^{-1}) and the sludge source flow at each of the two distributors by the symbol Q_0 the net withdrawal (suction) rate of water Q_{suc} within the container is

$$Q_{suc} = 4\,Q_{fl} - 2\,Q_0 \qquad \text{(no back flush)} \qquad (3\text{-}1)$$

During back flush, one of the four filters is adding water to the container at the rate $Q_{fl,bf}$. In this case water is being withdrawn from the container at the net rate

$$Q_{suc} = 3Q_{fl} - Q_{fl,bf} - 2Q_0 \qquad \text{(back flush)} \qquad (3\text{-}2)$$

This suction rate must equal the flow into the gap which, in accord with the Bernoulli equation, is

$$Q_{suc} = C_D A_g \left[\frac{2(P_\infty - P_c)}{\rho_f} \right]^{1/2} \qquad (3\text{-}3)$$

where C_D is the "orifice" coefficient for the gap flow, A_g is the flow area of the gap, P_∞ is the pressure in the basin water surrounding the gap, P_c is the effective uniform pressure within the container and ρ_f is the density of water. Solving Eq. (3-3) for P_∞ - P_c yields

$$P_\infty - P_c = \frac{1}{2} \rho_f \left(\frac{Q_{suc}}{C_D A_g} \right)^2 \qquad (3\text{-}4)$$

It is of interest to evaluate the magnitude of the pressure drop $P_\infty - P_c$. Consider first the case of no back flush. The flow into each filter is $Q_{fl} = 4.42 \times 10^{-4}$ m^3 s^{-1} (7.0 gpm) and the sludge source flow at each distributor is $Q_0 = 4.73 \times 10^{-4}$ m^3 s^{-1} (7.5 gpm). Thus the net suction flow from Eq. (3-1) is

$$Q_{suc} = 8.20 \times 10^{-4} \text{ m}^3 \text{ s}^{-1} \text{ (13.0 gpm)} \quad \text{(no back flush)} \qquad (3\text{-}5)$$

The area of the 1.0 x 156.0 in^2 gap is $A_g = 0.1$ m^2. Thus from Eq. (3-4) with $C_D = 0.7$ (see, e.g., Steckler et al., 1984) and $\rho_f = 10^3$ kg m^{-3}

$$P_\infty - P_c = 6.89 \times 10^{-2} \text{ Pa} \qquad \text{(no back flush)} \qquad (3\text{-}6)$$

When back flush occurs $Q_{fl,b} = 3.15 \times 10^{-4}$ m^3 s^{-1} (5.0 gpm) and from Eq. (3-2)

$$Q_{suc} = 6.31 \times 10^{-5} \text{ m}^3 \text{ s}^{-1} \text{ (1.0 gpm)} \quad \text{(back flush)} \qquad (3\text{-}7)$$

The pressure drop across the gap is now

$$P_\infty - P_c = 4.06 \times 10^{-4} \text{ Pa} \qquad \text{(back flush)} \qquad (3\text{-}8)$$

Indeed the pressure in the container with or without back flush is only slightly below that just outside the gap in the basin water. These results suggest a number of physical processes that could potentially result in an outflow either locally or over the entire gap. These are

(1)   The sludge inlet flow may locally reverse the inflow.

(2)   Back flushing a filter that is close to the gap may locally overwhelm the inflow.

(3)   A streaming motion of basin water around the container may cause the pressure on the downstream side of the container to drop below P_c, potentially causing outflow on the downstream side.

(4)   A sufficiently high temperature difference between the surrounding basin water and the container water will result in a buoyantly driven outflow over the entire length of the gap.

3.2   Outflow Due to Sludge Discharge Flow or Filter Back Flushing

Process 1 does not result in an outflow. The sludge distributors are too far away from the gap to have an effect on the flow in the vicinity of the gap. This can be demonstrated by treating a sludge distributor as a point source for which the radial velocity field v_r is given by the simple formula

$$v_r = \frac{Q_0}{4\pi r^2} \tag{3-9}$$

where r is the radial distance from the distributor. From Bernoulli's equation the pressure field surrounding the distributor is

$$P = P_c - \frac{1}{2}\rho\,v_r^2 = P_c - \frac{1}{2}\rho\left(\frac{Q_0}{4\pi r^2}\right)^2 \tag{3-10}$$

The pressure rises to within 0.01% of P_c in a radial distance of only about 0.01 m. Thus the sludge flow into the tank has a negligible effect on pressure drop and flow in the vicinity of the gap.

Much like the sludge distributors, the influence of the two-dimensional line source flow from a filter during back flush can be shown to diminish to zero a few centimeters away from the filter. Thus it is reasonable to assume that the container pressure P_c is below the surrounding basin pressure everywhere in the container. In other words, the normal operation of the filters and the sludge distributors will not by itself result in outflow.

3.3   Container Outflow Due to the Basin Current

The basin current gives rise to a pressure distribution along the outside surface of the container. The wake that forms on the downstream side of the container is mainly responsible for this distribution. The current is known to flow normal to one of the small sides of the container (hereafter referred to as the upstream side). A simple pressure distribution is assumed. The pressure along the upstream side and along the essentially sealed (no gap) large sides of the container, which are parallel to the current, is the basin pressure P_∞. On the downstream side (end surface) of the container the pressure P_d is

$$P_d = P_\infty - \frac{K}{2} \rho_f u_\infty^2 \tag{3-11}$$

where u_∞ is the basin current velocity and K is a constant whose value is between zero and unity. The basin cross-flow velocity can be bounded by a value of $u_\infty = 10^{-3}$ m s^{-1}. This is based upon assuming 120 gpm flow through a basin bay through a cross-sectional area defined by 30 feet wide (less than the approximately 40 feet width of a bay) and 3 feet deep (the container top is submerged by about 2.5 feet). The actual cross-flow value is likely lower. Measurements of pressure distributions around a circular cylinder indicate that K $\cong$ 0.75 (Churchill, 1988). We will assume that this value is valid for the rectangular container. Thus from Eq. (3-11) the pressure drop across the outside of the container, from the upstream side to the downstream side, is $P_\infty - P_d = 3.75 \times 10^{-4}$ Pa, and from Eqs. (3-6) and (3-8)

$$P_d - P_c = 6.83 \times 10^{-2} \text{ Pa} \qquad \text{(no back flush)} \tag{3-12}$$

$$P_d - P_c = 3.12 \times 10^{-5} \text{ Pa} \qquad \text{(back flush)} \tag{3-13}$$

Since $P_\infty > P_d > P_c$ no flow leaves the container through the gap along the upstream side and no flow leaves the container through the gap along the downstream side.

The critical basin flow velocity $u_{\infty,cr}$ above which flow will enter the gap of area $A_g/2$ along the downstream end is obtained by setting P_d in Eq. (3-11) equal to P_c in Eq. (3-3) and solving the result for u_∞:

$$u_{\infty,cr} = \frac{1}{K^{1/2}}\left(\frac{2Q_{suc}}{C_D A_g}\right)$$

(3-14)

The predicted critical basin flow velocities are $u_{\infty,cr} = 2.08 \times 10^{-3}$ m s^{-1} with back flushing and $u_{\infty,cr} = 2.71 \times 10^{-2}$ with no back flushing. Both of these estimates are above the basin cross flow velocity $u_\infty = 10^{-3}$ m s^{-1}.

Because of the basin current the flow into the upstream end of the container will be somewhat higher than the flow into the downstream end. A volume flow rate balance on the container provides the following equation:

$$C_D\left(\frac{A_g}{2}\right)\left[\frac{2(P_\infty - P_c)}{\rho_f}\right]^{1/2} + C_D\left(\frac{A_g}{2}\right)\left[\frac{2(P_d - P_c)}{\rho_f}\right]^{1/2} = Q_{suc}$$

(3-15)

The first and second terms in the above equation are, respectively, Bernoulli's equation for flow into the upstream-end gap of area $1/2\ A_g$ and Bernoulli's equation for flow into the downstream-end gap of area $1/2\ A_g$. Eliminating P_d between Eqs. (3-11) and (3-15) yields the following equation for $P_\infty - P_c$ in dimensionless form

$$x + (x^2 - K)^{1/2} = q$$

(3-16)

where

$$x = \frac{[2(P_\infty - P_c)/\rho_f]^{1/2}}{u_\infty}$$

(3-17)

$$q = \frac{2Q_{suc}}{C_D A_g u_\infty} \qquad (3\text{-}18)$$

Physical solutions to Eq. (3-16) for x obey the condition $u_\infty \leq u_{\infty,cr}$ (or, equivalently, $q > K^{1/2}$). Solving Eq. (3-16) for x yields

$$x = \frac{q}{2} + \frac{K}{2q} \qquad (3\text{-}19)$$

Once x is obtained from Eq. (3-19), the flows into the container are

$$Q_{suc,u} = C_D \left(\frac{A_g}{2}\right) \left[\frac{2(P_\infty - P_c)}{\rho_f}\right]^{1/2} = C_D \left(\frac{A_g}{2}\right) u_\infty x \qquad (3\text{-}20)$$

$$Q_{suc,d} = C_D \left(\frac{A_g}{2}\right) \left[\frac{2(P_c - P_d)}{\rho_f}\right]^{1/2} = C_D \left(\frac{A_g}{2}\right) u_\infty (x^2 - K)^{1/2} \qquad (3\text{-}21)$$

where the subscripts suc,u and suc,d, refer to the upstream and downstream inlet flows. As already mentioned, the appropriate parameter values for insertion into Eqs. (3-18) to (3-21) are $A_g = 0.1$ m^2, $C_D = 0.7$, $u_\infty = 10^{-3}$ m s^{-1}, and $K = 0.75$. If all the filters are operating the net withdrawal rate of water in the container is, as previously calculated, $Q_{suc} = 8.20 \times 10^{-4}$ m^3 s^{-1} (see Eq. 3-5). During back flush, one of the four filters is adding water to the container and water is being withdrawn from the container at the net rate $Q_{suc} = 6.31 \times 10^{-5}$ m^3 s^{-1} (see Eq. 3-7). The dimensionless suction rates for the case of all filters operating and for back flushing are respectively $q = 23.5$ and $q = 1.84$.

The corresponding dimensionless container pressures for no back flush and back flush are, from Eq. (3-19), $x = 11.8$ and $x = 1.12$. From Eqs. (3-20) and (3-21) the basin flow rates through the upstream and downstream sides of the container when all four filters are operating are essentially equal to one another and are

$$Q_{suc,u} = 4.11 \times 10^{-4}\,m^3\,s^{-1} \quad , \quad Q_{suc,d} = 4.10 \times 10^{-4}\,m^3\,s^{-1} \quad \text{(no back flush)} \tag{3-22}$$

For the back flush case there is a difference between the upstream and downstream inlet flows.

$$Q_{suc,u} = 3.88 \times 10^{-5}\,m^3\,s^{-1} \quad , \quad Q_{suc,d} = 2.43 \times 10^{-5}\,m^3\,s^{-1} \quad \text{(back flush)} \tag{3-23}$$

3.4 Outflow Induced by Container Temperature Rise Above the Basin Temperature

The temperature of the container can be higher than that of the basin because of pumping power and the perhaps because of water sources used for sludge retrieval. The container water temperature is driven by the inlet flow rate and supply temperature (this is the water source from the settlers), the net suction flow rate into the container (which carries in water at the basin temperature), and by convective heat transfer through the container walls. Decay power can be shown to be negligible when the inlet water temperature is more than about 1 °C above the basin temperature. In the discussion that follows, the container water temperature is assumed to be greater than the basin water temperature, but the induced flow depends only on the absolute value of the temperature difference, not its sign.

The flow induced by container-to-basin temperature differences is a counter-current natural exchange flow. Warmer, slightly less dense water inside the container flows outward through the gap and is replaced by cooler, slightly more dense water from the basin. The counter-current flow can be prevented or "purged" by a sufficiently strong pressure-induced upstream- or downstream suction flow into the container, q_p. The relationship between suction flow that prevents counter-current flow and the container-basin temperature difference ΔT is given by (Epstein and Kenton, 1989):

$$q_p = \frac{2C_D}{3}\left[2\,(A_g/2)^2\,\delta_g\,g\,\beta\,\Delta T\right]^{1/2} \tag{3-24}$$

where δ_g is the height of the gap (0.0254 m), g is the acceleration of gravity, and β is the coefficient of thermal expansion ($\beta = 2.07 \times 10^{-4}$ K^{-1}). Solving for ΔT gives the temperature difference above which countercurrent exchange flow will appear in the gap:

$$\Delta T = \frac{9 \, q_p^2}{2 \, C_D^2 A_g^2 \delta_g g \beta} \tag{3-25}$$

During normal operation q_p is the suction flow rate through the upstream or downstream gap (4.13×10^{-4} m^3 s^{-1}, see Eq. 3-22) and from Eq. (3-25) we estimate that countercurrent outflow requires the container water temperature to be $\Delta T = 3$°C above the basin water temperature. During back flush, $q_p = Q_{suc,d} = 2.61 \times 10^{-5}$ m^3 s^{-1}, and outflow through the downstream gap will occur when the temperature in the container is only $\Delta T = 0.012$°C above the basin value.

When there is no pressure-driven flow (no suction) at all, the counter-current flow rate attains its maximum value given by

$$Q_{cco} = \frac{C_D}{3} \left[(A_g / 2)^2 \, \delta_g \, g \, \beta \, \Delta T \right]^{1/2} \tag{3-26}$$

When the suction flow is less than the purge flow, $0 < Q_{suc} < q_p$, the counter-current exchange flow rate is given by

$$Q_{cc} = Q_{cco} \left(1 - \frac{Q_{suc}}{q_p} \right)^{3/2} \tag{3-27}$$

The counter-current flow rate as a function of container water temperature rise above the basin is shown in Fig. 3-1. Again the value of suction flow $Q_{suc} = 13$ gpm during normal operation, and $Q_{suc} = 1$ gpm during back flush. As noted in the foregoing, during normal operation there is no counter-current flow until the container water temperature is 3 °C above the basin value.

It is more instructive to examine the counter-current exchange flow that can occur for various values of the net suction flow. In Fig. 3-2, the value of Q_{suc} is varied between 1 and 15 gpm, and the counter-current exchange flow is plotted for various values of the temperature difference between the container and basin. In the construction of Fig. 3-2 the temperature difference was related to the value of q_p via Eq. (3-24). The flows are nonzero when the suction flow is less than the threshold value for purging.

Figure 3-2 can be used to choose a container suction flow that will prevent escape of sludge particles for a given container water temperature. The next step is to examine possible values of container water temperatures. Container water temperature T_{wc} evolves according to the following energy balance:

$$
\rho_f c_{pf} \frac{d(T_{wc} - T_\infty)}{dt} = \rho_f c_{pf} (2Q_o)(T_o - T_\infty) - \rho_f c_{pf} (4Q_{fl} + Q_{cc})(T_{wc} - T_\infty) - hA_{wc}(T_{wc} - T_\infty)
$$

$$(3\text{-}28)$$

where T_∞ is the basin water temperature, T_o is the inlet water temperature, $\rho_f = 1000$ kg/m^3 and $c_{pf} = 4184$ J/kg/K are the water density and specific heat, respectively, Q_o and Q_{fl} are the inlet and filter flows per inlet and filter, respectively, Q_{cc} is the total counter-current flow through the upstream and downstream gaps, A_{wc} is the container wall area, the heat transfer coefficient for natural convection is given by

$$
h = 0.103 \, k_f \left(\frac{g \, \beta \left(T_{wc} - T_\infty \right)}{v_f \, \alpha_f} \right)^{1/3}
$$

$$(3\text{-}29)$$

and additional properties appearing are thermal conductivity $k_f = 0.60$ W/m/K, kinematic viscosity $v_f = 10^{-6}$ m^2/s, and thermal diffusivity $\alpha_f = 1.4 \times 10^{-7}$ m^2/s.

Container water temperature versus time is shown for various assumed inlet water temperatures in Fig. 3-3. Note that even if the inlet water temperature is 5 °C above the basin,

the container water temperature is only 1.5 °C above the basin. In fact, an inlet temperature of slightly over 11 °C above the basin is required for the basin water temperature to be 3 °C above the basin value. This does not seem realistic, and strongly suggests that counter-current flow cannot occur during normal operations, only during back flushing. Finally, note that the time scale to attain steady container water temperature is about 5 hours.

The following conclusions may be drawn from this discussion:

(1)   For the given water addition, filter flow, and back flush flow rates, sludge particle loss from SCS-CON-230 is not credible except by thermal convection during back flushing. This is based on demonstrating that it is not credible for the container inlet water temperature to be consistently 11 °C or more greater than the basin temperature.

(2)   For an assumed bounding inlet water temperature 4 °C above the basin temperature, the water container temperature will be about 1.2 °C above the basin temperature, and this will be attained on a time scale that is short compared to the filling time. Counter-current flow will occur during back flushing. Sludge particle loss to the basin is expected during back flushing.

(3)   Sludge particle loss from the container can be prevented by maintaining a net container suction flow of 8 gpm if the bounding container inlet water temperature is 4 °C above the basin temperature (which leads to a container temperature about 1.2 °C above the basin).

(4)   For operation periods during which particles are settling in the container but no retrieval is occurring, continued water supply and filter operation might be beneficial because this maintains net suction from the basin and prevents particle escape due to counter-current flow except in the event of a backflush.
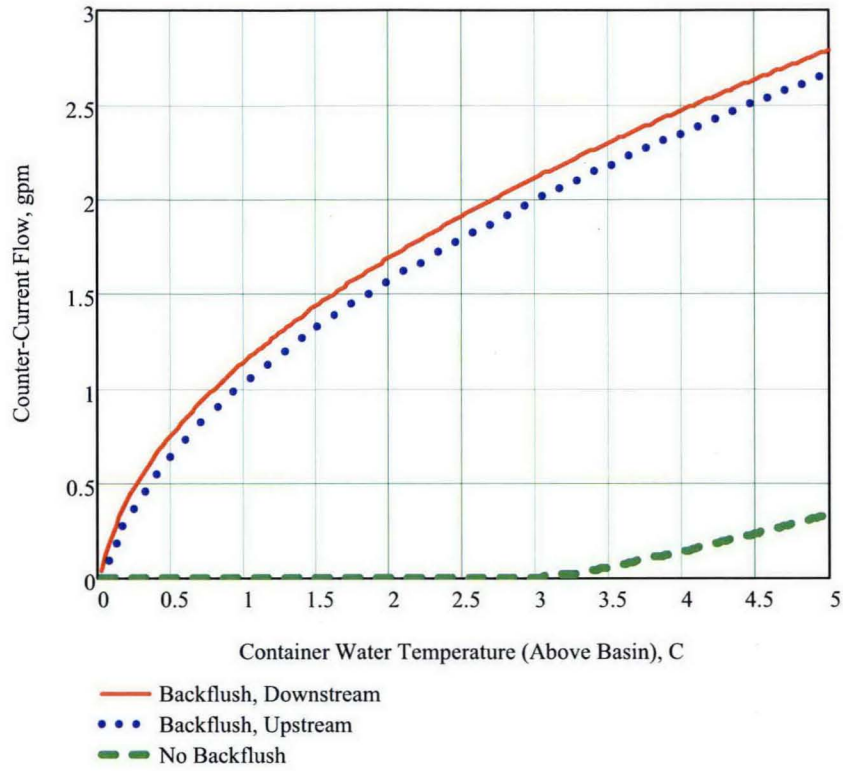
Figure 3-1   Countercurrent exchange flow between container and
basin as function of container water temperature.
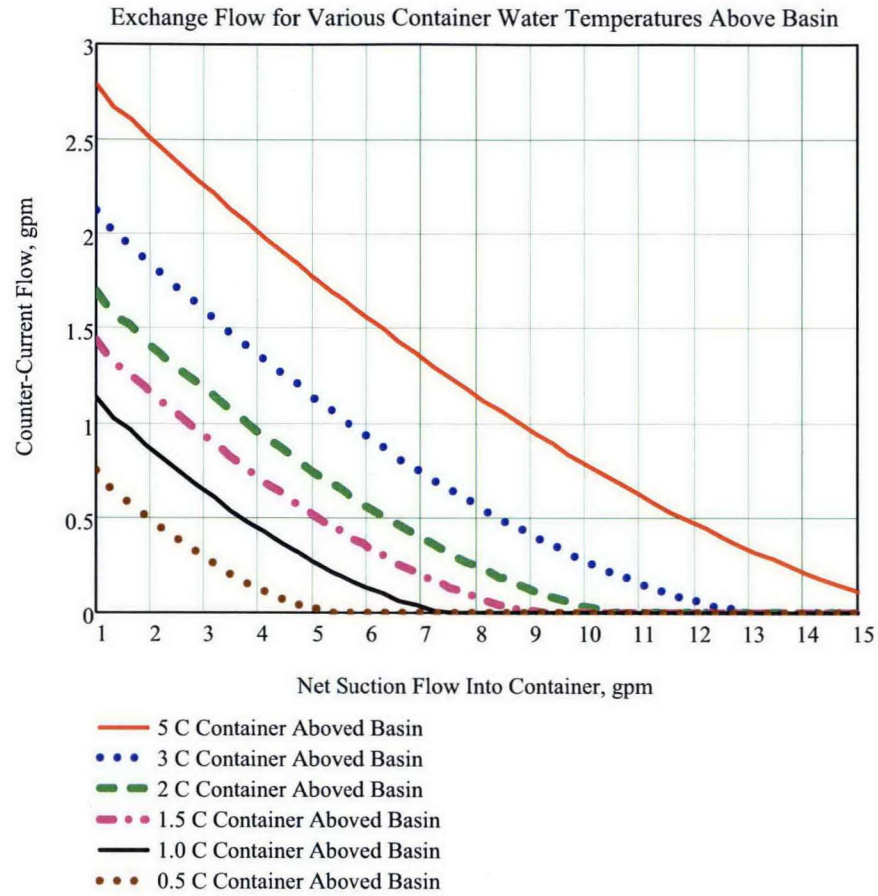
Figure 3-2   Countercurrent exchange flow between basin and container for various container water temperatures above the basin temperature as function of net suction.
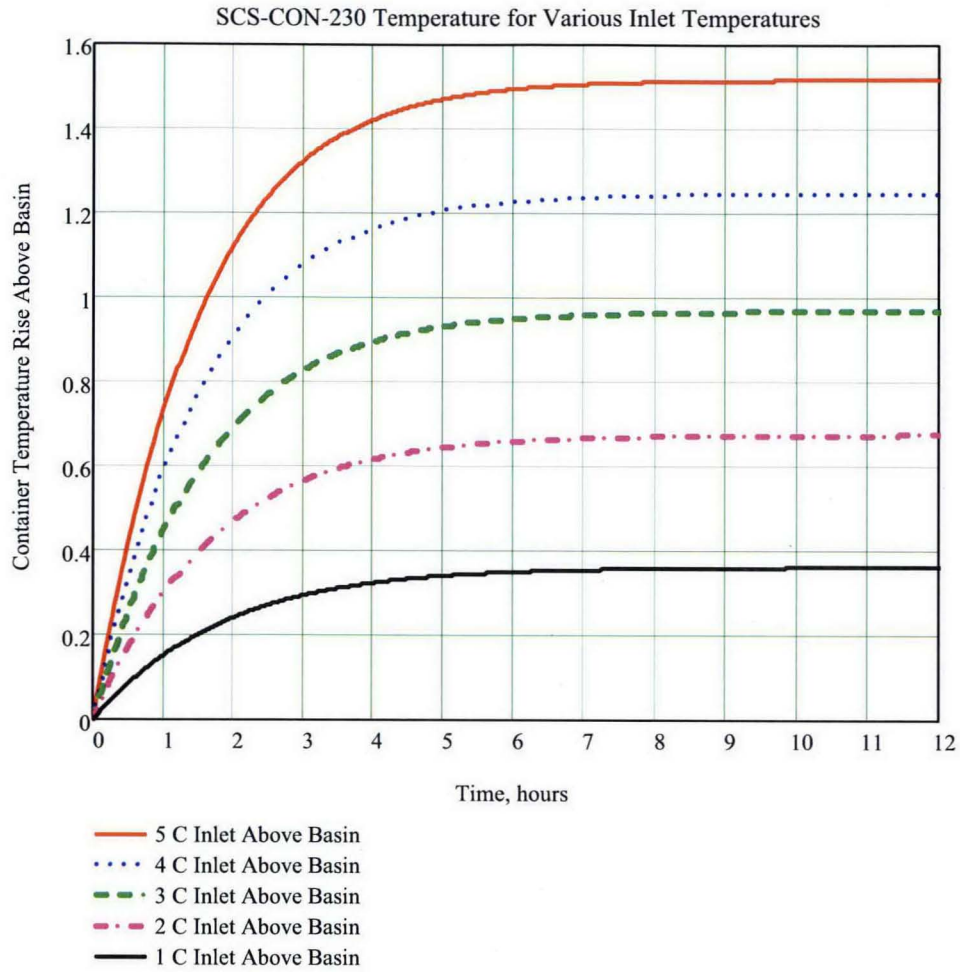
Figure 3-3   Container water temperature history for various inlet water temperatures.

4.0 SLUDGE PARTICLES SEDIMENTATION, FILTRATION AND OUTFLOW IN CONTAINER SCS-CON-230

4.1 Model Assumptions

In this section a theory is developed and applied to predict the fractions of the sludge particles discharged to the container that settle to the bottom of the container, arrive at the filters and flow out of the container. The major assumptions underlying the theory are:

(1)   The container is well-mixed by the sludge discharge buoyancy so that the particle concentration is uniform throughout the container (see Section 2.0).

(2)   The sludge particle size distribution is log-normal.

(3)   Most of the particles are small enough so that their settling velocity is accurately represented by Stoke's law.

(4)   Resuspension of settled sludge particles by the negatively buoyant sludge plume is neglected.

(5)   The sludge particles are spherical or they can be represented by equivalent spheres.

Assumptions 1 is conservative. Many particle size distributions that occur in nature and industry have been found to follow the log-normal distribution (Assumption 2). It is shown in Appendix C that for the maximum effective particle density assumed here (6000 kg m^{-3}) and for the log-normal particle size distribution characteristics selected (mass median particle diameter $d_{1/2} = 10$ μm and maximum particle diameter $d_{max} = 500$ μm), most of the particles (94% by mass) settle at a rate given by Stokes law (Assumption 3). A detailed discussion and justification of Assumption (4) is given in Appendix A. Assumption (5) involves the neglect of deviations from Stokes law by irregular particle shapes and the neglect of the fact that when two spherical solid particles collide they do not form another spherical particle. One can introduce shape

factors to correct the equations for nonspherical particle behavior. However the numerical values of these shape factors are usually unknown. In the authors' experience one can just as well investigate departures from spherical particle behavior by retaining the spherical particle assumption and varying the particle density in Stokes law and by varying the capture coefficient that appears in the particle coagulation terms.

4.2   Conversion of the Particle Size Distribution Equation to a System of Ordinary Differential Equations

The basic equation describing the change with time of the size distribution of a spatially homogeneous suspension due to particle coagulation and due to removal by sedimentation, filtration and outflow and particle addition due to the presence of a source (sludge distributors) is

$$\frac{\partial n(v,t)}{\partial t} = -\frac{n(v,t)u_{sed}(v)}{h_{sed}} - \frac{n(v,t)u_{fl}}{h_{fl}} - \frac{n(v,t)u_{out}}{h_{out}} + \dot{n}_p(v)$$
$$+ \frac{1}{2} \int_0^v K_g(\bar{v}, v-\bar{v}) n(\bar{v},t) n(v-\bar{v},t) d\bar{v} - \int_0^\infty K_g(\bar{v},v) n(\bar{v},t) n(v,t) d\bar{v}$$

$$(4-1)$$

Here $n(v,t)$ is the size distribution function, defined such that $n(v,t)dv$ is the number concentration of particles (particles m^{-3}) in the particle volume size range v to $v + dv$ at time t, $u_{sed}(v)$ is the Stoke's gravitational (sedimentation) velocity, u_{fl} is the filter inlet velocity that carries particles of all sizes to the filters, u_{out} is the outlet flow velocity that carries particles of all sizes through the gap and out of the container and $\dot{n}_p(v)dv$ is the rate of introduction of particles per unit volume of the suspension (container) in the size range v to $v + dv$. The symbol h denotes the effective heights for sedimentation (sed), filtration (fl), and outflow (out); it is the suspension (container) volume divided by sedimentation area (container floor), or total filter area, or gap outflow area, respectively. The integral terms are the gravitational particle coagulation term that represent the collection of small particles by larger falling particles. The kernel $K_g(\bar{v},v)$ that appears in the coagulation terms is the frequency of binary collisions between particles of volume v and $\bar{v}$ (in units $m^3 s^{-1}$).

Equation (4-1) may be converted to an ordinary differential equation by multiplying it by v^γ, where γ is a constant, and integrating over particle volume v from 0 to ∞; namely,

$$\frac{d}{dt}\int_0^\infty v^\gamma n(v,t)dv = -\frac{1}{h_{sed}}\int_0^\infty v^\gamma n(v,t)u_{sed}(v)dv$$

(4-2)

$$-\frac{u_{fl}}{h_{fl}}\int_0^\infty v^\gamma n(v,t)dv - \frac{u_{out}}{h_{out}}\int_0^\infty v^\gamma n(v,t)dv + \int_0^\infty v^\gamma \dot{n}_p(v)dv$$

$$+\frac{1}{2}\int_0^\infty \int_0^v v^\gamma K_g\left(\overline{v},v-\overline{v}\right)n\left(\overline{v},t\right)n\left(v-\overline{v},t\right)d\overline{v}dv$$

$$-\int_0^\infty \int_0^\infty v^\gamma K_g\left(\overline{v},v\right)n\left(\overline{v},t\right)n\left(v,t\right)d\overline{v}dv$$

The integral,

$$X_\gamma(t) = \int_0^\infty v^\gamma n(v,t)dv$$

(4-3)

that appears in the time derivative on the left-hand-side of Eq. (4-2) can represent a general property of the sludge suspension. For example, for $\gamma = 0$, X_0 is simply equal to the total number concentration of suspension particles:

$$N(t) = X_0(t) = \int_0^\infty n(v,t)dv$$

(4-4)

If $\gamma = 1$, $X_1(t)$ is the total volume (or mass) concentration of suspension particles in units of volume of particles per volume of space:

$$V(t) = X_1(t) = \int_0^\infty vn(v,t)dv$$

(4-5)

If $\gamma = 2/3$, $X_{2/3}(t)$ is proportional to the suspension surface area distribution.

The integral represented by $X_\gamma(t)$ is referred to in the literature as the γ'th moment of the particle size number density distribution function. Thus Eq. (4-2) represents a set of ordinary differential equations for the moments. The moments and the integrals on the right-hand-side of Eq. (4-2) can be integrated once the functional form of the distribution function $n(v,t)$ is assumed. The exact number of "moment equations" (4-2) that must be solved is equal to the number of time-dependent parameters that appear in the distribution. The number density distribution function is assumed to be of the following log-normal form:

$$n(v,t)dv = \frac{N(t)}{\sqrt{2\pi} \ln[\sigma(t)]} \bullet \exp\left[-\frac{\left\{ \ln\left(\frac{v}{v_g(t)} \right)^{1/3} \right\}^2}{2\ln^2[\sigma(t)]} \right] d\ln v^{1/3} \qquad (4-6)$$

where $N(t)$ is the total instantaneous number concentration of particles in the suspension, $v_g(t)$ is the instantaneous number median particle volume of the suspension, and $\sigma(t)$ is the instantaneous geometric standard deviation of the suspension.

Substitution of Eq. (4-6) into Eq. (4-3) yields the following expression for the moments of the log-normal distribution:

$$X_\gamma(t) = N(t)[v_g(t)]^\gamma \exp\left\{ \frac{9\gamma^2}{2}[\ln\sigma(t)]^2 \right\} \qquad (4-7)$$

Using the zeroth, first and second moments:

$$X_0(t) = N(t) \qquad (4-8)$$

$$X_1(t) = N(t)\, v_g(t) \exp\left\{ \frac{9}{2}[\ln\sigma(t)]^2 \right\} \qquad (4-9)$$

$$X_2(t) = N(t)[v_g(t)]^2 \exp\left\{ 18[\ln\sigma(t)]^2 \right\} \qquad (4-10)$$

As already mentioned, the zeroth and first moments can be associated with those quantities which are capable of experimental measurement – the total number of particles and the total mass of particles, respectively. The second moment given by Eq. (4-10) has little physical significance and is chosen because it has been used successfully in the past by log-normal aerosol code developers and because it is convenient to deal with mathematically. A better choice for the required third moment might be $X_{2/3}$, which represents the total suspension surface area.

It will prove convenient to invert Eqs. (4-8) to (4-10) so that the time-dependent parameters of the log-normal distribution are expressed in terms of the three moments of the distribution function. The results of the required algebraic manipulations are

$$N(t) = X_0(t) \tag{4-11}$$

$$v_g(t) = \frac{X_1(t)^2}{X_0(t)^{3/2} X_2(t)^{1/2}} \tag{4-12}$$

$$\ln \sigma(t) = \frac{1}{3} \left\{ \ln \left(\frac{X_0(t) X_2(t)}{X_1^2(t)} \right) \right\}^{1/2} \tag{4-13}$$

It remains to establish the functional forms for the sedimentation velocity $u_{sed}(v)$ and the gravitational coagulation kernal $K_g(\overline{v}, v)$ in Eq. (4-2). Once this is accomplished differential equations for X_γ (or for N, v_g and σ) can be obtained by direct integration of the integrals in Eq. (4-2). The sedimentation velocity for the sludge particles is given by Stoke's law (see Assumption 3 in Section 4.1). The deposition velocity for spherical particles is

$$u_{sed}(v) = \frac{2}{9} \left(\frac{3}{4\pi} \right)^{\frac{2}{3}} \frac{(\rho_s - \rho_f) g v^{2/3}}{\mu_f} \tag{4-14}$$

where g is the gravitational constant, ρ_s is the density of the particle material, and ρ_f, μ_f are the density and viscosity of the water component of the sludge suspension.

Particles of different sizes will settle at different rates under the influence of gravity and thereby create relative motion between them that leads to collisions and coagulation. Consider a large particle of radius $\bar{r}$ as it settles through a suspension of smaller particles of radius r. The smaller particles will collide with the larger particle by the mechanisms of inertia and interception. A particle capture coefficient $\varepsilon(r,\bar{r})$ is defined as the ratio of the actual frequency of collisions to the frequency that would obtain if the small particles were fixed and not pushed aside by the flow around the large particle. Clearly, the collision frequency kernel for gravitational coagulation is

$$K_g(r,\bar{r}) = \varepsilon(r,\bar{r})\,\pi(r+\bar{r})^2\left[u_{sed}(\bar{r}) - u_{sed}(r)\right] \quad ; \quad r \le \bar{r} \tag{4-15}$$

The value of $\varepsilon(r,\bar{r})$ is less than unity and is not known to good accuracy. The following functional form based on the work of Fuchs (1964) and Pruppacher and Klett (1978) is adopted here:

$$\varepsilon(r,\bar{r}) = \frac{3\varepsilon_0}{2}\left(\frac{r}{r+\bar{r}}\right)^2 \quad ; \quad r \le \bar{r} \tag{4-16}$$

There is a controversy over the proper numerical value of the constant coefficient ε_0 in the above equation which to the best of the authors' knowledge has not yet been resolved. In the Fuchs' model $\varepsilon_0 = 1.0$ and in the Pruppacher-Klett model $\varepsilon_0 = 1/3$. Of course lower numerical values of ε_0 may be employed to model nonspherical particles. Combining Eqs. (4-15) and (4-16) gives

$$K_g(\bar{r},r) = \frac{3\pi}{2}\varepsilon_0 r^2\left[u_{sed}(\bar{r}) - u_{sed}(r)\right] \quad ; \quad r \le \bar{r} \tag{4-17}$$

or, by converting particle radii to volume:

$$K_g(\bar{v},v) = \frac{\pi}{3}\left(\frac{3}{4\pi}\right)^{4/3}\frac{\varepsilon_0(\rho_s - \rho_f)g}{\mu_f}v^{2/3}\left(\bar{v}^{2/3} - v^{2/3}\right) \quad ; \quad v \le \bar{v} \tag{4-18}$$

Repeating the above development for a large particle of radius r settling through a suspension of smaller particles of radius $\bar{r}$, the appropriate coagulation equation for $v > \bar{v}$ is obtained:

$$K_g\left(\bar{v}, v\right) = \frac{\pi}{3}\left(\frac{3}{4\pi}\right)^{4/3} \frac{\varepsilon_0 \left(\rho_s - \rho_f\right)g}{\mu_f} \bar{v}^{2/3}\left(v^{2/3} - \bar{v}^{2/3}\right) \quad ; \quad v > \bar{v} \qquad (4\text{-}19)$$

Substituting Eqs. (4-6), (4-14), (4-18) and (4-19) into the integral terms in Eq. (4-2), performing the indicated integrations for $\gamma = 0,1,2$ and using Eqs. (4-11) to (4-13) to express all quantities in terms of X_0, X_1, and X_2 gives the differential equations for the first three integral moments:

$$\frac{dX_0}{dt} = -\frac{B}{h_{sed}} X_0\left(\frac{X_1^8}{X_0^7 X_2}\right)^{\frac{1}{9}} - \left(\frac{u_{fl}}{h_{fl}} + \frac{u_{out}}{h_{out}}\right)X_0 + \dot{N}_p$$
$$-\frac{3\pi}{4}\left(\frac{3}{4\pi}\right)^{2/3}\varepsilon_0 B X_0^2\left(\frac{X_1^8}{X_0^7 X_2}\right)^{\frac{2}{9}}\left\{1 - \left(\frac{X_0 X_2}{X_1^2}\right)^{\frac{4}{9}} \text{erfc}\left[2\ln\sigma(t)\right]\right\} \qquad (4\text{-}20)$$

$$\frac{dX_1}{dt} = -\frac{B}{h_{sed}} X_0\left(\frac{X_1 X_2}{X_0^2}\right)^{\frac{5}{9}} - \left(\frac{u_{fl}}{h_{fl}} + \frac{u_{out}}{h_{out}}\right)X_1 + \dot{N}_p v_{g,p} \exp\left[\frac{9}{2}(\ln\sigma_p)^2\right] \qquad (4\text{-}21)$$

$$\frac{dX_2}{dt} = -\frac{B}{h_s} X_0\left(\frac{X_2^5}{X_0 X_1^4}\right)^{\frac{4}{9}} - \left(\frac{u_{fl}}{h_{fl}} + \frac{u_{out}}{h_{out}}\right)X_2 + \dot{N}_p v_{g,p}^2 \exp\left[18(\ln\sigma_p)^2\right]$$
$$+\frac{3\pi}{2}\left(\frac{3}{4\pi}\right)^{2/3}\varepsilon_0 B X_0^2\left(\frac{X_1^{10}X_2^{10}}{X_0^{20}}\right)^{\frac{1}{9}}\left\{1 - \left(\frac{X_0 X_2}{X_1^2}\right)^{\frac{4}{9}} \text{erfc}\left[2\ln\sigma(t)\right]\right\} \qquad (4\text{-}22)$$

In the above equations the subscript p pertains to the known (specified) particle size distribution properties at the source (sludge distributors; see below), and

$$B = \frac{2}{9}\left(\frac{3}{4\pi}\right)^{2/3}\frac{g(\rho_s - \rho_f)}{\mu_f} \qquad\qquad (4\text{-}23)$$

The details of integrating the double integrals in the particle coagulation rate terms are not straightforward and are given in Appendix B.

Since $N(t)$, $v_g(t)$ and $\sigma(t)$ are related to the moments X_0, X_1, and X_2 via Eqs. (4-11) to (4-13), the differential equation set (4-20) to (4-22) is sufficient to determine the evolution of the sludge suspension particle size distribution once the source particle size distribution properties $v_{g,p}$ and σ_p are specified. Of course, the source-sludge particle size spectrum must be of the log-normal form

$$\dot{n}_p(v)\,dv = \frac{\dot{N}_p}{\sqrt{2\pi}\,\ln\sigma_p}\exp\left[-\frac{\left\{\ln\left(\frac{v}{v_{g,p}}\right)^{1/3}\right\}^2}{2\ln^2\sigma_p}\right]d\ln v^{1/3} \qquad (4\text{-}24)$$

where $\dot{N}_p$ is the total rate of introduction of particles per unit volume of the container. In setting up the numerical calculations that follow it is convenient to work only with representative particle diameters of the source-sludge particle size distribution instead of the quantities $v_{g,p}$ and σ_p. The two diameters selected here are $d_{1/2}$ and d_{max} defined as the particle diameters such that 50% and 99.9% of the total mass (or volume) of the particles is in particles of diameters smaller than $d_{1/2}$ and d_{max}, respectively. For a log-normal particle suspension

$$\frac{d_{1/2}}{d_{g,p}} = \exp\left[3\left(\ln\sigma_p\right)^2\right] \qquad\qquad (4\text{-}25)$$

$$\frac{d_{max}}{d_{g,p}} = \exp\left[3\left(\ln\sigma_p\right)^2 + \frac{11}{5}\sqrt{2}\,\ln\sigma_p\right] \qquad\qquad (4\text{-}26)$$

when $d_{g,p}$ is the number median particle diameter related to the number median particle volume through

$$d_{g,p} = \left(\frac{6\, v_{g,p}}{\pi} \right)^{1/3} \tag{4-27}$$

Dividing Eq. (4-26) by Eq. (4-25) yields the desired expression for σ_p

$$\ln \sigma_p = \frac{5}{11\sqrt{2}} \ln \left(\frac{d_{max}}{d_{1/2}} \right) \tag{4-28}$$

Also, from Eqs. (4-25) and (4-27)

$$v_{g,p} = \frac{\pi}{6} d_{g,p}^3 = \frac{\pi}{6} d_{1/2}^3 \exp\left[-9 \left(\ln \sigma_p \right)^2 \right] \tag{4-29}$$

or

$$d_{g,p} = d_{1/2} \exp\left[-\frac{9}{3} \left(\ln \sigma_p \right)^2 \right] \tag{4-30}$$

5.0   TRANSIENT MODEL RESULTS

In this section, transient simulations are performed using the model equations for the suspended particle size distribution developed in the preceding section. Transient simulations are capable of providing the volume of particles that escape from the container, the volume suspended, the volume on filters, and the volume settled as a function of time while conditions such as the incoming particle volume fraction and back flush operations are allowed to vary with time. Crucial input parameters regarding particle size distribution, particle density, and simulation of operations are discussed first. Case selection and inputs are then summarized. A detailed results example is provided in order to explain the time history of the various particle volumes (suspended, on filters, settled, and escaped). Results are summarized and conclusions are noted. Figures are arranged at the end of the section to improve organization of the material.

5.1   Particle Size Distribution and Particle Density

The particle size distribution used for this work is a log-normal distribution based upon canister sludge data. Figure 5-1 presents data for KW canister sludge, KE canister sludge, and sludge simulant reported in [Schmidt and Zacher, 2007] Table 6. There is a notable difference between the KW and KE sample cumulative volumes at a 1 micron particle size, and the median particle size range is between about 6 and 18 microns. It is desirable to select a particle size distribution for container filling simulation that falls inside the available data.

The cumulative distribution function for a log-normal particle size distribution up to a given diameter d is given by

$$F(d) = \frac{1}{2}\left\{1 + \text{erf}\left[\frac{\ln\left(d/d_{g,p}\right)}{\sqrt{2}\ln(\sigma)} - \frac{3\ln(\sigma)}{\sqrt{2}}\right]\right\} \qquad (5\text{-}1)$$

where symbols were previously defined in Section 4. As noted previously, the distribution parameters $v_{g,p}$ and σ are found by specifying the median particle diameter and defining that 99.9% of the particles are below a maximum size, here taken as 500 microns.

Figure 5-2 presents a comparison of data in Figure 5-2 with two possible log-normal distributions. The distribution chosen for this work has a median particle size of 10 microns and the corresponding standard deviation parameter value is 3.516. This distribution matches the KE data at the low end, matches the average of the medians for KE and KW samples, and approaches 100% faster than the KE sample.

The average particle density of sludge simulant reported in [Schmidt and Zacher, 2007] Table 5 is 6.0 g/cc. KW canister sludge is higher than this average and KE canister sludge is lower than this average, with a design basis range from 4.6 g/cc to 6.7 g/cc.

While the settler system was operating, we can expect that larger, denser particles fell out near the upstream end, while smaller, less dense particles fell out near the downstream end. The settlers are to be retrieved from the upstream end toward the downstream end, so during simulations of operations variation in the particle density will be considered as described below.

5.2   Simulation of Operations

There are three important aspects of operations that require idealization for simulation: The overall timeline for retrieval operations including supply of inlet water from the settlers and operation of the filters, the time history for incoming particles, and the timing and duration of back flush operations. Assumed operations are described and justified here.

The basic timeline for operations is explained in [Hofferber, 2008], with verbally transmitted clarification as described here. Broadly speaking, an individual settler tube will be cleaned out over approximately a one week period (five working days), and due to personnel logistics the actual retrieval operations will only occur for about four hours per day.

The solids retrieval operation involves the use of high pressure pumping bursts to mobilize settled material followed by a waiting period to reduce the amount of suspended solids. The target suspended solids concentration is 2 weight percent (wt. %). The main part of the retrieval operation is a set of actions known as a "5 x 1 retrieval" in which a short burst of high pressure flow is used for mobilization, followed by a waiting period until the suspended solids are below 2 wt. % for more than 30 seconds, followed by retrieving the hose one foot (duration not specified), and repeating. Successive 5 x 1 retrievals commence at increasing penetration depths until the tube is clear. The peak solids fraction during bursts may be about 10 wt. %.

The timeline just described clearly indicates that for brief periods of time, several seconds to something less than about a minute, there may be a concentration of suspended solids that exceed 2 wt. %, followed by an equal or longer duration in which the suspended solids concentration is below 2 wt. %. The effective duty cycle duration is on the order of minutes, which is very brief compared to the daily operations duration.

A filter back flush operation is initiated on a pre-set pressure drop across the filters, which has been described verbally to correspond to between 1/8" and ¼" filter cake buildup. During a back flush, the four filter assemblies are pulsed one at a time at 5 gpm average back flush flow for three seconds each. Next, one filter assembly is isolated and pulsed at 5 gpm average for 15 seconds, followed by a 2 minute plus 15 second rest period; the pulse duration is about 1 second in duration. This isolation and pulse step is repeated for each filter. The overall duration of a back flush operation is therefore a bit over 10 minutes, but the back flush operation itself consists of a series of very brief flow reversals.

The main justification for simplified operations simulation is the brief nature of unit operations compared to the time scale for a change in the suspended particle concentration. It will be seen from simulation results that the unit operations time scale, which varies over a range between about one second, fifteen seconds, and thirty seconds, is much less than the characteristic time to change the suspended particle concentration, which is on the order of ten minutes to an hour. In particular, during container filling, it will be seen that the suspended particle concentration tends to approach a steady value. A continuous operation simulation leads

to a higher suspended particle concentration on average than a discontinuous operations simulation because greater particle coagulation and settling occurs for a discontinuous process compared to that for a continuous process. For this reason, an idealized operation that "smears out" or homogenizes the rate of particle addition yields slightly conservative results in the sense of maximizing particle escape from the containers, compared to an idealized operation that adds particles in "bursts" over a duty cycle.

The primary assumption to simplify operations simulation, to be proven by simulation, is that daily settler tube operations can be considered independent. This is a reasonable assumption because there are about twenty hours of particle settling time between daily operations.

A secondary assumption is that both the particle addition and back flush "burst" operations can be idealized by more homogeneous operations. This assumption will be tested by comparing homogeneous versus simulated burst operations. It will be shown that homogeneous particle addition is the worst case in terms of allowing escape of material. Back flush operations by their nature occur only periodically, but the individual filter operation can be idealized as a single continuous type of operation. This is consistent with the model formulation in which the particles are assumed to be well-mixed in the container, so that the location of each individual filter is a moot point.

Therefore, two kinds of operations scenarios will be developed here: Uniform addition of particles over a time period within the four hour daily shift, and duty cycle addition of particles during the daily shift in which the particle volume fraction is alternately some non-zero constant value and then zero.

First consider a timeline for simulation of retrieval from a single settler tube. The goal of the simulation is to understand the potential for particle escape from the container to the basin. As discussed in Section 3, the identified mechanism for particle escape is counter-current flow between the container and basin that is induced by a temperature difference. Escape can occur during filter back flushing, or if flow into and out of the container is stopped. Normally, inflow

and filter outflow will only occur during retrieval operations, and these flows would be stopped after a daily shift and reinitiated at the beginning of the next day's operation.

We know in advance that turning off the flow will allow particle escape. Therefore, to minimize the potential for particle escape, it is desirable to operate the filter system for some duration after particle retrieval. In order to fit the simulation into the operations timeline, it is assumed that particles will be retrieved for a duration less than four hours, and that container inflow/outflow will continue for the remainder of the four hour daily shift to allow some particle settling, and finally that daily operation will end with a filter back flush.

Next, consider particle retrieval. The estimated total sludge volume in the all settler tubes is 5.4 m^3 [Schmidt, 2006]. For this work, we consider a hypothetical worst-case tube to contain 0.80 m^3. At 35 vol. % solids [Schmidt, 2006] this yields 0.28 m^3 particles. Sludge is retrieved in five working days corresponding to a retrieval duration of 20 hours or 72,000 s. The average inlet flow to the container is 15 gpm or 9.46 $\times 10^{-4}$ m^3/s. The average flowing particle volume fraction α is related to the total particle volume V_p, inlet flow rate Q, and duration t: $V_p = \alpha\, Q\, t$. The value of α for the homogeneous and duty cycle operations simulations must satisfy this equation, so α is implied by whatever total retrieval duration is chosen. For reference, the average value of α corresponding to 20 hours of particle retrieval duration is 0.411 vol.%. The corresponding mass fraction μ is given by $\mu = (\rho_p/ \rho_f)\alpha$ so it depends upon the density ratio between incoming particles and water. This ratio is 6 for average particles, and therefore the average mass fraction during 30 hours retrieval is 2.5 wt%. While this is slightly larger than the target value of 2 wt. %, it is consistent with the described operation because there will be bursts of higher mass fraction approaching 10%.

As mentioned above, the first retrieval operations for a settler tube are expected to yield relatively higher density particles and the last operations are expected to yield relatively lower density particles. For this work, three different densities will be considered to correspond to daily retrieval on day 1 (highest), day 3 (lower), and day 5 (lowest). It will be seen that substantial settling of particles occurs over a period of hours, so in fact daily operations are essentially completely independent. Thus, variation in particle density to correspond to the

variation during retrieval is equivalent to simply running simulations of a daily operation and examining various densities for sensitivity.

Filter back flush operation can be idealized by periodically changing the container outflow rate for a duration of 60 seconds, which is the approximate total duration of flushing flow during a back flush cycle. The remaining question is the frequency of a back flush cycle. A frequency of 30 minutes is used here based on noting the corresponding filter cake thickness that is developed during test simulations. Because the total particle volume and the retrieval time are selected to provide a somewhat conservative (but not unrealistic) potential for particle escape, the real back flush frequency that could be expected in practice is more likely to lie between one and two hours.

During back flush simulation, particles accumulated on the filters are released back into the container. The particle size distribution of these particles is assumed to be the same as the distribution of suspended particles. This is justified by noting that the suspended particle size distribution quickly attains a steady state.

Given all the considerations above, the two operations simulation timelines that will be used here are as follows:

Uniform Addition Cases:

- Nominal average flow occurs for a duration of 4 hours plus one minute (inflow is 15 gpm, filter outflow is 28 gpm, net suction from the basin is 13 gpm).

- Back flush operation occurs every 30 minutes for a duration of one minute (net filter outflow is 16 gpm, net suction from the basin is 1 gpm). The last minute of container inflow/outflow is a back flush operation.

- Particles are added at a uniform volume fraction over a duration of 3.5 hours. The volume fraction to add the assumed 0.28 m³ particles over five daily shifts is 0.47 vol. %.

Duty Cycle Cases:

- Nominal average flow occurs for a duration of 4 hours plus one minute (inflow is 15 gpm, filter outflow is 28 gpm, net suction from the basin is 13 gpm).

- Back flush operation occurs every 30 minutes for a duration of one minute (net filter outflow is 16 gpm, net suction from the basin is 1 gpm). The last minute of container inflow/outflow is a back flush operation.

- Particles are added at a uniform volume fraction over a duration of 20 minutes, followed by zero particle addition for 40 minutes. This duty cycle is repeated four times, so particle addition ends at 3 hours 20 minutes. The volume fraction of particles when they are added is 1.23 vol. %.

Note that the duration for particle settling after addition and before flow shutoff is about the same for the uniform and duty cycle case timelines. The 20/40 on/off cycle for particles was chosen so that bursts of greater than 2 wt. % would be used. It is understood that particles would not be added above 2 wt. % for 20 minutes. However, this does at least allow simulation of the real fact that particles would for some period of time be added at greater than 2 wt. %. The real issue is the frequency of the duty cycle: 20/40 versus 2/4 for example. A duty cycle of 2 minutes of particles followed by 4 minutes of water, repeated 10 times an hour, would produce results that are virtually indistinguishable from the uniform addition cases. So, the logic in choosing a duty cycle duration is to purposely provide a time-dependent boundary condition that differs from the uniform addition case and yet allows particle bursts at greater than 2 wt. %.

The incoming water temperature will be a flow-rate-weighted average of the water temperature used in the high pressure lance and the basin water temperature. Considering an even flow split, it does not seem credible to use a water temperature more than 4 °C above the basin value. The effect of pump power is negligible. In the next section, specific cases are listed that allow for variation in incoming particle density and water supply temperature.

5.3   Case Selection and Input Summary

Based upon particle density data presented previously and the expected qualitative nature of density variation within a settler tube, three particle densities are chosen: 6 g/cc, 4 g/cc, and 2 g/cc. It is assumed that the nominal inlet flow to the container will be about 2 °C above the basin temperature, and sensitivity to inlet flow 4 °C above the basin temperature will be evaluated. This results in the set of cases summarized in Table 5-1. An operations variation case, 1D, is included to examine the potential benefit of extending container flow beyond 4 hours, and it is only applied to the lighter-than nominal density baseline case 1B. Note that in each case there is a daily particle volume added of 56 Liters. In all cases a pre-existing retrieved settled sludge volume of 4 m^3 is assumed so that the suspended concentration is higher than it would be if the container were initially empty.

Table 5-1   Settler Sludge Retrieval Case Summary

Case	Operation Type for Particle Addition	Particle Density	Inlet Water Temperature	Figures
1A	Uniform	6 g/cc	2 °C	5-3A,B
1B	Uniform	4 g/cc	2 °C	5-4A,B
1C	Uniform	2 g/cc	2 °C	5-5A,B
2A	Duty Cycle	6 g/cc	2 °C	5-6A,B
2B	Duty Cycle	4 g/cc	2 °C	5-7A,B
2C	Duty Cycle	2 g/cc	2 °C	5-8A,B
3A	Uniform	6 g/cc	4 °C	5-9A,B
3B	Uniform	4 g/cc	4 °C	5-10A,B
3C	Uniform	2 g/cc	4 °C	5-11A,B
1D	Uniform, Extended Container Flow*	4 g/cc	2 °C	5-12A,B
*For all cases except 1D, container water inflow/outflow ends at 4 hours one minute. In case 1D, container water inflow/outflow ends at 6 hours one minute.				

5.4   <u>Detailed Results Discussion</u>

Detailed results are explained here for cases 1B and 2B. In all cases, three or four figures are provided on two pages in Section 5.7, as follows:

<u>Page 1, Top: Time history of particle volume, Liters</u>.

Volumes are shown for suspended (solid line), settled (dotted line), escaped to basin (dashed line), and filter cake (dot-dash line) particles.

In the uniform addition example, Figure 5-4A, the volume of suspended particles gradually increases to a nearly steady level, but exhibits a series of spiky increases every half hour corresponding to back flushing. The filter cake particle volume grows at a constant rate during normal filter operation and suddenly drops to zero during a back flush operation. The end of particle addition at 3.5 hours is followed by a before the final back flush, and the suspended volume gradually decreases thereafter. The volume of settled particles steadily increases and plateaus as the suspended volume diminishes. It is difficult to see the escaped particle volume on the same scale as these other volumes.

In the duty cycle addition example, Figure 5-7A, The suspended particle volume can be seen to initially increase for 20 minutes, then decline briefly for 10 minutes, and suddenly increase somewhat with the first back flush operation, and then decline until 1 hour. At that time a second back flush increases the suspended volume, and the suspended volume continues to increase due to the next duty cycle of particle addition. Otherwise behavior is similar to that of uniform addition.

<u>Page 2, Bottom: Time history of escaped particle volume, Liters</u>

The volume of just escaped particles is shown because it is difficult to observe on the same scale as the other volumes.

In both cases (Figures 5-4A and 5-7A) the escaped volume increases in a series of steps while there is water flow to and from the container. Each step increase corresponds to a back flush operation. The size of the steps varies as the suspended particle concentration increases, and as the temperature of container water increases (discussed below).

After water flow to the container is terminated at four hours in both cases, particles are free to escape the basin because of counter-current flow. The rate of escape declines primarily because the suspended particle concentration declines over a period of several hours, and secondarily because the container water temperature decreases.

The escaped particle volume is affected primarily by suspended particle concentration, which therefore means that it varies strongly with particle density. In general the largest contribution to particle escape is after water shutoff.

Page 2, Top: Time history of suspended particles, Liters.

The volume of suspended particles is shown on a logarithmic scale due to its dynamic range and in particular so that the suspended volume at the end of the simulation can be seen.

The behavior of suspended particle volume was discussed above. This plot is included so that the long-term suspended particle volume after daily operations can be seen. Behavior is similar in both the uniform addition and duty cycle cases (Figures 5-4B and 5-7B).

The key difference between individual cases the effect of particle density. For 6 g/cc particles and uniform addition (Figure 5-3B) the suspended volume declines by a factor of 100 during the first 6 hours after water shutoff, leaving less than 0.2 L suspended. This is less than the escaped particle volume, indicating little longer-term potential for particle escape, and demonstrating that daily operations are essentially independent with regard to the potential for particle escape. For the 4 g/cc variation (Figure 5-4B) there is a similar factor of 100 decline in suspended volume and remaining suspended volume is about about 0.3 L, which is again less than the escaped volume. But for the 2 g/cc variation (Figure 5-5B) there is only about a factor

of 10 decline in suspended volume and the final value of 7 L is comparable to the final escaped volume of 5 L, indicating some remaining potential for particle escape. However, the slope of the suspended volume curve indicates that a value of about 1 L can be expected within 24 hours, so that daily operations can be considered independent even in the extreme case of such light particles.

Page 2, Bottom: Time history of container water temperature, °C.

The temperature difference between container water and basin water is given. Note that the actual value of either temperature is not important, only the difference between values, because it is the difference that drives counter-current flow and particle escape. This figure is only given for the "A" case in each group because the temperature history is the same for all cases with a group defined by the operation type and incoming water temperature.

Because the incoming water temperature is constant and because the duration of water addition is the same in all cases except 1D, the water temperature history is the same for the uniform addition case at 2 °C (Figure 5-3B) and the duty cycle case at 2 °C (Figure 5-6B). A peak value is attained at the end of water addition, about 0.7 °C difference between container and basin. The decline after water addition is primarily due to heat transfer through the container walls, and only secondarily due to counter-current flow. For water addition at 4 °C above the basin value, the peak temperature difference is about 1.25 °C (Figure 5-9B). The reason that the water temperature does not decline all the way to the basin value is due to the decay power transferred from sludge to water in the container.

5.5   Summary of Case Results

Results for particle escape are summarized in Table 5-2. The final escape fraction is estimated by adding 10% of the final suspended volume to the final escaped volume and dividing by the daily added volume of 56 L (The 10% figure is deduced by examining the difference in escape from 10 to 16 hours for case group 1). Conclusions are presented in the next section.

Table 5-2   Particle Escape Results Summary

Case	Final Escaped Volume, Liter	Final Suspended Volume, Liter	Final Escape Fraction	Figures
1A uniform, 6 g/cc, 2 °C	1.2	0.15	2.2%	5-3A,B
1B uniform, 4 g/cc, 2 °C	2.0	0.35	3.6%	5-4A,B
1C uniform, 2 g/cc, 2 °C	4.8	7.0	9.8%	5-5A,B
2A duty, 6 g/cc, 2 °C	1.0	< 0.1	1.8%	5-6A,B
2B duty, 4 g/cc, 2 °C	1.8	0.2	3.3%	5-7A,B
2C duty, 2 g/cc, 2 °C	4.8	5.5	9.6%	5-8A,B
3A uniform, 6 g/cc, 4 °C	1.7	0.15	3.1%	5-9A,B
3B uniform, 4 g/cc, 4 °C	2.8	0.35	5.1%	5-10A,B
3C uniform, 2 g/cc, 4 °C	6.2	7.5	12.4%	5-11A,B
1D uniform, 4 g/cc, 2 °C*	1.15	0.3	2.1%	5-12A,B
*For all cases except 1D, container water inflow/outflow ends at 4 hours one minute. In case 1D, container water inflow/outflow ends at 6 hours one minute. Compare 1D to 1B.				

The results table can be interpreted as follows: If you know the average particle density retrieved in a given daily campaign, the results table provides the escape fraction for that day. Results for 6 g/cc cases should be considered to represent average expected behavior, and results for 4 g/cc cases should be considered to represent a the impact of reasonable variation in expected particle density. Results for 2 g/cc cases represent an extreme case that might arise in practice near the end of retrieval for a given settler tube. The total fraction of escaped particles for a settler tube can be estimated by assuming some fraction of particles at 6 g/cc, some fraction

of particles at 4 g/cc, and some fraction at 2 g/cc, and weighting the results in Table 5-2 by the assumed fractions. For example, using a weighting of 60% at 6 g/cc, 30% at 4 g/cc, and 10% at 2 g/cc for case 1 yields an overall escape fraction of 3.4%.

The impact of filters is estimated by noting the suspended particle concentration for case 1B, which in the steady state is about 25 L in a container volume of about 14,000 L (due to pre-existing sludge) yielding 0.18%. In the absence of filter flow, the rate of outflow to the basin is equal to the rate of inflow from the settler tube. The average incoming particle volume fraction is 0.47%. Therefore the fraction of particles escaping is 0.18/0.47 = 38%.

5.6 Conclusions

Conclusions may be summarized as follows:

(1)   Results for long-term suspended particle volume demonstrate that daily retrieval campaigns are independent of one another with respect to the potential for particle escape.

(2)   Results are not very sensitive to assumed idealizations of operations, and the simple case of uniform particle addition provides a bounding but not unrealistically high estimate for particle escape.

(3)   The most important sludge property that governs the potential for particle escape is particle density. The parameter of second interest to results is the temperature of water entering the container. This depends mostly on the water supply temperature for the high pressure mobilization lance.

(4)   The escape fraction for particles of average expected density (6 g/cc) is between about 1% and 2% depending on the inlet water temperature (Cases 2A and 3A). The escape fraction for particles of less than average expected density (4 g/cc) is between about 2% and 6% (Cases 2B and 3B). The escape fraction for extremely light particles could range from about 8% to 13% (Cases 2C and 3C).

(5)   Extending filter operation for a few hours after the end of daily particle retrieval does have a clear benefit (compare cases 1B and 1D). It is recommended that filters be operated for at least 30 minutes after the last particle retrieval, corresponding to the assumed operation here, because that is when the suspended particle volume is highest and extended operation has a clear benefit.

(6)   The impact of filters is substantial; without them, about 1/3 of added particles would escape.

5.7   Section 5 Figures
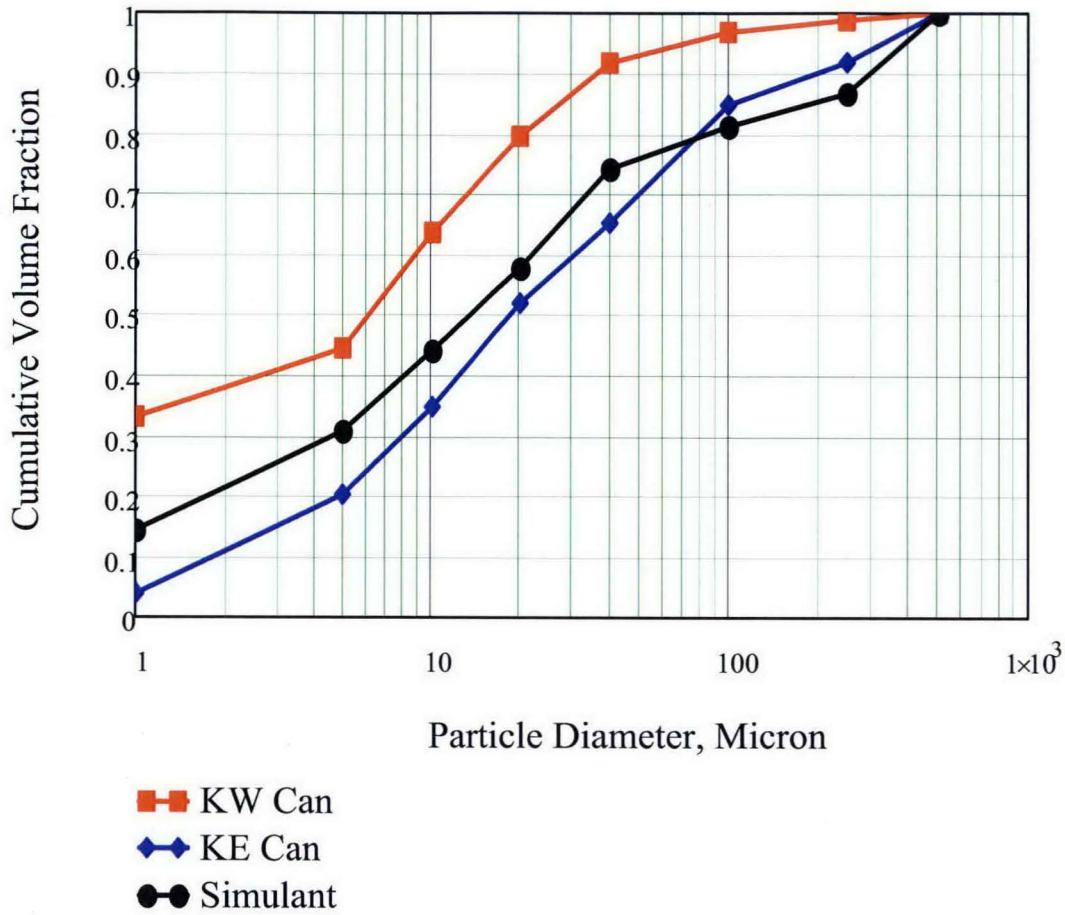
Figure 5-1   PNNL particle size and data [Schmidt and Zacher, 2007].
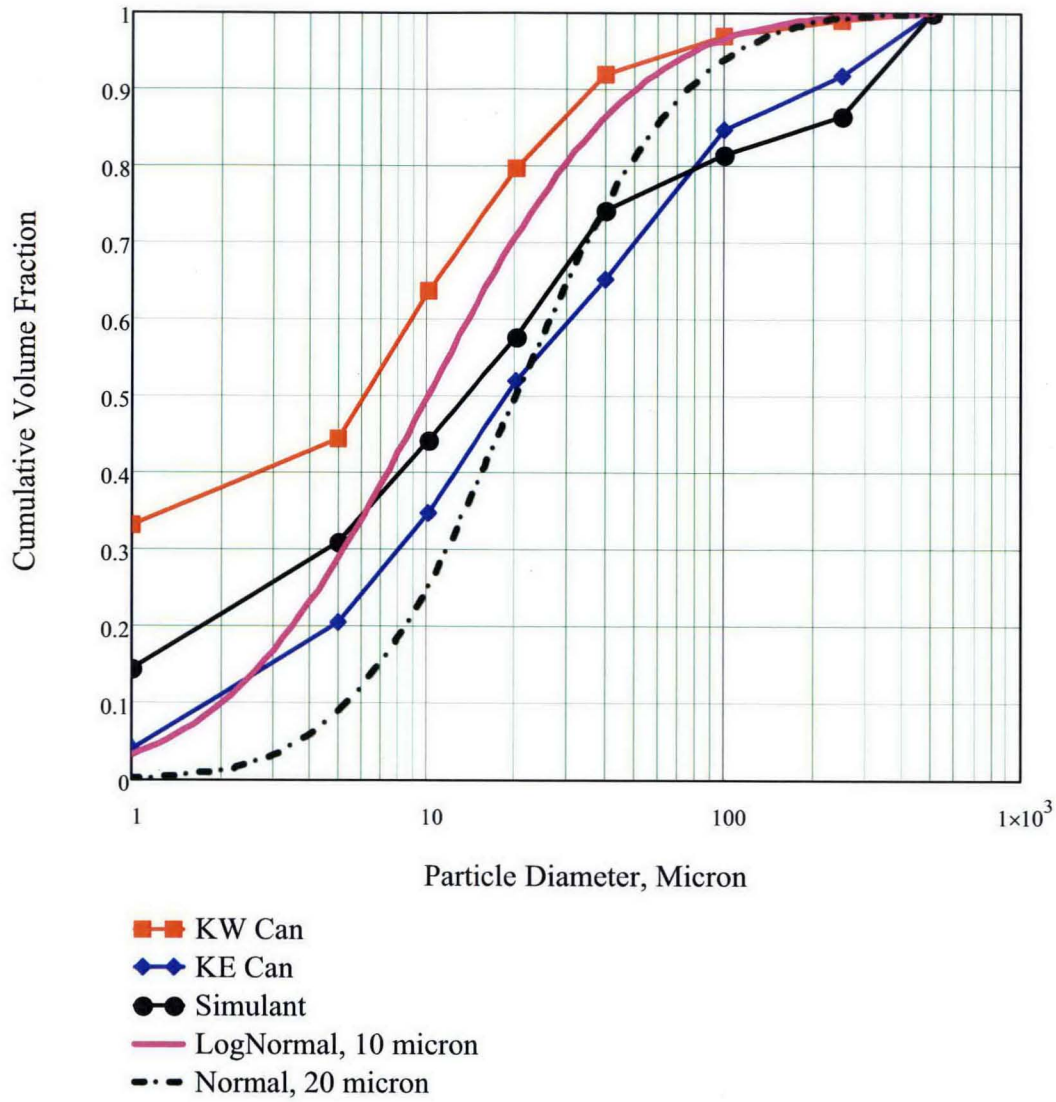
Figure 5-2   Comparison of log-normal distributions and data.
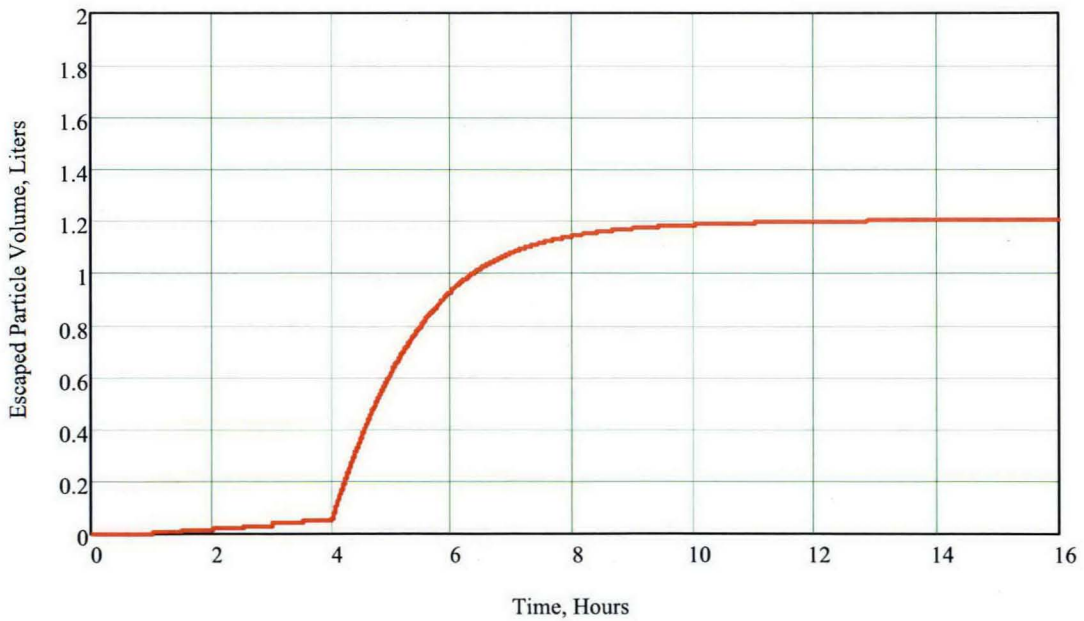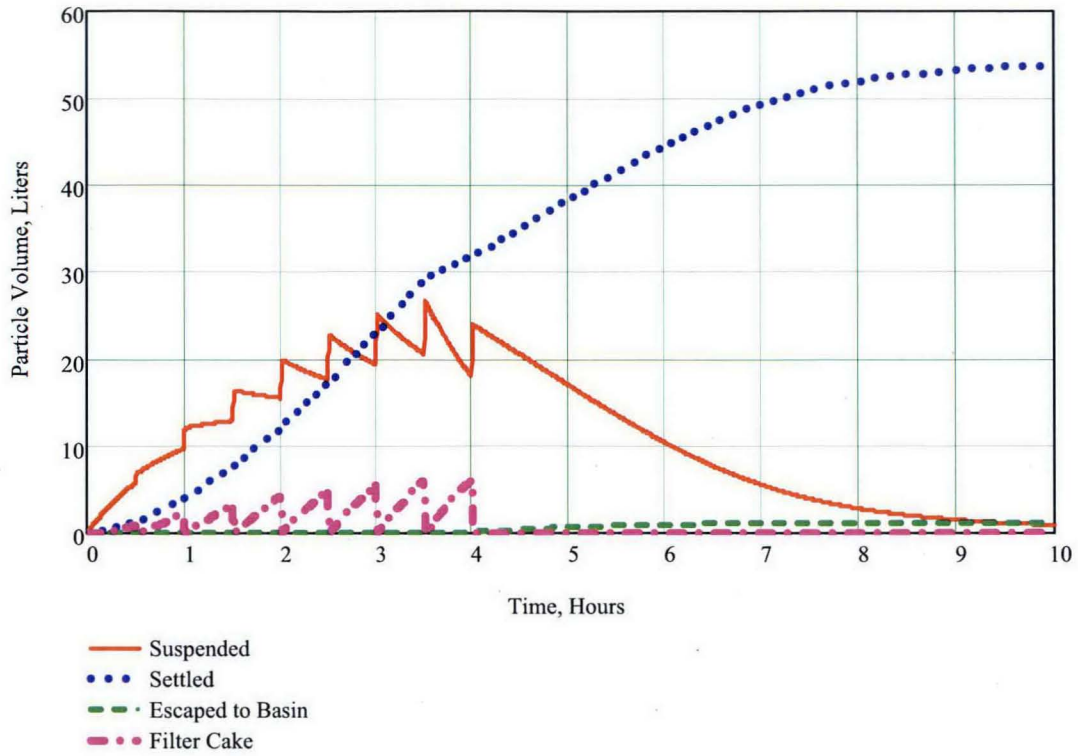
Figure 5-3A   Case 1A results
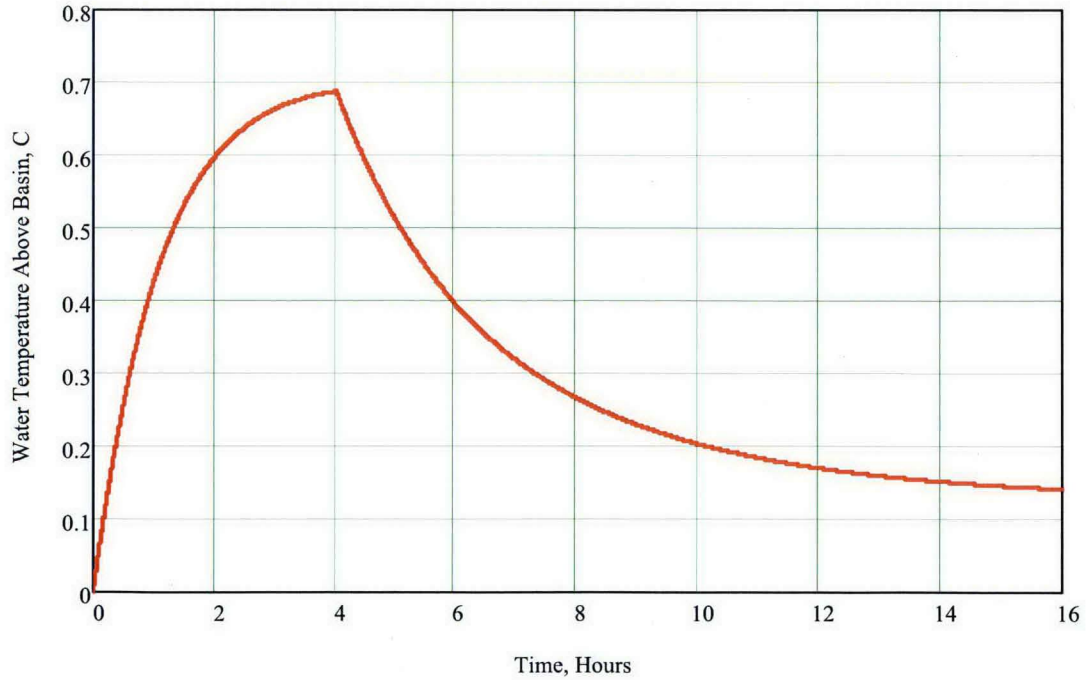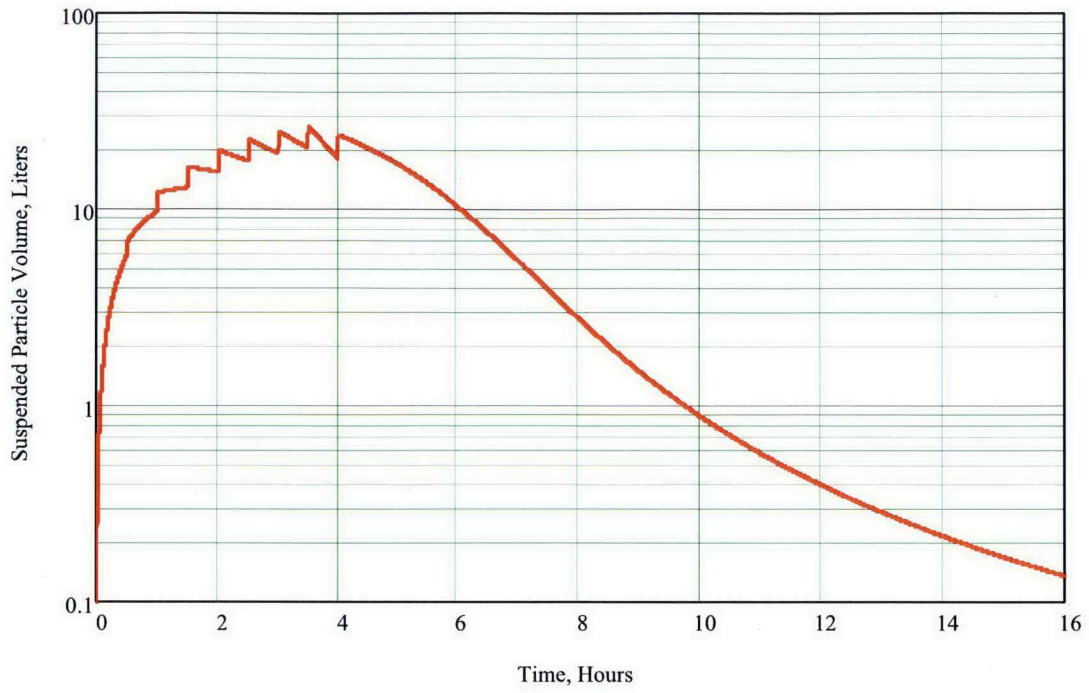
Figure 5-3B   Case 1A results, continued.
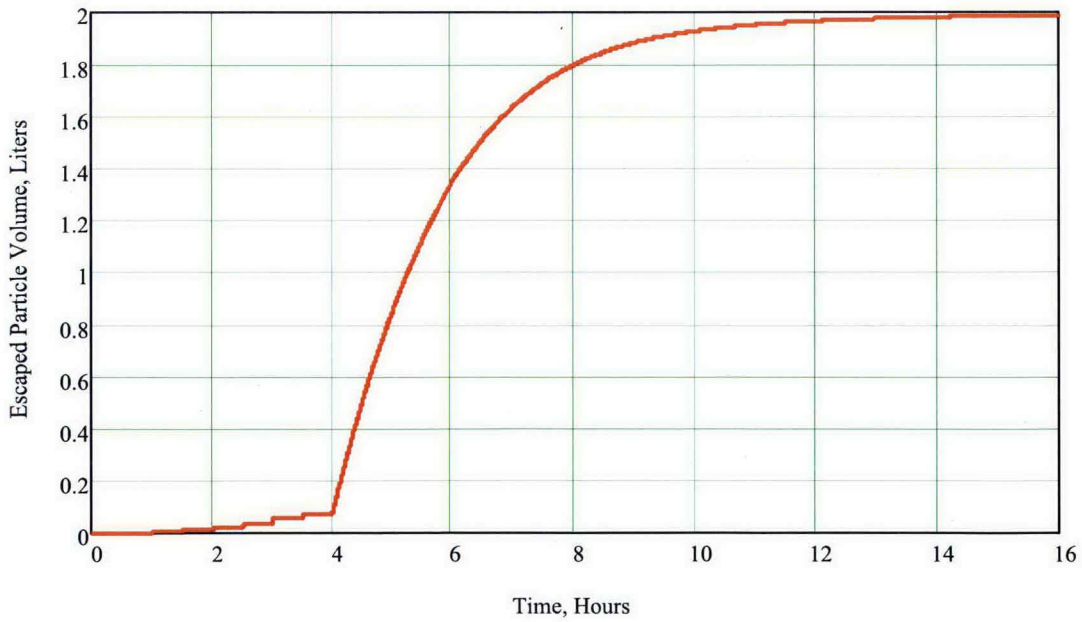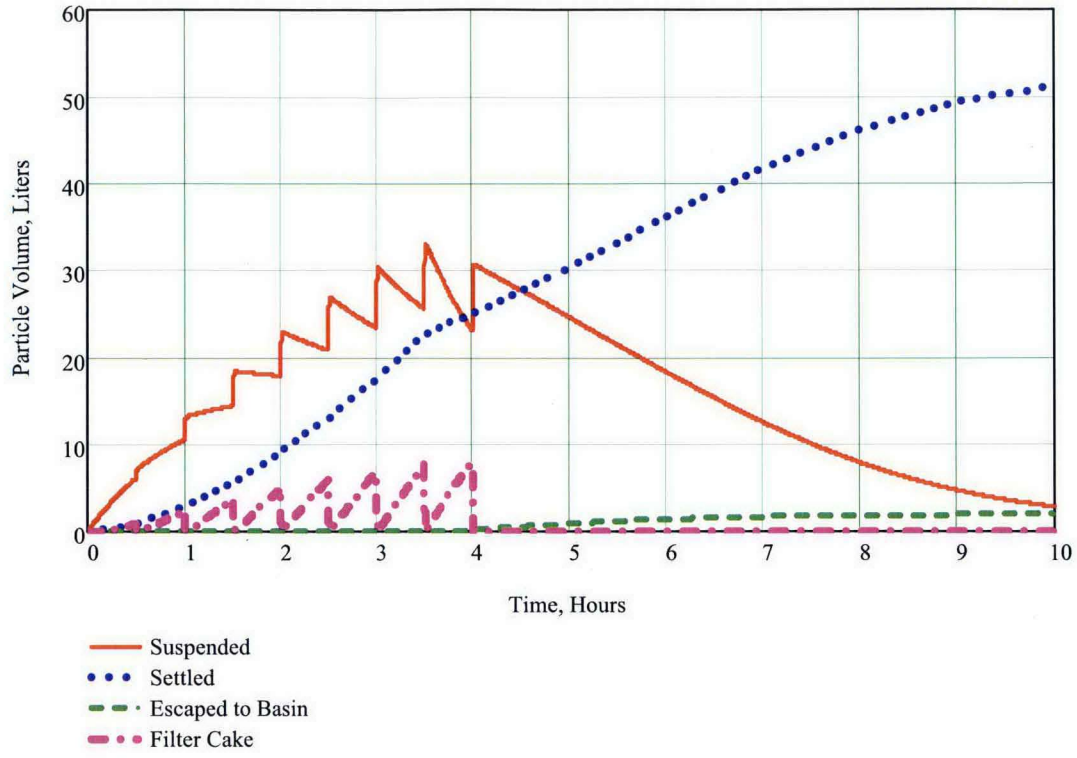
Figure 5-4A   Case 1B results.
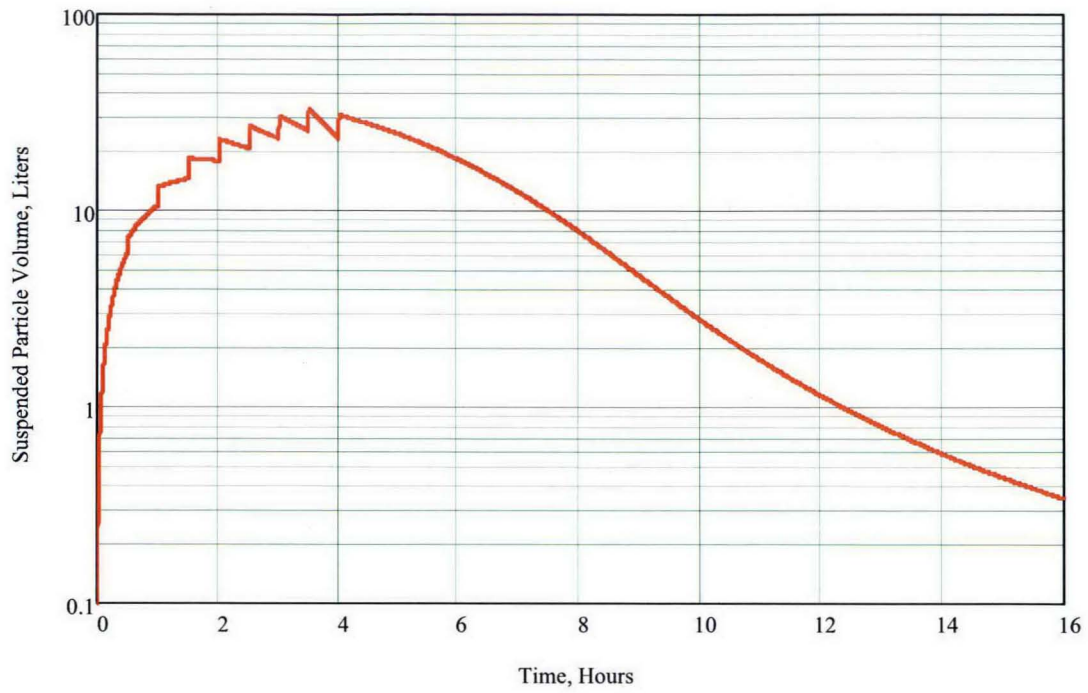
Figure 5-4B   Case 1B results, continued.
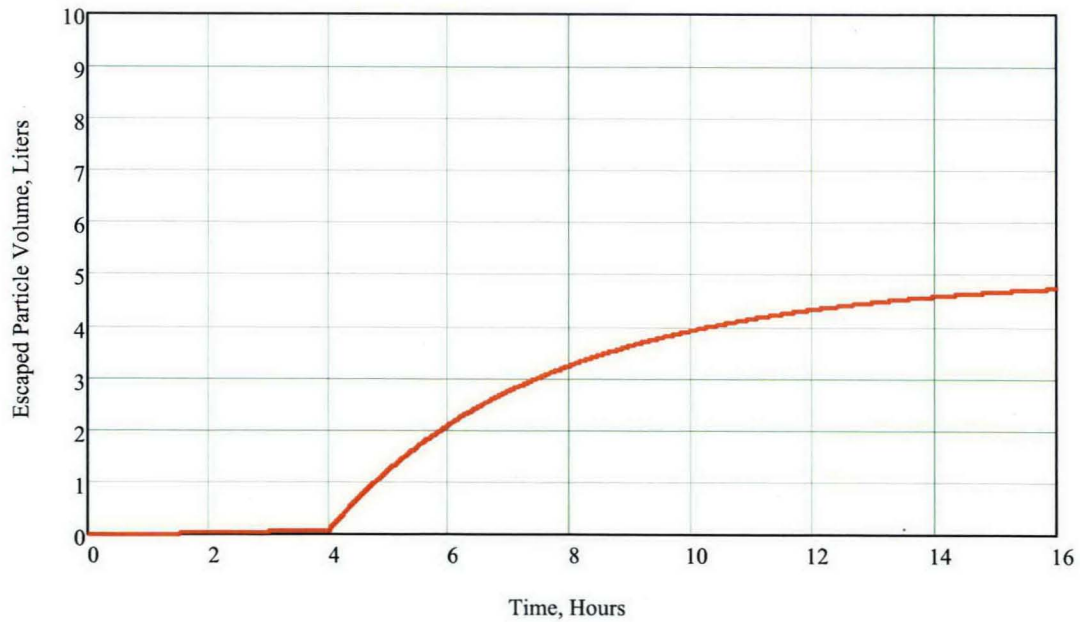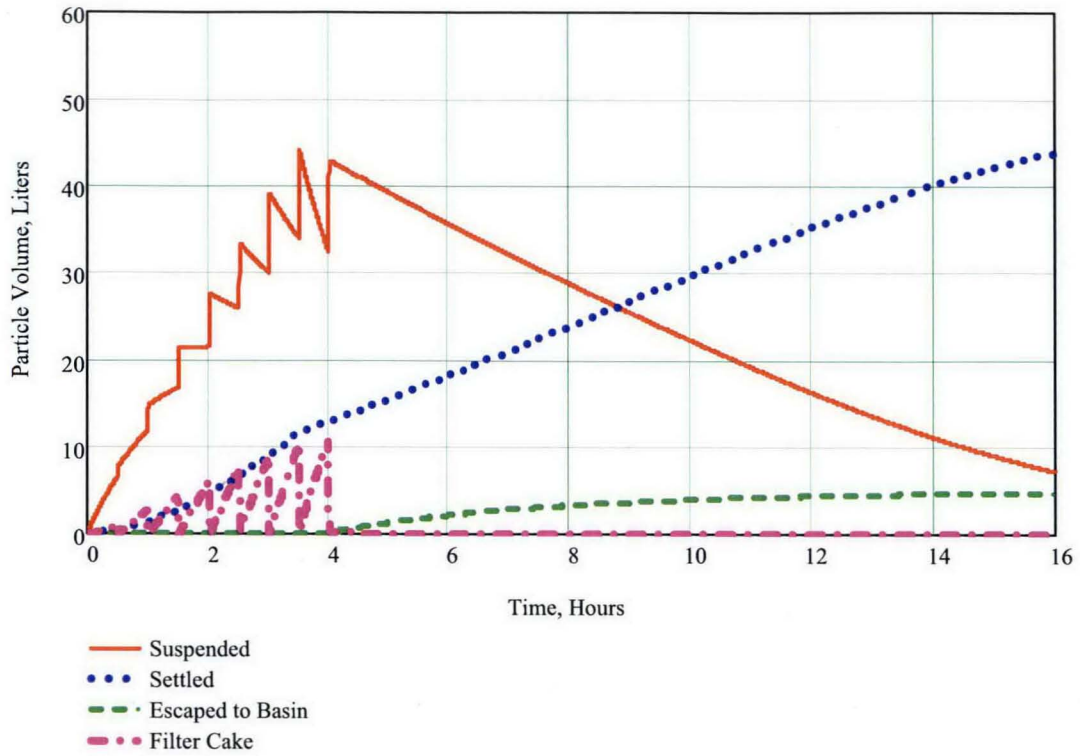
Figure 5-5A   Case 1C results.
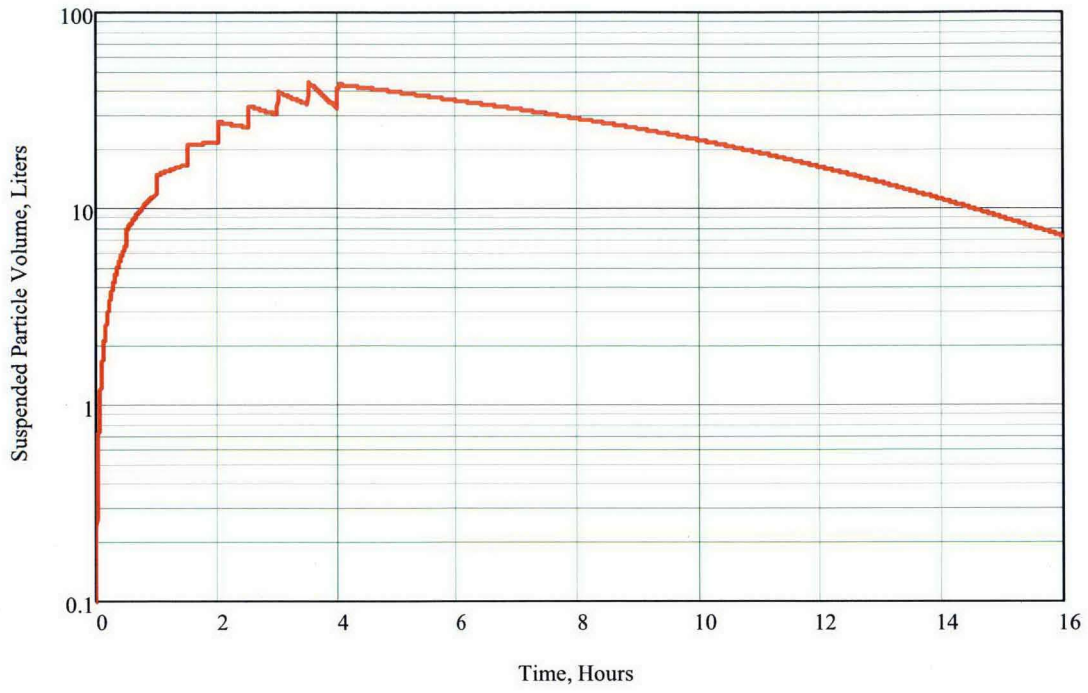
Figure 5-5B   Case 1C results, continued.
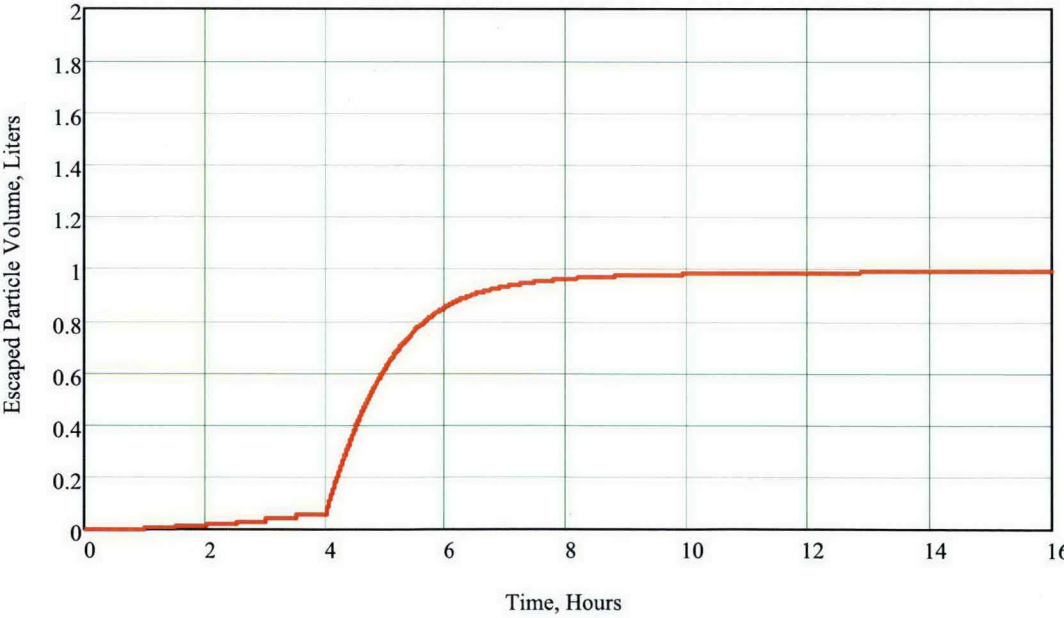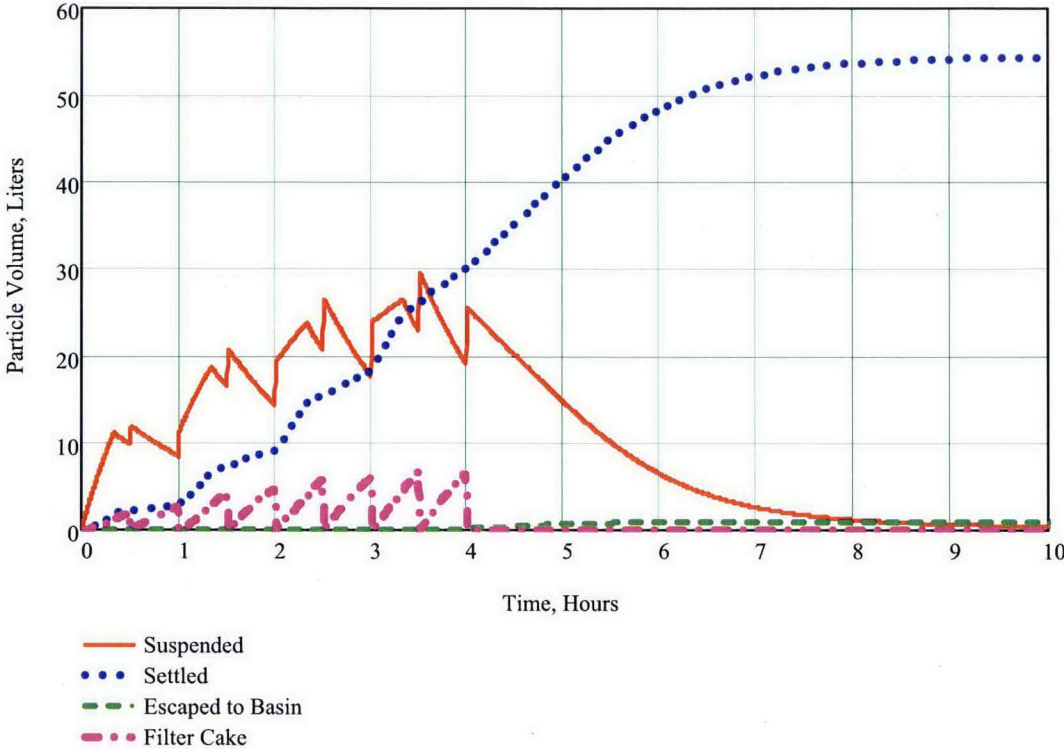
Figure 5-6A   Case 2A results.
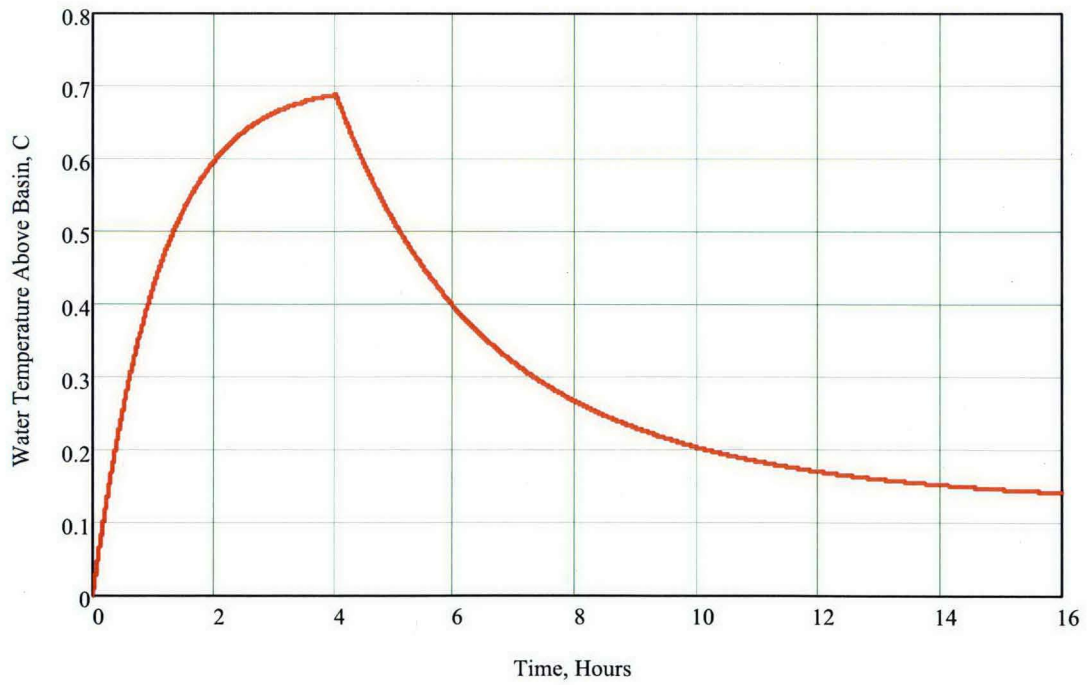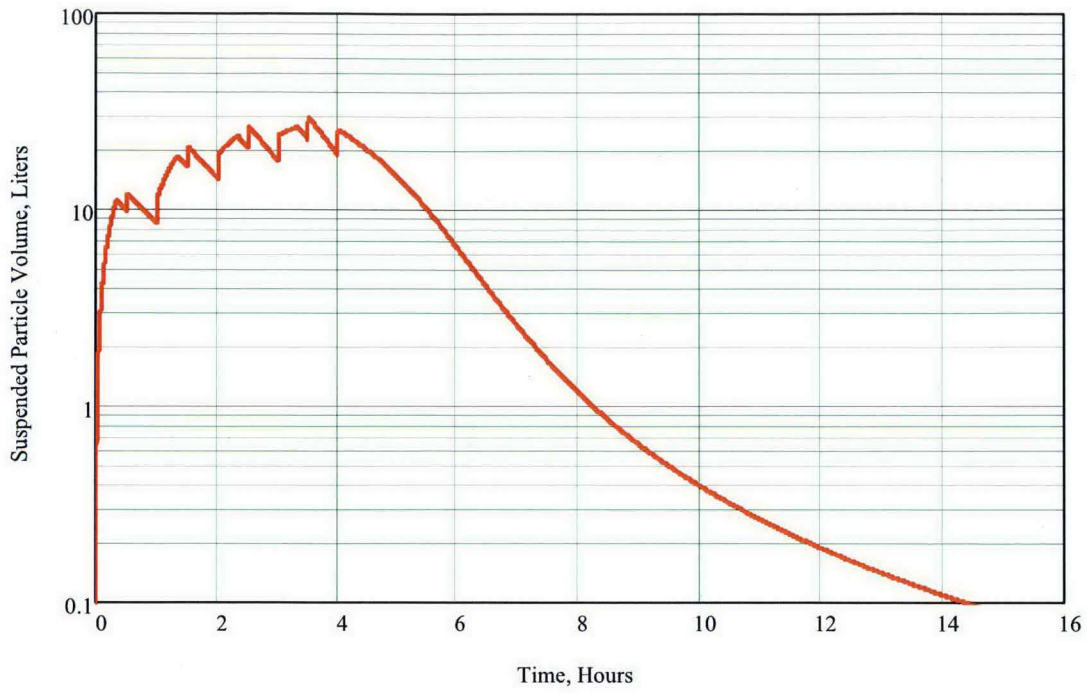
Figure 5-6B   Case 2A results, continued.
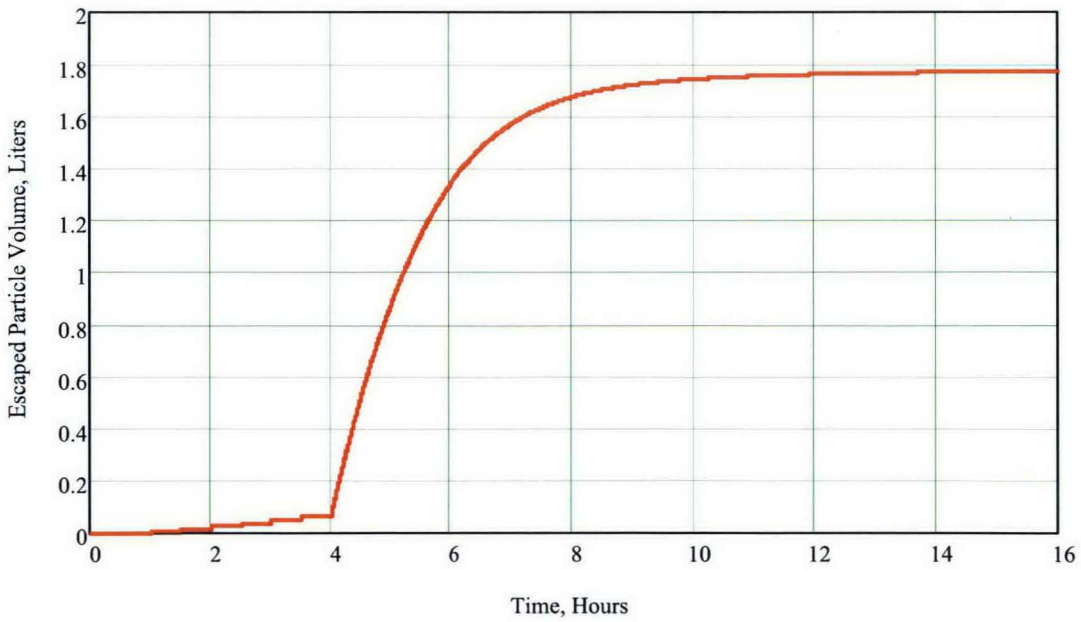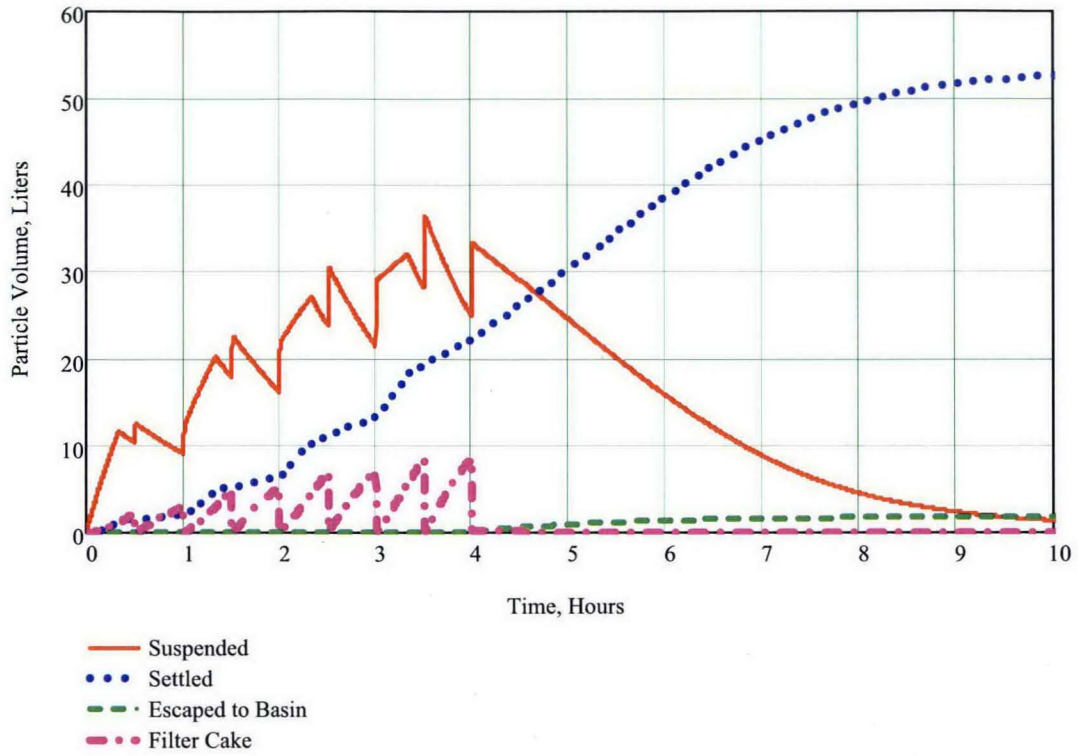
Figure 5-7A   Case 2B results.
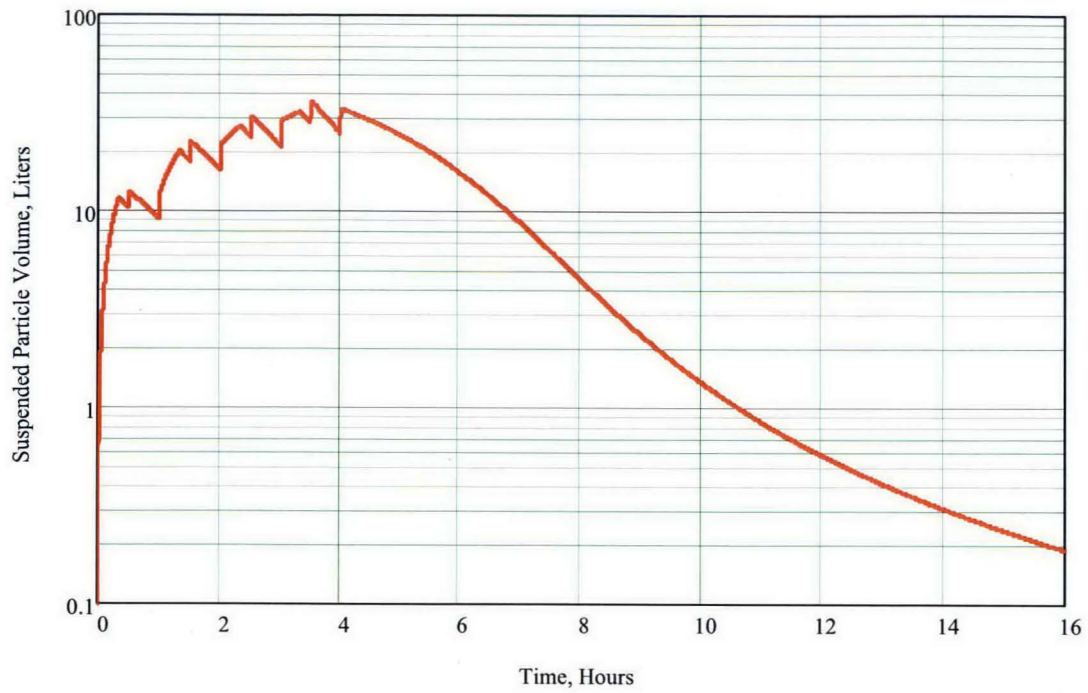
Figure 5-7B   Case 2B results, continued.
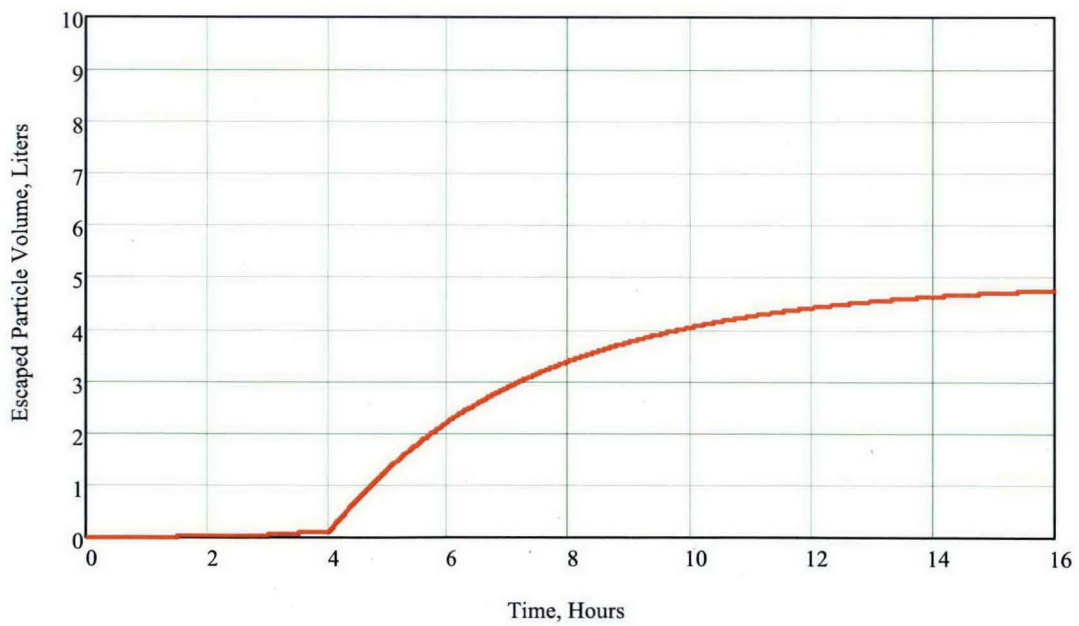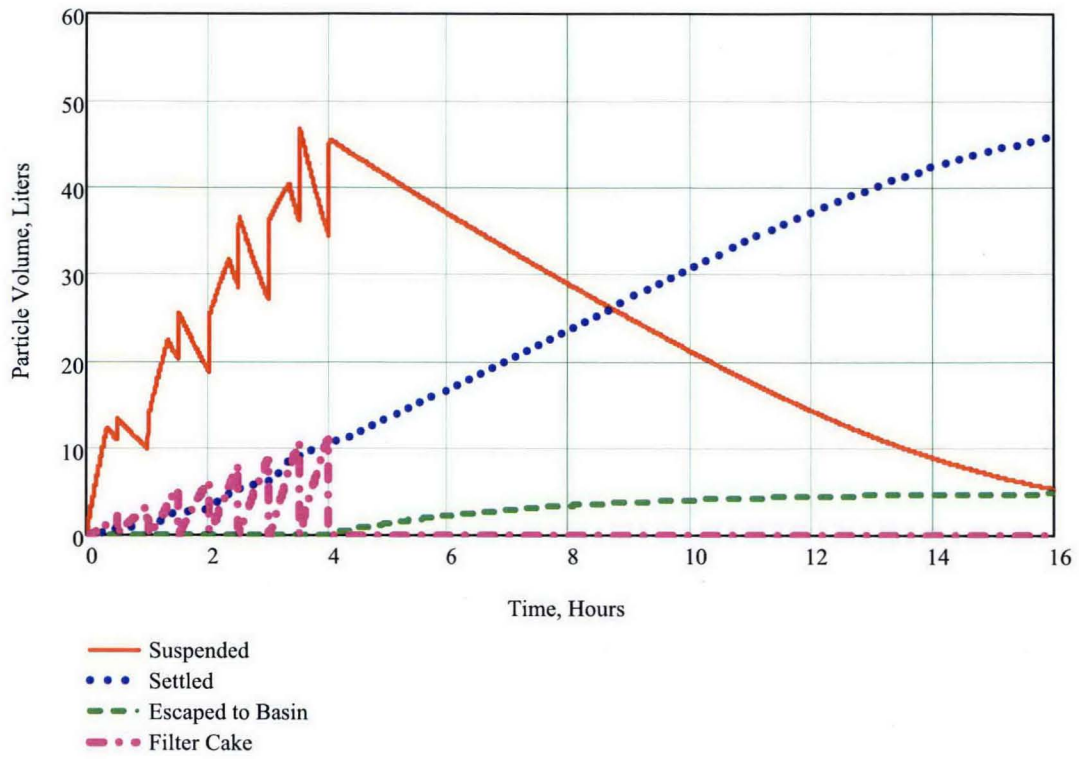
Figure 5-8A   Case 2C results.
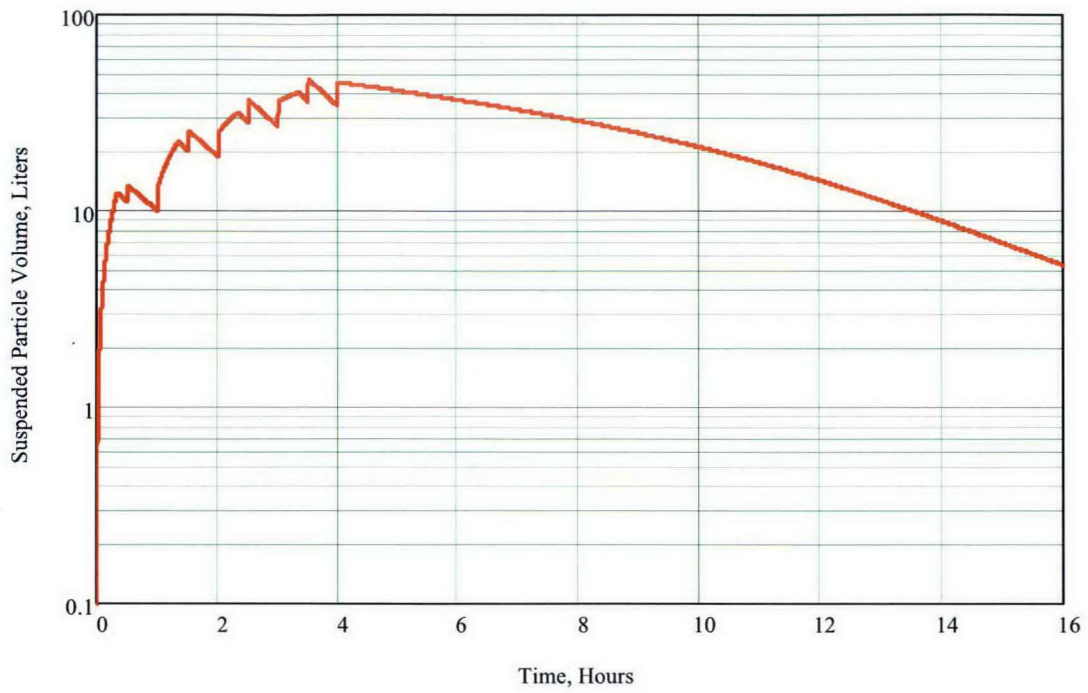
Figure 5-8B   Case 2C results, continued.
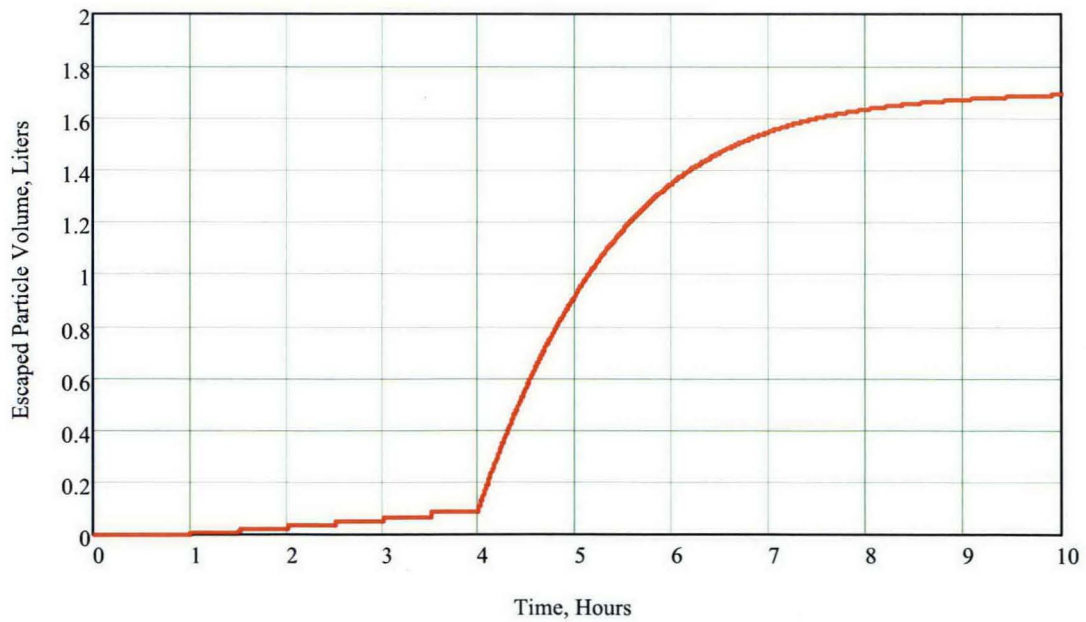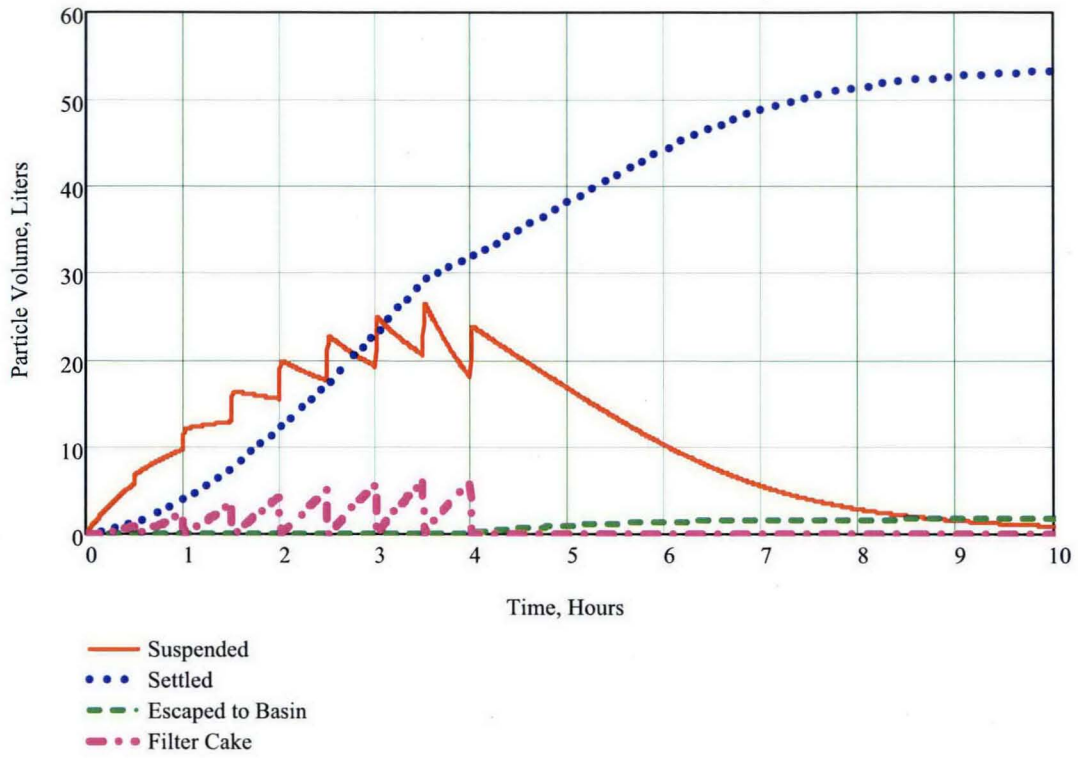
Figure 5-9A   Case 3A results.
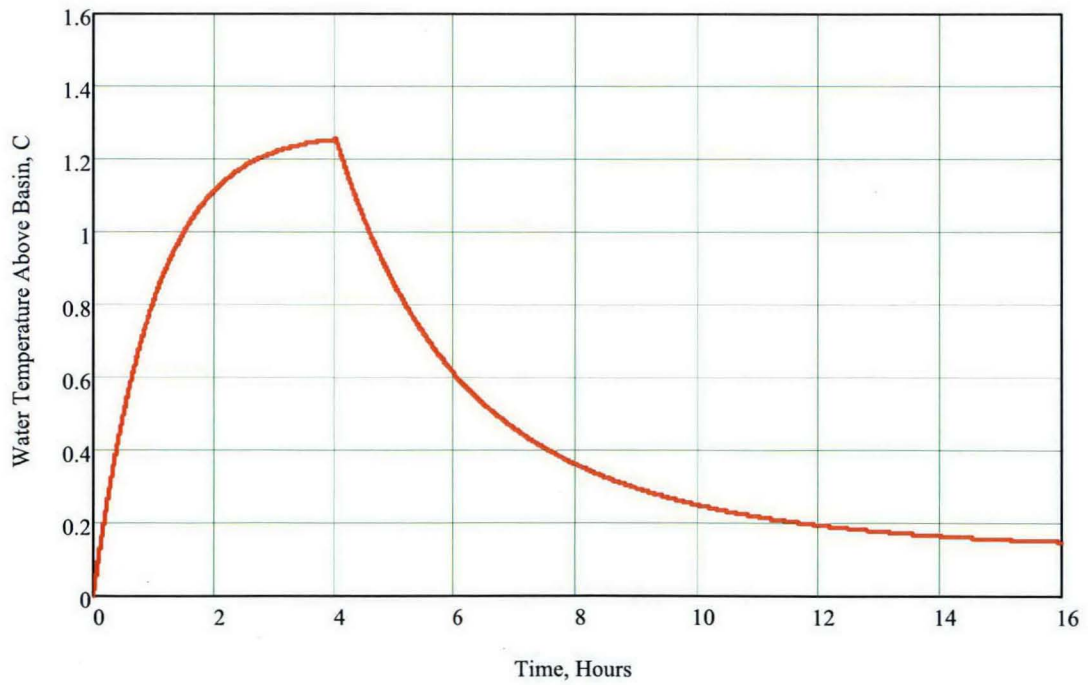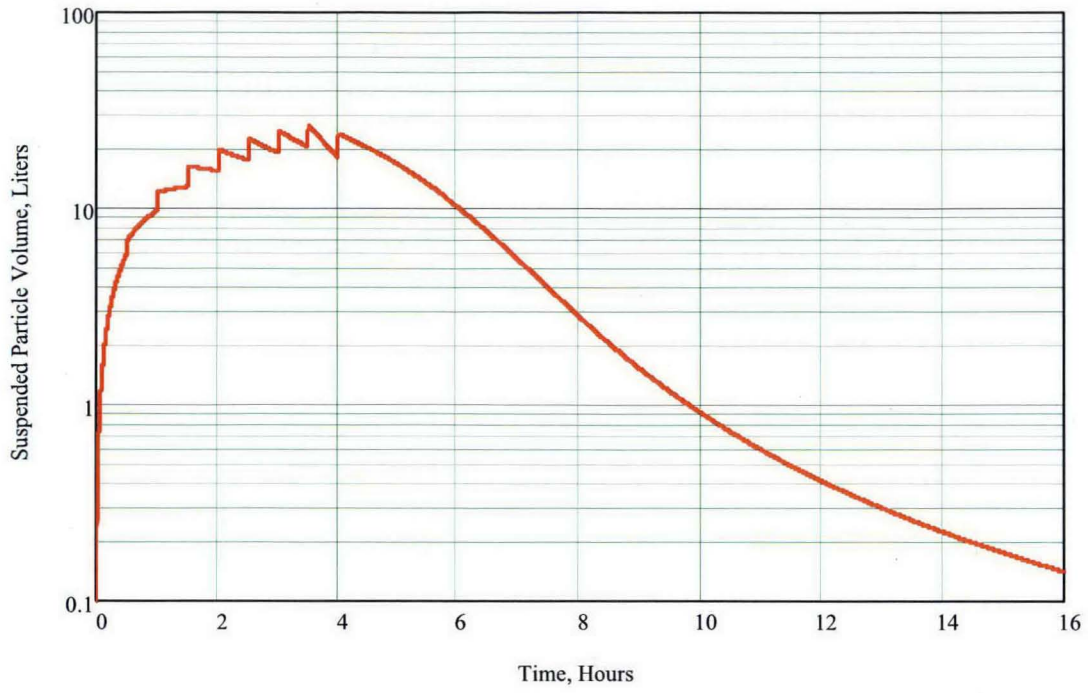
Figure 5-9B   Case 3A results, continued.
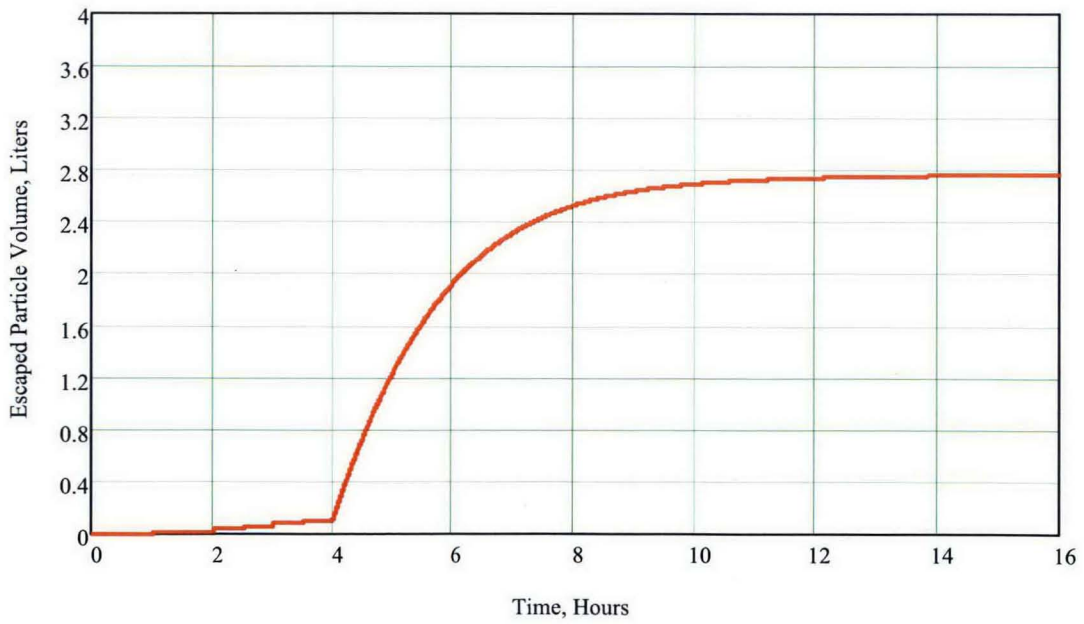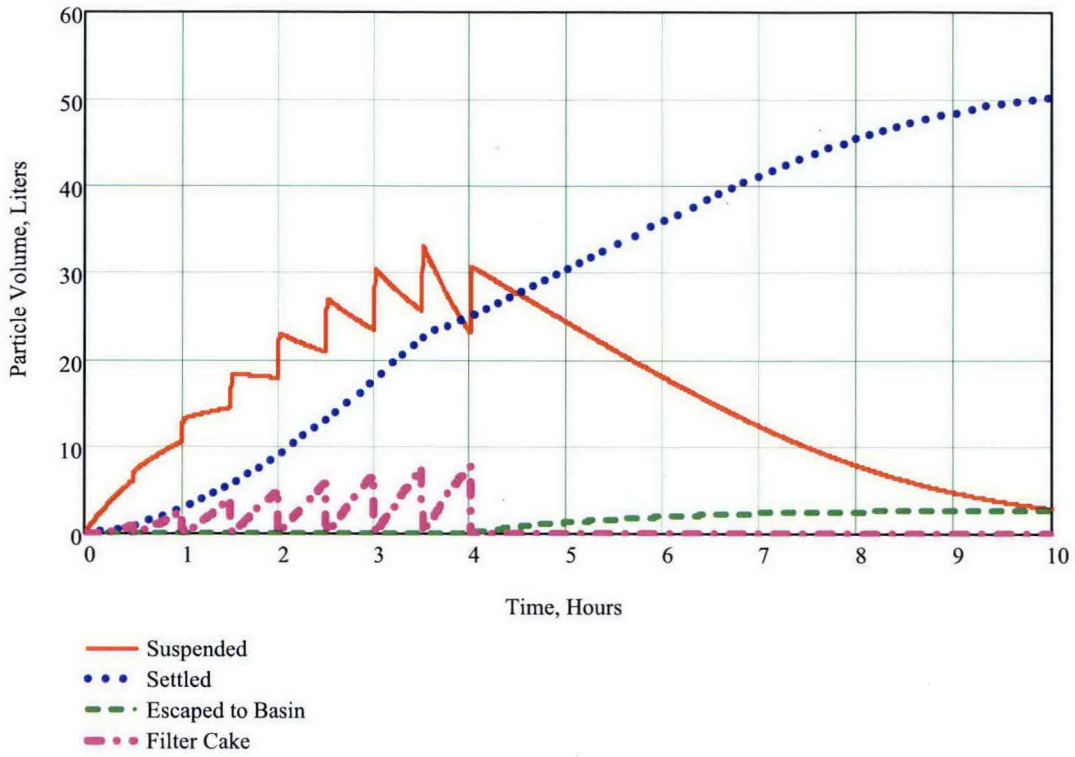
Figure 5-10A   Case 3B results.
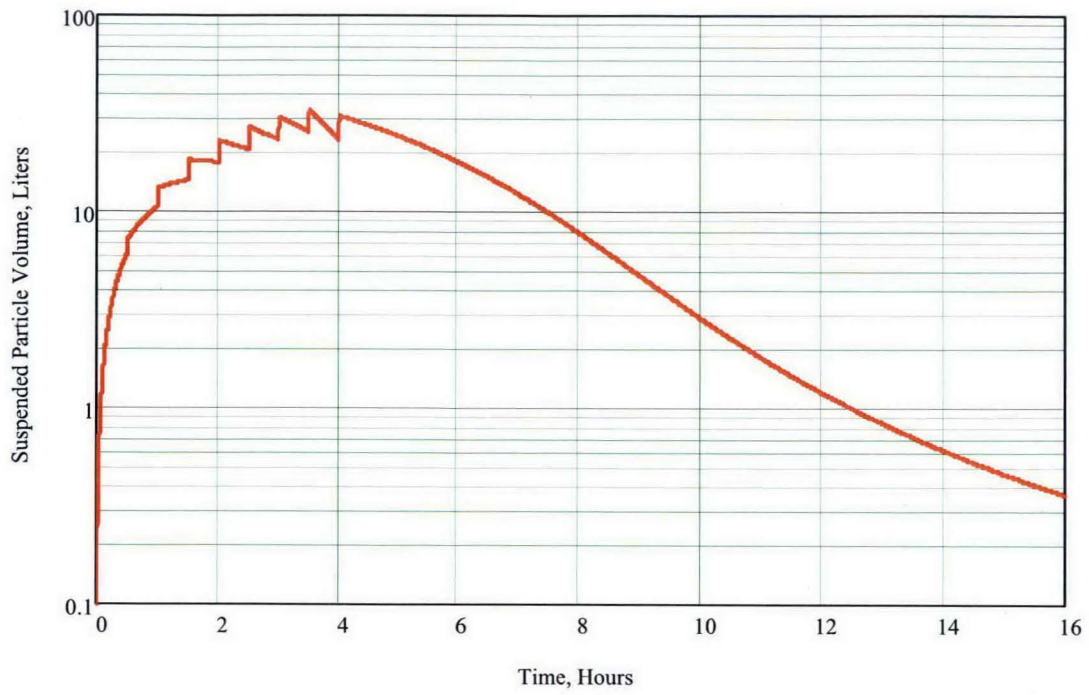
Figure 5-10B   Case 3B results, continued.
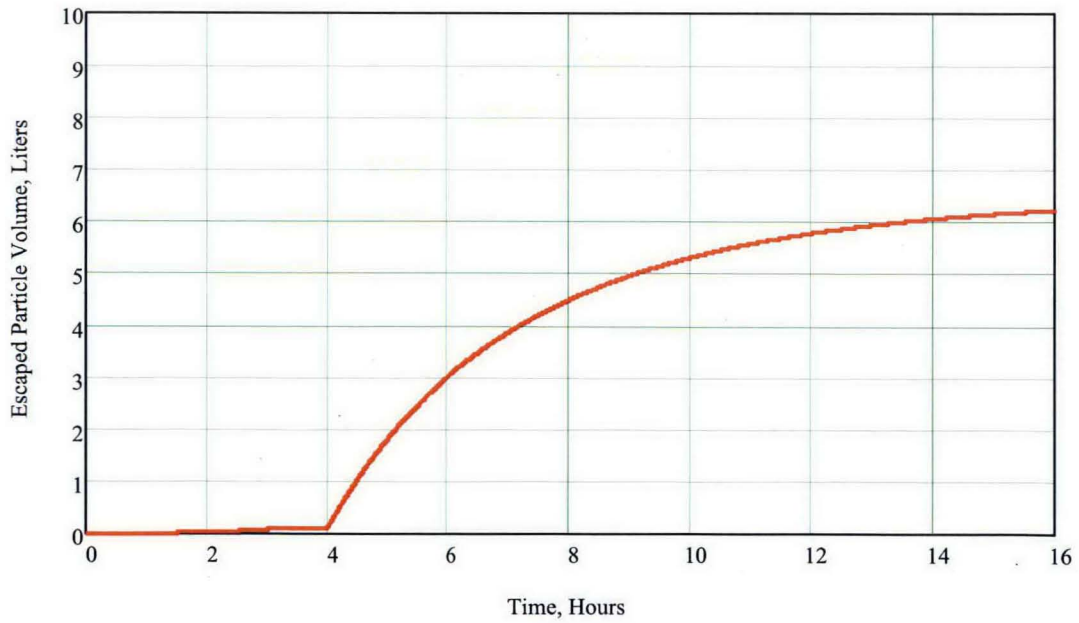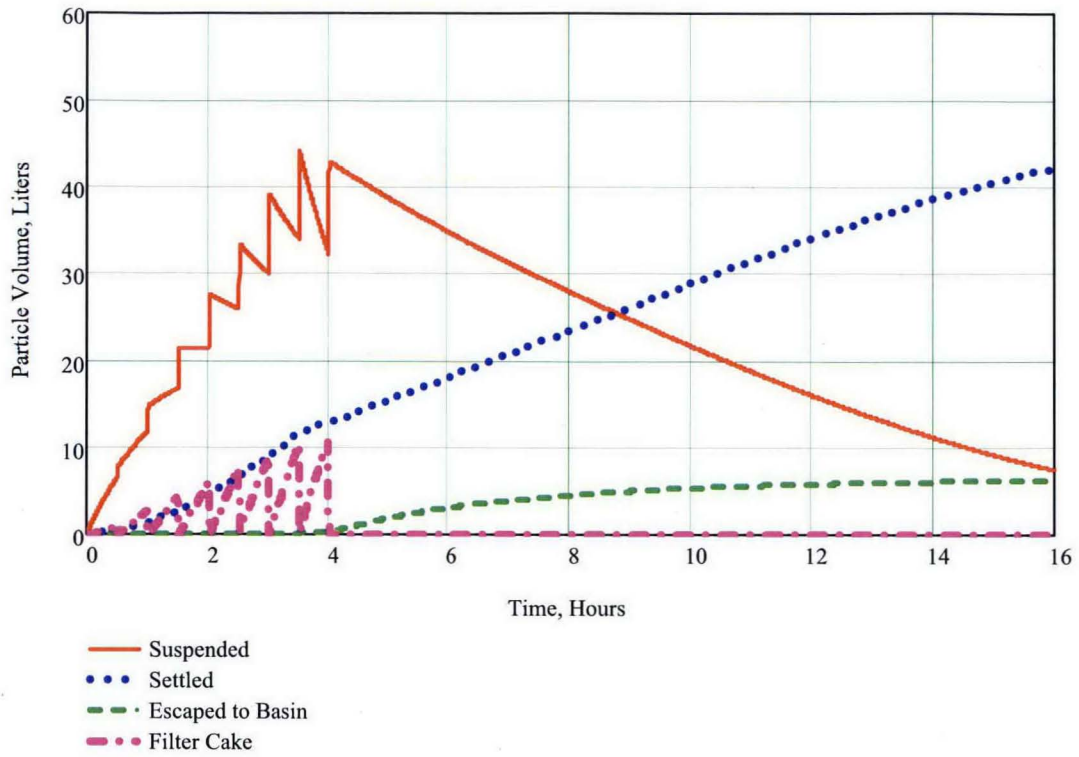
Figure 5-11A Case 3C results.
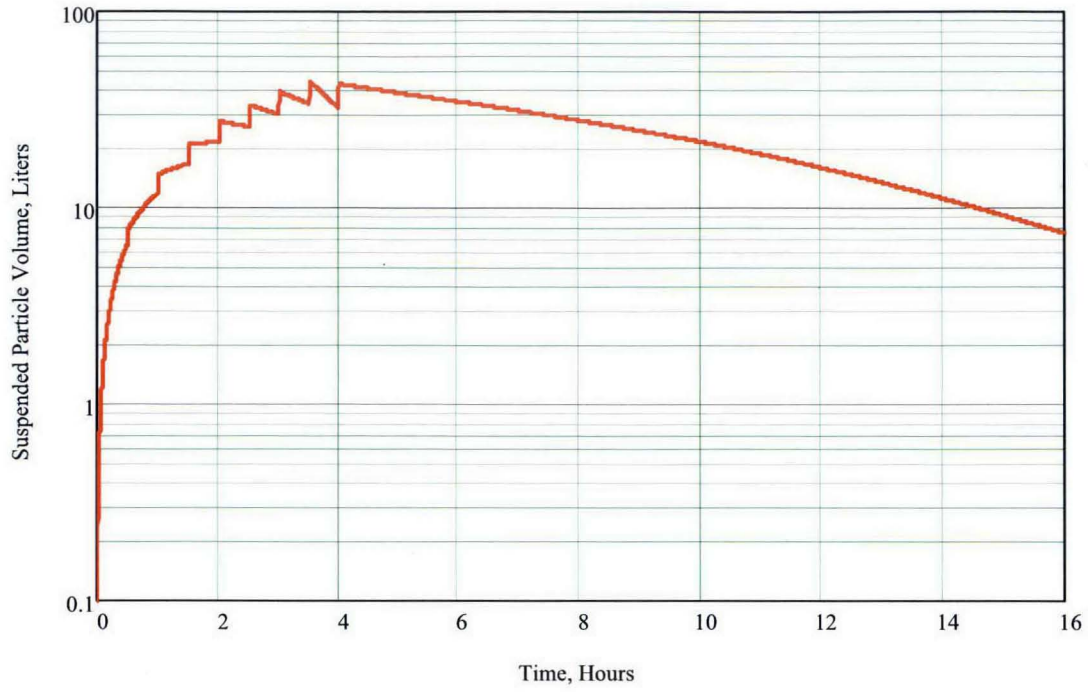
Figure 5-11B   Case 3C results, continued.

Figure 5-12A Case 1D results.
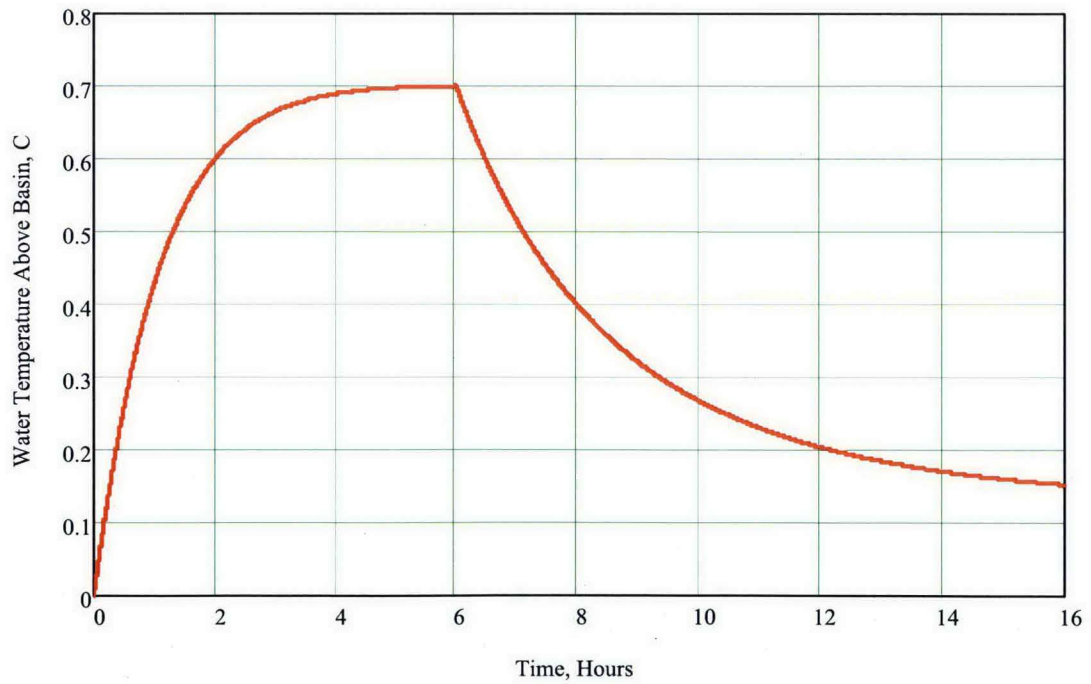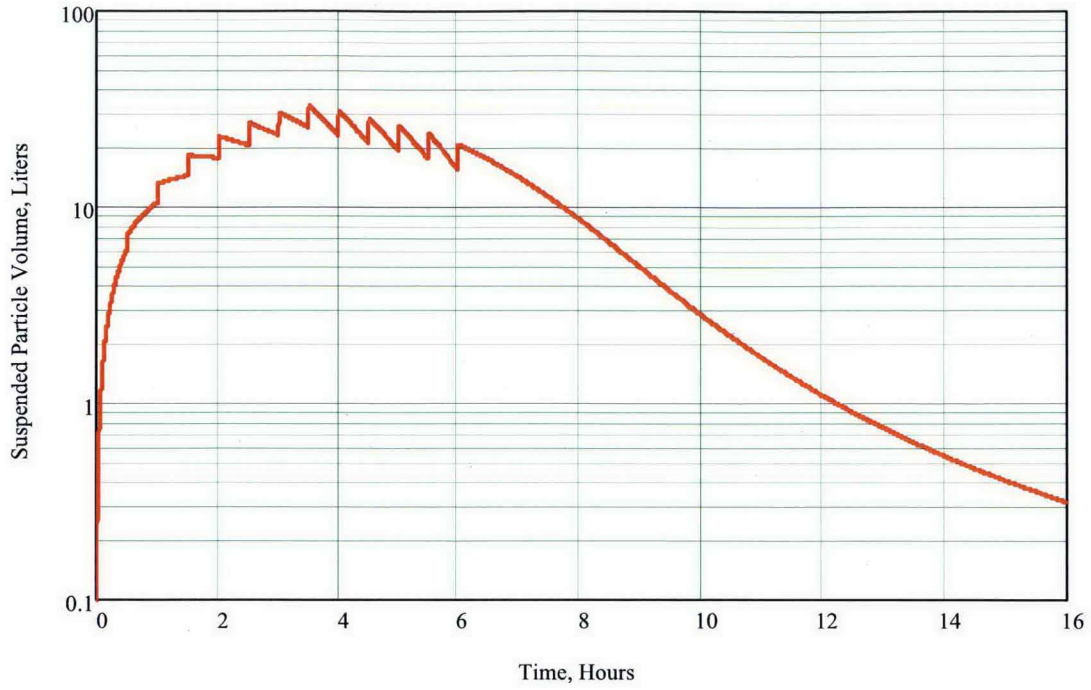
Figure 5-12B Case 1D results, continued.

5.8 Simulation Model Implementation Notes

The preceding results were obtained by rendering equations of Sections 3 and 4 in a Mathcad™ Version 11 spreadsheet. Some model implementation notes are given here in order to clarify which equations are solved and what assumptions pertain.

The model integrates equations for 8 state variables during the simulation duration:

X_0 Zeroth moment of the distribution, per Eq. (4-20),

X_1 First moment of the distribution, per Eq. (4-21),

X_0 Second moment of the distribution, per Eq. (4-22),

T_{wc} Container water temperature, per Eq. (3-28),

V_{sed} Settled (sedimented) solids volume,

V_{fil} Filter deposited solids volume,

V_{esc} Escaped (to basin) solids volume, and

V_{sor} Total source solids volume.

The volume derivatives are given by:

$$\frac{dV_{sed}}{dt} = \frac{B}{h_{sed}} X_0 \left(\frac{X_1 X_2}{X_0^2} \right)^{\frac{5}{9}} V \tag{5-2}$$

$$\frac{dV_{fil}}{dt} = \frac{u_{fl}}{h_{fl}} X_1 V - \frac{V_{fil}}{10} \delta_{bf} \tag{5-3}$$

$$\frac{dV_{esc}}{dt} = \frac{u_{out}}{h_{out}} X_1 V \tag{5-4}$$

$$\frac{dV_{sor}}{dt} = \alpha_o Q_o \delta_{sor} \tag{5-5}$$

The equation for settled volume is simply the first term of Eq. (4-21) multiplied by container volume because the units of X_0 are per unit volume. The first term for the filter cake volume accounts for addition. The on/off back flush function parameter δ_{bf} is defined as $\delta_{bf} = 1$ during a back flush and δ_{bf} is $= 0$ otherwise; the second term adds filter cake back to the suspended solids with an arbitrary time constant of 10 seconds. Similarly, the total source volume of solids is controlled by an on/off source function δ_{sor}.

To account for particle addition during a back flush, Eqs. (4-20) through (4-22) are modified to add the following terms, respectively:

$$+ \frac{V_{fil}}{10V} \frac{1}{v_{g,p} \exp\left[\frac{9}{2}(\ln \sigma_p)^2\right]} \delta_{bf} \qquad \text{(add to 4-20)} \qquad (5\text{-}6)$$

$$+ \frac{V_{fil}}{10V} \delta_{bf} \qquad \text{(add to 4-21)} \qquad (5\text{-}7)$$

$$+ \frac{V_{fil}}{10V} v_{g,p} \exp\left[\frac{27}{2}(\ln \sigma_p)^2\right] \delta_{bf} \qquad \text{(add to 4-22)} \qquad (5\text{-}8)$$

The modification to Eq. (4-21), Eq. (5-7), follows directly from Eq. (5-3). The other factors in Eq. (5-6) and (5-8) follow from the relationships between the moments given in Eqs. (4-8) through (4-10):

$$\frac{X_0}{X_1} = \frac{1}{v_{g,p} \exp\left[\frac{9}{2}(\ln \sigma_p)^2\right]} \qquad (5\text{-}9)$$

$$\frac{X_2}{X_1} = \frac{v_{g,p}^2 \exp\left[18(\ln \sigma_p)^2\right]}{v_{g,p} \exp\left[\frac{9}{2}(\ln \sigma_p)^2\right]} = v_{g,p} \exp\left[\frac{27}{2}(\ln \sigma_p)^2\right] \qquad (5\text{-}10)$$

and the same ratios apply for any rate of change terms. The assumption underlying Eqs. (5-6) through (5-8) is that the suspended particle size distribution does not vary too much between

back flush cycles, so that the suspended and filter cake size distributions are effectively the same. Also, the rate of change of water temperature Eq. (3-28) is modified to account for decay power

$$+ Q_v \left(X_1 V + V_{fil} + 0.5 V_{sed} \right) \qquad \text{(add to 3-28)} \qquad \text{(5-11)}$$

where Q_v is the decay power per unit solids volume, the first term represents the contribution from suspended solids, the second term is the contribution from filter cake solids, and the last term contains the underlying, conservative assumption that half the decay power of settled sludge is transferred upward into the container water (the other half is transferred via container walls to the basin).

Values for the state variables must be initialized. The water temperature is initialized to the basin water temperature, and all integrated volumes are set to zero except that an initial value may be assigned to the settled volume to account for pre-existing sludge. Parameters for the particles in the container are initialized as follows:

- A small value of the initial mass M_o is chosen for a case,

- The median size of source particles $d_{1/2}$ is chosen for a case,

- The distribution parameters σ_p and $v_{g,p}$ for source particles are derived from the median size and the maximum size (500 microns) using Eq. (4-28) and then Eq. (4-29),

- The first moment is initialized as $X_0 = M_o/(\rho_p V)$ where ρ_p is particle density, and

- The zeroth and second moments are initialized from the first moment using the ratios in Eq. (5-9) and (5-10) respectively.

During the course of a simulation, the derivative functions as described above are evaluated at every time step. At any given time, the number of back flushing filters, the water source rate, and the particle source rate are found from case-specific specifications. These are used to find the total net suction rate and the upstream and downstream suction rates using Eq. (3-1) or (3-2) with Eqs. (3-15), (3-20), and (3-21). Given the container water temperature (an integrated state variable) the counter-current exchange flow rate with the basin is found from Eq.

(3-27) which uses (3-26) and (3-24). The loss terms of the form $\lambda = u/h$ in Eqs. (4-20) through (4-22) are given by Q/V where Q is the appropriate volume flow rate (filter or counter-current exchange). The source term in Eq. (4-21) is replaced by $\alpha_o Q_o \delta_{sor} / V$, and the ratios in Eq. (5-9) and (5-10) are applied to replace the source terms in Eq. (4-20) and (4-22) respectively.

6.0 REFERENCES

Baines, W. D. and Turner, J. S., 1969, "Turbulent Buoyant Convection from a Source in a Confined Region," J. Fluid Mech. 37, pp. 51-80.

Carey, S. N., Sigurdsson, H. and Sparks, R. S. J., 1988, "Experimental Studies of Particle-Laden Plumes," J. Geophys. Res. 93, pp. 314-322.

Churchill, S. W., 1988, Viscous Flows, Butterworths, Stoneham, MA, p. 337.

Cohen, R. E. and Vaughan, E. U., 1974, "Approximate Solution of the Equations for Aerosol Agglomeration," J. Colloid Interface Science 35, pp. 612-623.

Epstein, M. and Kenton, M. A., 1989, "Combined Natural Convection and Forced Flow Through Small Openings in a Horizontal Partition, With Special Reference to Flows in Multicompartment Enclosures," J. Heat Transfer 111, pp. 980-987.

Epstein, M. and Fauske, H. K., 2001, "Mass of Flammable Material Produced by Continuous Fuel-Gas and Volatile Liquid Fuel Releases," Combustion Science and Technology 171, pp. 89-118.

Halow, J. S., 1973, "Incipient Rolling, Sliding and Suspension of Particles in Horizontal and Inclined Turbulent Flow," Chem. Engng. Sci. 28, pp. 1-12.

Hofferber, G.A., 2008, Test Report for IWTS Settler Tank Retrieval Equipment Development Test, KBC-37619 Rev. 0, May.

Kumagai, M., 1984, "Turbulent Buoyant Convection from a Source in a Confined Two-Layer Region," J. Fluid Mech. 147, pp. 105-131.

Martin, H., 1977, "Heat and Mass Transfer Between Impinging Gas Jets and Solid Surfaces," Advances in Heat Transfer 13, pp. 1-59.

Morton, B. P., Taylor, G. I. and Turner, J. S., 1956, "Turbulent Gravitational Convection from Maintained and Instantaneous Sources," Proc. Royal Society, Series A 234, pp. 1-23.

Rajaratnam, N., 1976, Turbulent Jets, Elsevier, New York.

Saffman, P. G., 1965, "The Lift Force on a Small Sphere in a Slow Shear Flow," J. Fluid Mech. 22, pp. 385-400.

Schlichting, H., 1960, Boundary Layer Theory, McGraw-Hill, New York.

Schmidt, A. J., 2006, Spent Nuclear Fuel Project Technical Databook, Vol. 2, Sludge, HNF-SD-SNF-TI-015, Revision 13A, Fluor Hanford, Richland, WA, June.

Schmidt, A.J., and Zacher, A.H., 2007, Composition and Technical Basis for K Basin Settler Sludge Simulant for Inspection, Retrieval, and Pump Testing, PNNL-16619, Rev. 1, Pacific Northwest National Laboratory, Richland, WA, June.

Steckler, K. D., Baum, H. R. and Quintiere, J. G., 1984, "Fire Induced Flows Through Room Openings – Flow Coefficients," 20th Symposium (Int.) on Combustion, The Combustion Institute, pp. 1591-1600.

APPENDIX A

Resuspension of Sludge Particles

The settled sludge particle deposit at the bottom of the container is subject to the shear forces exerted by the negatively buoyant sludge plumes that flow to the bottom of the tank and spread out over the particle deposit. Resuspension of previously deposited sludge particles by the sludge plume may begin when the sludge particle layer grows in depth and the surface of the sludge layer is close enough to the sludge distributor ports for the impingement plume flow to dislodge particles from the surface.

The conditions for resuspension are derived by first estimating the mainstream water velocity u_∞ parallel to the sludge surface that is required to remove a particle. A steady turbulent flow of water passes over the sludge particle deposit and a representative adhering sludge particle at the surface is regarded as an isolated sphere that is small enough to be submerged in the laminar sublayer. If the surface of the particle deposit can be regarded as a flat solid surface, immediately adjacent to the surface of the sludge deposit (within the laminar sublayer) the water velocity u as a function of distance y from the surface is (Schlichting, 1960)

$$u = \frac{fu_\infty^2}{2v_f} y \qquad (A-1)$$

where v_f is the kinematic viscosity of the flowing water and f is the friction factor for turbulent flow over a flat plate. Obviously the surface of the sludge particle layer is rough and porous and cannot truly be considered a flat plate for which Eq. (A-1) is valid. Moreover, the concept of the laminar sublayer may have no importance for completely rough surfaces. However, the flow velocity gradient du/dy near a smooth flat plate is more steep than that near a rough surface (Schlichting, 1960). Also the velocity u of the flow in contact with a surface particle is less than that calculated by Eq. (A-1) owing to the "shielding" provided by adjacent particles. It will be seen below that the lift force acting on a particle is proportional to u and du/dy. Therefore Eq. (A-1) results in a conservative (high) estimate of the force available to dislodge a particle from the sludge deposit.

Saffman (1965) derived an expression for the lift force F_L acting on a sphere in a linear velocity field. The numerical coefficient in the force expression was corrected by Halow (1973) to bring it into agreement with experimental data. The equation for the lift force for a sphere initially at rest on a surface is

$$F_L = 8.09 \, d^2 \, (v_f \kappa)^{1/2} \rho_f \, u(d/2) \tag{A-2}$$

Here d is the particle diameter, u(d/2) is the water velocity evaluated at a distance from the surface equal to one-half the spherical particle diameter and κ is the velocity gradient. From Eq. (A-1)

$$u(d/2) = \frac{fu_\infty^2 d}{4 \, v_f} \tag{A-3}$$

$$\kappa = \frac{du}{dy} = \frac{fu_\infty^2}{2 \, v_f} \tag{A-4}$$

Thus Eq. (A-2) becomes

$$F_L = 1.43 \, \frac{f^{3/2} \rho_f u_\infty^3 d^3}{v_f} \tag{A-5}$$

To determine the minimum possible water velocity u_∞ at which a spherical particle is dislodged from the surface of the sludge deposit, the lift force is set equal to the minimum particle adhesion force given by the weight of the particle. Thus it is possible for the particle to be entrained by the water flow when

$$F_L \geq (\rho_s - \rho_f) g \left(\frac{\pi d^3}{6} \right) \tag{A-6}$$

or, from Eq. (A-5), the liquid velocity criterion for particle liftoff is

$$u_\infty \geq u_{\infty,sus} = \frac{0.72}{f^{1/2}} \left[\frac{(\rho_s - \rho_f)g\, v_f}{\rho_f} \right]^{1/3} \tag{A-7}$$

It turns out that the resuspension velocity $u_{\infty,sus}$ is independent of particle size. Consider the typical parameter values for the SCS-CON-230 application, $v_f = 10^{-6}$ m^2 s^{-1}, $\rho_s = 6 \times 10^3$ kg m^{-3}, $\rho_f = 10^3$ kg m^{-3} and $f = 0.02$ for a rough surface. Inserting these numbers into Eq. (A-7) gives

$$u_{\infty,sus} = 0.19 \text{ m s}^{-1} \tag{A-8}$$

for the minimum water velocity required to lift a sludge particle off the top of the particle layer.

The maximum velocity of the water at the surface of the particle deposit is achieved within the stagnation zone of the falling sludge plume. The velocity profile in the stagnation region of a jet issuing from a nozzle in close proximity of the impingement surface is well known. It is clear from the measurements reported in Martin (1977) and Rajaratnam (1976) that the peak fluid velocity parallel to the surface is approximately equal to the fluid velocity at the nozzle exit plane. We choose an imaginary nozzle in the sludge plume deflection region at the surface of the settled particle layer and identify the nozzle exit plane velocity and radius with the sludge plume radius and velocity at the surface. By virtue of this physically reasonable identification (for turbulent flow) the peak water velocity at and parallel to the surface of the particle deposit is given by Eq. (2-5) evaluated at the top of the particle deposit, a distance z below the sludge distributor. Therefore the criterion for the onset of sludge particle resuspension is obtained by equating v in Eq. (2-5) with u_∞ in Eq. (A-7) and solving the result for z:

$$z \leq z_{sus} = \frac{0.44\, f^{3/2} \alpha_0 Q_0}{E_0^2 v_f} \tag{A-9}$$

The above criterion states that if the top of the growing, settled particle layer rises to within a vertical distance z_{sus} of the sludge distributor given by the right-hand side of Eq. (A-9)

sludge particle resuspension will occur. Using the appropriate parameter values, namely $Q_0 = 4.73 \times 10^{-4}$ m^3 s^{-1}, $\alpha_0 = 0.02$, $v_f = 10^{-6}$ m^2 s^{-1}, $E_0 = 0.12$ and $f = 0.02$, we conclude that if the vertical distance between the top of the settled particle layer and the sludge distributors is less than $z_{sus} = 0.82$ m sludge particle resuspension is possible.

It is important to mention that particle resuspension, if it occurs, will be confined to only a small fraction of the surface area of the settled particle layer. The radial water velocity profile $u_\infty(r)$ at the top of the particle layer due to the impinging sludge plume may be inferred from the information in Martin (1977) and Rajaratnam (1976) on forced jets, together with the imaginary nozzle model discussed in the foregoing, and is

$$u_\infty(r) = \begin{cases} \dfrac{v(z)}{2R(z)} r & 0 < r < 2R(z) \\ \dfrac{2R(z)v(z)}{r} & 2R(z) < r \end{cases} \qquad \text{(A-10)}$$

where $v(z)$ and $R(z)$ are given by Eqs. (2-5) and (2-7) respectively and z is the elevation of the sludge distributors above the settled particle layer. The radial distance r in Eq. (A-10) is measured along the surface of the particle layer from the sludge plume axis-surface point of impingement at $r = 0$. The water velocity $u_\infty(r)$ just above and parallel to the surface and directed outward toward the periphery of the sludge plume is zero at $r = 0$ and increases as r increases. The velocity reaches a peak value equal to $v(z)$ at $r = 2R(z)$, that is at a radial location outside the boundary of the plume where it makes contact with the surface of the particle layer. The water velocity $u_\infty(r)$ then decreases as r is increased beyond $2R(z)$ and ultimately comes back to zero at $r = \infty$.

Particle entrainment will occur within a ring shaped surface area between two circles of inner radius r_i $[0 < r_i < 2R(z)]$ and outer radius r_0 $[2R(z) < r_0 < \infty]$. At these radial locations the water velocity is equal to the critical water velocity $u_{\infty,sus}$ for the onset of particle lifting (see Eqs. A-7 and A-8). From Eq. (A-10) the radial boundaries of the particle entrainment zone are

$$r_i = \frac{2R(z)u_{\infty,sus}}{v(z)} \tag{A-11}$$

$$r_0 = \frac{2R(z)v(z)}{u_{\infty,sus}} \tag{A-12}$$

The surface area A_{sus} over which particle resuspension occurs beneath one impinging sludge plume is

$$A_{sus} = \pi\left(r_0^2 - r_i^2\right) = 4\pi R(z)^2 \left\{ \left[\frac{v(z)}{u_{\infty,sus}}\right]^2 - \left[\frac{u_{\infty,sus}}{v(z)}\right]^2 \right\} \tag{A-13}$$

or, from Eqs. (2-5), (2-7) and (A-9)

$$A_{sus} = 4\pi\left(\frac{6}{5}E_0\right)^2 z^2 \left[\left(\frac{z_{sus}}{z}\right)^{2/3} - \left(\frac{z}{z_{sus}}\right)^{2/3}\right] \tag{A-14}$$

Now $A_{sus} = 0$ at $z = 0$ and at $z = z_{sus}$. Thus A_{sus} must exhibit a maximum in the interval $0 < z < z_{sus}$. It is a simple matter to show that the maximum surface area $A_{sus,max}$ occurs at

$$z_{max} = 2^{-3/4} z_{sus} \tag{A-15}$$

and that $A_{sus,max}$ is

$$A_{sus,max} = \pi\left(\frac{6}{5}E_0 z_{sus}\right)^2 \tag{A-16}$$

Recall that our estimate of the critical sludge distributor-to-settled particle surface separation distance for the onset of resuspension is $z_{sus} = 0.82$ m. Thus, from Eq. (A-16)

$$A_{sus,max} = 0.044 \text{ m}^2 \qquad\qquad (A-17)$$

This area is a negligible fraction of the total surface area of the settled particle bed (5.5 m^2).

APPENDIX B

Gravitational Coagulation Integrals for Moment Equations

By introducing the change in variables $\xi = v - \bar{v}$ into the coagulation integrals in Eq. (4-2) and noting that the kernal $K_g(v, \bar{v})$ is always symmetrical with respect to v and $\bar{v}$, the gravitational coagulation terms can be shown to transform to (see, e.g., Cohen and Vaughan (1974)

$$I_g(\gamma) = \frac{1}{2} \int_0^\infty \int_0^\infty \left[(\bar{v} + v)^\gamma - \bar{v}^\gamma - v^\gamma \right] K_g(\bar{v}, v) \, n(\bar{v}, t) \, n(v, t) \, dv d\bar{v} \tag{B-1}$$

Recall from Eqs. (4-18) and (4-19) that $K_g(\bar{v}, v)$ is a piecewise continuous function that has one form in the interval $0 < v \le \bar{v}$ and another form in the interval $\bar{v} < v < \infty$. Therefore the interior integral in Eq. (B-1) must be expanded into two components as follows:

$$I_g(\gamma) = \frac{1}{2} \int_0^\infty \left\{ \int_0^{\bar{v}} \left[(\bar{v} + v)^\gamma - \bar{v}^\gamma - v^\gamma \right] K_g(\bar{v}, v) \, n(\bar{v}, t) \, n(v, t) \, dv \right.$$
$$\left. + \int_{\bar{v}}^\infty \left[(\bar{v} + v)^\gamma - \bar{v}^\gamma - v^\gamma \right] K_g(\bar{v}, v) \, n(\bar{v}, t) \, n(v, t) \, dv \right\} d\bar{v} \tag{B-2}$$

Substituting Eq. (4-6) for n(v,t)dv and n($\bar{v}$,t)d$\bar{v}$ and Eqs. (4-18) and (4-19) for $K_g(\bar{v}, v)$ in the first and second interior integrals, respectively, and eliminating the resulting integration variables v and $\bar{v}$ in favor of ξ and $\bar{\xi}$, where

$$\xi = \frac{\ln\left[\dfrac{v}{v_g(t)} \right]^{1/3}}{\sqrt{2} \ln \sigma(t)} \quad , \quad \bar{\xi} = \frac{\ln\left[\dfrac{\bar{v}}{v_g(t)} \right]^{1/3}}{\sqrt{2} \ln \sigma(t)} \tag{B-3}$$

Eq. (B-2) becomes for $\gamma = 0,1,2$:

$$I_g(0) = -\frac{\pi}{6}\left(\frac{3}{4\pi}\right)^{\frac{4}{3}}\frac{\varepsilon_0 g(\rho_s - \rho_f)}{\mu_f}N^2 v_g^{\frac{4}{3}} \times$$

$$\left\{ \int_{-\infty}^{\infty} e^{(2\sqrt{2}\ln\sigma)\overline{\xi}-\overline{\xi}^2} \int_{-\infty}^{\overline{\xi}} e^{(2\sqrt{2}\ln\sigma)\xi-\xi^2}\, d\xi d\overline{\xi} - \int_{-\infty}^{\infty} e^{-\overline{\xi}^2} \int_{-\infty}^{\overline{\xi}} e^{(4\sqrt{2}\ln\sigma)\xi-\xi^2}\, d\xi d\overline{\xi} \right. \tag{B-4}$$

$$\left. + \int_{-\infty}^{\infty} e^{(2\sqrt{2}\ln\sigma)\overline{\xi}-\overline{\xi}^2} \int_{\overline{\xi}}^{\infty} e^{(2\sqrt{2}\ln\sigma)\xi-\xi^2}\, d\xi d\overline{\xi} - \int_{-\infty}^{\infty} e^{(4\sqrt{2}\ln\sigma)\overline{\xi}-\overline{\xi}^2} \int_{\overline{\xi}}^{\infty} e^{-\xi^2} d\xi d\overline{\xi} \right\}$$

$$I_g(1) = 0 \tag{B-5}$$

$$I_g(2) = \frac{\pi}{3}\left(\frac{3}{4\pi}\right)^{\frac{4}{3}}\frac{\varepsilon_0 g(\rho_s - \rho_f)}{\mu_f}N^2 v_g^{\frac{10}{3}} \times$$

$$\left\{ \int_{-\infty}^{\infty} e^{(5\sqrt{2}\ln\sigma)\overline{\xi}-\overline{\xi}^2} \int_{-\infty}^{\overline{\xi}} e^{(5\sqrt{2}\ln\sigma)\xi-\xi^2}\, d\xi d\overline{\xi} - \int_{-\infty}^{\infty} e^{(3\sqrt{2}\ln\sigma)\overline{\xi}-\overline{\xi}^2} \int_{-\infty}^{\overline{\xi}} e^{(7\sqrt{2}\ln\sigma)\xi-\xi^2}\, d\xi d\overline{\xi} \right. \tag{B-6}$$

$$\left. + \int_{-\infty}^{\infty} e^{(5\sqrt{2}\ln\sigma)\overline{\xi}-\overline{\xi}^2} \int_{\overline{\xi}}^{\infty} e^{(5\sqrt{2}\ln\sigma)\xi-\xi^2}\, d\xi d\overline{\xi} - \int_{-\infty}^{\infty} e^{(7\sqrt{2}\ln\sigma)\overline{\xi}-\overline{\xi}^2} \int_{\overline{\xi}}^{\infty} e^{(3\sqrt{2}\ln\sigma)\xi-\xi^2} d\xi d\overline{\xi} \right\}$$

The double integrals in Eqs. (B-4) and (B-6) are made considerably easier to evaluate with the knowledge that

$$\int_{-\infty}^{\overline{\xi}} e^{a\xi-\xi^2}\, d\xi = \frac{\sqrt{\pi}}{2}e^{\left(\frac{a}{2}\right)^2}\left[1 + \mathrm{erf}\left(\overline{\xi} - \frac{a}{2}\right)\right] \tag{B-7}$$

$$\int_{\overline{\xi}}^{\infty} e^{a\xi-\xi^2}d\xi = \frac{\sqrt{\pi}}{2}e^{\left(\frac{a}{2}\right)^2}\left[1 - \mathrm{erf}\left(\overline{\xi} - \frac{a}{2}\right)\right] \tag{B-8}$$

$$\int_{-\infty}^{\infty} e^{-x^2}\, \mathrm{erf}\left(x + a\right) dx = \sqrt{\pi}\, \mathrm{erf}\left(\frac{a}{\sqrt{2}}\right) \tag{B-9}$$

The definite integral in Eq. (B-9) could not be found in published tables of integrals available to the authors and was derived by the authors.

Considering all the terms in Eqs. (B-4) and (B-6), the particle coagulation functions reduce to the remarkably simple results

$$I_g(0) = -\frac{3\pi}{4}\left(\frac{3}{4\pi}\right)^{\frac{2}{3}} \varepsilon_0 BN^2(t)\, v_g(t)^{\frac{4}{3}}\, e^{4[\ln\sigma(t)]^2} \left\{1 - e^{4[\ln\sigma(t)]^2}\, \mathrm{erfc}\left[2\ln\sigma(t)\right]\right\} \qquad (B-10)$$

$$I_g(2) = \frac{3\pi}{2}\left(\frac{3}{4\pi}\right)^{\frac{2}{3}} \varepsilon_0 BN^2(t)\, v_g(t)^{\frac{10}{3}}\, e^{25[\ln\sigma(t)]^2} \left\{1 - e^{4[\ln\sigma(t)]^2}\, \mathrm{erfc}\left[2\ln\sigma(t)\right]\right\} \qquad (B-11)$$

APPENDIX C

Validity of Stokes Law Particle Settling Rate

Many experimental data have been taken for flow around spheres, and charts of the drag force (or friction factor) versus flow Reynolds number Re is available in numerous text books on fluid mechanics. From these charts it is clear that Stoke's law is valid for Re $\lesssim$ 1.0, or from the definition of Re the criterion for Stokes settling of a source sludge particle (spherical) of diameter d_p is

$$\frac{u_{sed} d_p}{v_f} \lesssim 1.0 \tag{C-1}$$

The Stokes law sedimentation velocity u_{sed} is

$$u_{sed} = \frac{\left(\rho_s - \rho_f\right) g\, d_p^2}{18\, \mu_f} \tag{C-2}$$

Eliminating u_{sed} between the above two equations gives the following condition on the source sludge particle diameter for the validity of Stokes law

$$d_p \lesssim \left(\frac{18\, \mu_f^2}{\rho_f \left(\rho_s - \rho_f\right) g}\right)^{1/3} \tag{C-3}$$

The question of interest is what is the fraction f of the mass of the inflowing sludge particles contained in particles below the size given by Eq. (C-3). Now for a log-normal distribution of inflowing sludge particles the cumulative particle size distribution curve (f versus d_p) is

$$f = \frac{1}{2}\left[1.0 + \mathrm{erf}\left(\frac{\ln(d_p / d_{g,p})}{\sqrt{2}\, \ln\sigma_p} - \frac{3\ln\sigma_p}{\sqrt{2}}\right)\right] \tag{C-4}$$

where [see Eqs. (4-28) and (4-30)]

$$\ln \sigma_p = \frac{5}{11\sqrt{2}} \ln \left(\frac{d_{max}}{d_{1/2}} \right) \tag{C-5}$$

$$d_{g,p} = d_{1/2} \exp \left[-\frac{9}{3} \left(\ln \sigma_p \right)^2 \right] \tag{C-6}$$

The numerical calculations reported in Section 5 employ the following physical parameter values $\rho_s = 6000$ kg m^{-3} (maximum effective sludge particle density), $\rho_f = 1000$ kg m^{-3}, $\mu_f = 10^{-3}$ kg m^{-1} s^{-1}, $d_{max} = 500$ μm, and $d_{1/2} = 10$ μm. From Eq. (C-3) the maximum diameter of the particles that settle in accord with Stokes law is $d_p = 71.6$ μm. From Eqs. (C-5) and (C-6) $\ln \sigma_p = 1.257$ and $d_{g,p} = 8.71 \times 10^{-2}$ μm. Finally, from Eq. (C-4) the fraction of inflowing particles that exhibit a terminal Stokes velocity is

$$f = \frac{1}{2} \left[1.0 + erf \, (1.109) \right] = 0.942 \tag{C-7}$$

Thus only about 6.0% of the sludge particles settle at rates slower than that given by Stokes law. Note that our calculations show that the median particle size of the suspended sludge particles is smaller than that of the incoming sludge particles. Therefore Eq. (C-7) is a lower bound estimate of the fraction of the particles that obey Stokes law.

APPENDIX D

Quality Assurance Documents

Included here are:

1.   Notes on authorship, review, and documentation (This page),
2.   Calculation Note Cover Sheet (Page D-2), and
3.   Calculation Note Methodology Checklist (Page D-3).

Authorship and review were conducted as follows:
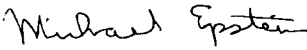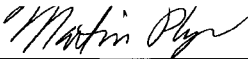
- Section 1 pages 1-1 and 1-2, were authored by Michael Epstein and reviewed by Martin Plys. Section 1 pages 1-3 through 1-9, were authored by Martin Plys and reviewed by Michael Epstein.
- Sections 2, 3, and 4 were authored by Michael Epstein and reviewed by Martin Plys, with one exception: Figures in Section 3 were authored by Martin Plys and reviewed by Jens Conzen.
- Section 5 was authored by Martin Plys and reviewed by Jens Conzen.
- Appendices A, B, and C were authored by Michael Epstein and reviewed by Martin Plys.

The review conducted by Martin Plys involved checking all derivations and numerical results. A Mathcad Version 11 file was created to document the checking. This review is documented in a separate memorandum to the QA file.
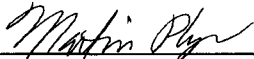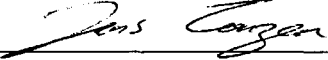
Calculations that generated Section 3 figures and all results in Section 5 were performed in a linked set of Mathcad Version 11 worksheets. The review conducted by Jens Conzen involved checking the correct implementation of equations in the report, review of the self-checks embedded in the calculation worksheets, checking detailed test cases for correct performance, and checking production calculations for reasonable results and consistency with detailed test cases. This review is documented in a separate memorandum to the QA file.

D-2

FAUSKE & ASSOCIATES, LLC

CALCULATION NOTE COVER SHEET
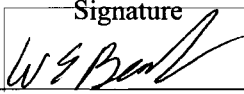
SECTION TO BE COMPLETED BY AUTHOR(S):

Calc-Note Number _____ FAI/09-091 _____ Revision Number ___ 0 ___.

Title ___ Sludge Particle Separation Efficiencies for the Rectangular SCS-CON-230 Container ___.

_____.

Project __ K-Basins Closure Project _____. Project Number or Shop Order _____ DESH 11A ___.

Purpose: See Section 1.0.

Results Summary: See Section 1.0.

References of Resulting reports, Letters, or Memoranda (Optional): N/A

Author(s): Name (Print or Type)	Signature	Completion Date
Michael Epstein	*Michael Epstein*	June 29, 2009
Martin G. Plys	*Martin Plys*	June 29, 2009

SECTION TO BE COMPLETED BY VERIFIER(S):

Verifier(s): Name (Print or Type)	Signature	Completion Date
Martin G. Plys	*Martin Plys*	June 29, 2009
Jens Conzen	*Jens Conzen*	June 29, 2009

Method of Verification: Design Review ____, Independent Review or Alternate Calculations __X__, Testing ____.
Other (specify) _____.

SECTION TO BE COMPLETED BY MANAGER:

Responsible Manager: Name (Print or Type)	Signature	Approval Date
William E. Berger	*W E Berger*	June 29, 2009

CALC NOTE NUMBER _____**FAI/09-091**_____ PAGE ___**D-3**___

CALCULATION NOTE METHODOLOGY CHECKLIST

CHECKLIST TO BE COMPLETED BY AUTHOR(S)   **(CIRCLE APPROPRIATE RESPONSE)**

1. Is the subject and/or the purpose of the design analysis clearly stated?....................(YES) • NO   .

2. Are the required inputs and their sources provided?...(YES) • NO • N/A

3. Are the assumptions clearly identified and justified?..(YES) • NO • N/A

4. Are the methods and units clearly identified?...(YES) • NO • N/A

5. Are equations appropriate and correct?...(YES) • NO • N/A

6. Are results of evaluated equations correct?..(YES) • NO • N/A

7. Have the limits of applicability been identified?..(YES) • NO • N/A
    (i.e., Is the analysis for a 3 or 4 loop plant or for a single application?)

8. Are the results of literature searches, if conducted, or other background data
    provided?... YES • NO • (N/A)

9. Are all the pages sequentially numbered and identified by the calculation note
    number?..(YES) • NO

10. Is the project or shop order clearly identified?..(YES) • NO

11. Has the required computer calculation information been provided?............................. YES • NO • (N/A)

12. Were the computer codes used under configuration control? .... YES • NO • (N/A)

13. Was the computer code(s) used applicable for modeling the physical and/or
    computational problems identified? .... YES • NO • (N/A)
    (i.e., Is the correct computer code being used for the intended purpose?)

14. Are the results and conclusions clearly stated?...(YES) • NO

15. Are Open Items properly identified?...(YES) • NO • N/A

16. Were approved Design Control practices followed without exception? .... YES • NO • (N/A)
    (Approved Design Control practices refers to guidance documents within
    Nuclear Services that state how the work is to be performed, such as how to
    perform a LOCA analysis.)

NOTE: If NO to any of the above, Page Number containing justification _____
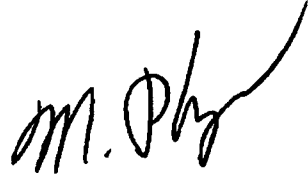
Attachment B

Review and Verification Files

Attachment B1

Attachment B1, *Review of FAI/09-91 Portions Modeled in MathCAD*

FAUSKE
& ASSOCIATES, LLC

WORLD LEADER IN NUCLEAR AND CHEMICAL PROCESS SAFETY

MEMO: MGP062609

DATE: June 26, 2009

TO: QA File 5.35; M. Plys; J. Conzens; M. Epstein

FROM: Marty Plys; Desk 1-630-887-5207, Cell 1-312-953-7299, plys@fauske.com

SUBJECT: **Review of FAI/09-91 Portions Authored by Michael Epstein**

I have reviewed the sections of FAI/09-91 that were authored by Michael Epstein. In my review I checked the derivations of all equations and I checked all numerical answers provided. In the case of various terms in the lognormal differential equations, the derivation was checked by numerical evaluation of integrals for example values.

Two pages of markup to the report are attached. Also attached is the Mathcad file used to document checking of numerical answers and derivations.

Review of FAI/09-91 Portions
Authored by Michael Epstein

Page 2 of 22

PRC-STP-00011, Rev. 0
Attachment B1
MGP062609
June 26, 2009

3-5 8.20×10^{-4} FAI/09-91 markups

3-7 6.31×10^{-5} per MGP review

3-8 4.06×10^{-4}

3-12 6.83×10^{-2}

3-13 $3.12 \times 10^{-}$

after 3-14: change 2.13×10^{-3}
           to 2.08×10^{-3}

p. 3-6 : $8.22 \to 8.20$
          $6.45 \to 6.31$

change $q = 1.84$ to $q = 1.80$
          $x = 11.8 \to x = 11.7$
          $x_0 = 1.12 \to x_0 = 1.11$

3-22 $4.13 \to 4.11$

3-23 $3.92 \to 3.88$
         $2.61 \to 2.43$

3-25 C_ϕ in denominator

4-1 $-$ sign before $\dfrac{n(v,t) u_{out}}{h \, \delta t}$

Review of FAI/09-91 Portions
Authored by Michael Epstein

Page 3 of 22

PRC-STP-00011, Rev. 0
Attachment B1
MGP062609
June 26, 2009

FAI/09-91 markup per MGP review

$$I_g(0) = -\frac{3}{4}\left(\frac{3}{4\pi}\right)^{\frac{2}{3}} \varepsilon_0 BN^2 v_s^{\frac{4}{3}} \int_{-\infty}^{\infty} \left\{ e^{(2\sqrt{2}\ln\sigma)\xi} \int_{-\infty}^{\xi} e^{(2\sqrt{2}\ln\sigma)\xi - \xi^2} d\xi \right. $$
$$\left. + e^{(2\sqrt{2}\ln\sigma)\xi} \int_{\xi}^{\infty} e^{(2\sqrt{2}\ln\sigma)\xi - \xi^2} d\xi - e^{(4\sqrt{2}\ln\sigma)\xi} \int_{\xi}^{\infty} e^{-\xi^2} d\xi \right\} e^{-\bar\xi^2} d\bar\xi \qquad \text{(B-4)}$$

$$I_g(1) = 0 \qquad\qquad e^{-\alpha\xi - \xi^2} \qquad\qquad \text{(B-5)}$$

$$I_g(2) = \frac{3}{2}\left(\frac{3}{4\pi}\right)^{\frac{2}{3}} \varepsilon_0 BN^2 v_s^{\frac{10}{3}} \int_{-\infty}^{\infty} \left\{ e^{(5\sqrt{2}\ln\sigma)\xi} \int_{-\infty}^{\xi} e^{(5\sqrt{2}\ln\sigma)\xi - \xi^2} d\xi \right. $$
$$\left. - e^{(5\sqrt{2}\ln\sigma)\xi} \int_{-\infty}^{\xi} e^{(7\sqrt{2}\ln\sigma)\xi - \xi^2} d\xi + e^{(5\sqrt{2}\ln\sigma)\xi} \int_{\xi}^{\infty} e^{(5\sqrt{2}\ln\sigma)\xi - \xi^2} d\xi \right. $$
$$\left. - e^{(7\sqrt{2}\ln\sigma)\xi} \int_{\xi}^{\infty} e^{(5\sqrt{2}\ln\sigma)\xi - \xi^2} d\xi \right\} e^{-\bar\xi^2} d\bar\xi \qquad \text{(B-6)} \qquad \checkmark$$

The double integrals in Eqs. (B-4) and (B-6) are made considerably easier to evaluate with the knowledge that

$$\int_{-\infty}^{\xi} e^{\alpha\xi - \xi^2} d\xi = \frac{\sqrt{\pi}}{2} e^{\left(\frac{a}{2}\right)^2} \left[1 + \text{erf}\left(\xi - \frac{a}{2}\right) \right] \qquad \text{(B-7)}$$

$$\int_{\xi}^{\infty} e^{\alpha\xi - \xi^2} d\xi = \frac{\sqrt{\pi}}{2} e^{\left(\frac{a}{2}\right)^2} \left[1 - \text{erf}\left(\xi - \frac{a}{2}\right) \right] \qquad \text{(B-8)}$$

$$\int_{-\infty}^{\infty} e^{-x^2} \text{erf}(x + a) dx = \sqrt{\pi}\, \text{erf}\left(\frac{a}{\sqrt{2}}\right) \qquad \text{(B-9)}$$

The definite integral in Eq. (B-9) could not be found in published tables of integrals available to the authors and was derived by the authors.

Review of FAI/09-91 Portions
Authored by Michael Epstein

Page 4 of 22

PRC-STP-00011, Rev. 0
Attachment B1
MGP062609
June 26, 2009

LOG-NORMAL WELL-MIXED SLUDGE IN SCS-CON-230

Calculate suspended sludge concentration, outflow to basin, outflow to filters.
FAI Report FAI/09-91, Sludge Particle Separation Efficiencies for the Rectangular
  SCS-CON-230 Container
Customer: CH2MHill Plateau Remediation, Richland WA
Contact: John Dearing, 509-372-1877, Jim Sloughter 509-373-0591
Authors: Michael Epstein derived the container pressure and log-normal equations.
    Marty Plys implemented and derived input values including PSD's.
    epstein@fauske.com, plys@fauske.com, 16W070 83rd Street, Burr Ridge, IL 60527

Note: No dimensions used because of Mathcad expects all vector elements to have the same
dimensions, which prohibits integration of quantities with different dimensions.

Equation Testing File:

This file is used to test Mike Epstein's equations in Sections 2, 3, and 4 of FAI/09-91.
This file also checks App. B against the log-normal equations of Section 4.
The first couple of pages are taken from SCS-CON-230-Model.mcd.

1.0 INPUTS - Generic

Conversion factors to be used here:

Inches to meters: $1 \cdot in = 0.025400\, m$ C to K: $T_k := 273.15$

gpm to m^3/s: $1 \cdot gpm = 6.30902 \times 10^{-5}\, m^3 \cdot s^{-1}$ $Gpm := \left(6.30902 \times 10^{-5}\right)^{-1}$

Other properties and constants:

Water density, viscosity, and $\rho_f := 1000$ $\mu_f := 10^{-3}$ $\beta := 2.07 \cdot 10^{-4}$
thermal expansion coefficient
Water thermal conductivity, $k_f := 0.60$ $c_{pf} := 4184$ $\nu_f := \dfrac{\mu_f}{\rho_f}$ $\alpha_f := \dfrac{k_f}{\rho_f c_{pf}}$
spec. heat, and diffusivity

Acceleration of gravity $g := 9.81$ $\nu_f = 1.0000 \times 10^{-6}$ $\alpha_f = 1.4340 \times 10^{-7}$

Review of FAI/09-91 Portions
Authored by Michael Epstein

Page 5 of 22

PRC-STP-00011, Rev. 0
Attachment B1
MGP062609
June 26, 2009

SCS-CON-230 Dimensions that follow are converted from inches to meters.
L = length, W = width, H = height, V = volume, Ac = cross-sectional area, Awc = wall area

$L := 142 \cdot 0.0254$ $L = 3.6068$

$H := 128 \cdot 0.0254$ $H = 3.2512$ **Height does not include eggcrate section on bottom**

$W := 60 \cdot 0.0254$ $W = 1.5240$

$V_c := L \cdot W \cdot H$ $V_c = 17.8711$

$A_c := W \cdot L$ $A_c = 5.4968$

$A_{wc} := 2 \cdot H \cdot (L + W)$ $A_{wc} = 33.3625$

Egg crate volume $V_{egg} := 0.98$

Gap flow area: The perimeter is given as the same upstream and downstream, but use separate variables in case of changes. Outflow occurs at the downstream width, need the effective height which is container volume/outflow area.

Gap thickness: $\delta_{gap} := 1 \cdot 0.0254$ $\delta_{gap} = 0.0254$

Upstream gap: $A_{gu} := 0.0254 \cdot (60 + 9 + 9) \cdot \delta_{gap}$ $A_{gu} = 0.0503$

Downstream gap $A_{gd} := 0.0254 \cdot (60 + 9 + 9) \cdot \delta_{gap}$ $A_{gd} = 0.0503$

Assumed wall thickness and $x_{wc} := 0.125 \cdot 0.0254$ $x_{wc} = 3.1750 \times 10^{-3}$

thermal cond. for heat loss $k_{wc} := 40$ Units W/m/K

Nominal inlet source is two distributors, with nominal solids fraction α:

Inlet flow, per source m**3/s $Q_o := 7.5 \cdot Gpm^{-1}$ $Q_o = 4.7318 \times 10^{-4}$

Solids frac, # inlets $\alpha_o := 0.02$ $N_o := 2$

Filter flow $Q_{fl} := 7 \cdot Gpm^{-1}$ $Q_{fl} = 4.4163 \times 10^{-4}$

Backflush flow rate $Q_{bf} := 5 \cdot Gpm^{-1}$ $Q_{bf} = 3.1545 \times 10^{-4}$

Loss coefficient (well known) and container pressure loss coefficient (conservative):

Loss coefficient: $C_D := 0.7$

Container K: $K_c := 0.75$

Review of FAI/09-91 Portions
Authored by Michael Epstein

Page 6 of 22

PRC-STP-00011, Rev. 0
Attachment B1
MGP062609
June 26, 2009

2.0 Check of Section 2 Equations

Eq. 2-9:
$$A_c = 5.4968 \qquad E_o := 0.12 \qquad H_d := 1.9 \qquad 2 \cdot \pi \cdot \left(\frac{6}{5}\right)^2 \cdot \frac{E_o^2 \cdot H_d^2}{A_c} = 0.0856$$

Eq. 2-12:
$$\frac{9 \cdot \pi \cdot E_o \cdot H_d^2}{5 \cdot A_c} = 0.4457$$

3.0 Check of Section 3 Equations

Eq. 3-5:
$$Q_n = 4.4163 \times 10^{-4} \qquad Q_n \cdot Gpm = 7.0000 \qquad Q_o = 4.7318 \times 10^{-4} \qquad Q_o \cdot Gpm = 7.5000$$

$$Q_{suc} := 4 \cdot Q_n - 2 \cdot Q_o \qquad Q_{suc} = 8.2017 \times 10^{-4} \qquad Q_{suc} \cdot Gpm = 13.0000$$

Eq. 3-6:
$$A_{gu} + A_{gd} = 0.1006 \qquad \rho_f = 1.0000 \times 10^3 \qquad C_D = 0.7000 \qquad Q_{suc} = 8.2017 \times 10^{-4}$$

$$A_g := 0.10 \qquad \frac{1}{2} \cdot \rho_f \left(\frac{Q_{suc}}{C_D \cdot A_g}\right)^2 = 0.0686$$

Eq. 3-7:
$$Q_{bf} = 3.1545 \times 10^{-4} \qquad Q_{bf} \cdot Gpm = 5.0000$$

$$Q_{suc} := 3 \cdot Q_n - 2 \cdot Q_o - Q_{bf} \qquad Q_{suc} \cdot Gpm = 1.0000 \qquad Q_{suc} = 6.3090 \times 10^{-5}$$

Eq. 3-8:
$$\frac{1}{2} \cdot \rho_f \left(\frac{Q_{suc}}{C_D \cdot A_g}\right)^2 = 4.0616 \times 10^{-4}$$

Review of FAI/09-91 Portions
Authored by Michael Epstein

Page 7 of 22

PRC-STP-00011, Rev. 0
Attachment B1
MGP062609
June 26, 2009

Between Eq. 3-11 and Eq. 3-12:

In-basin cross-flow velocity rounded value 1 mm/s justified by 120 gpm over 30 feet width and 1 m depth because gap is 2.5 feet submerged:

$$\frac{120 \cdot \left(6.30902 \times 10^{-5}\right)}{1 \cdot (30 \cdot 12 \cdot 0.0254)} = 8.2796 \times 10^{-4} \qquad u_{inf} := 0.001$$

$$K_c = 0.7500 \qquad \rho_f = 1.0000 \times 10^3 \qquad \frac{K_c}{2} \cdot \rho_f \cdot u_{inf}^2 = 3.7500 \times 10^{-4}$$

$$C_D = 0.7000 \qquad A_g = 0.1000$$

Eq. 3-12:
$$Q_{suc} := 13 \cdot Gpm^{-1} \qquad Q_{suc} = 8.2017 \times 10^{-4}$$

$$\frac{1}{2} \cdot \rho_f \left(\frac{Q_{suc}}{C_D \cdot A_g}\right)^2 - \frac{K_c}{2} \cdot \rho_f \cdot u_{inf}^2 = 0.0683$$

Eq. 3-13:
$$Q_{suc} := 1 \cdot Gpm^{-1} \qquad Q_{suc} = 6.3090 \times 10^{-5}$$

$$\frac{1}{2} \cdot \rho_f \left(\frac{Q_{suc}}{C_D \cdot A_g}\right)^2 - \frac{K_c}{2} \cdot \rho_f \cdot u_{inf}^2 = 3.1161 \times 10^{-5}$$

Eq. 3-14:
$$Q_{suc} := 13 \cdot Gpm^{-1} \qquad Q_{suc} = 8.2017 \times 10^{-4} \qquad \frac{1}{\sqrt{K_c}} \cdot \left(\frac{2 \cdot Q_{suc}}{C_D \cdot A_g}\right) = 0.0271$$

$$Q_{suc} := 1 \cdot Gpm^{-1} \qquad Q_{suc} = 6.3090 \times 10^{-5} \qquad \frac{1}{\sqrt{K_c}} \cdot \left(\frac{2 \cdot Q_{suc}}{C_D \cdot A_g}\right) = 2.0814 \times 10^{-3}$$

Review of FAI/09-91 Portions
Authored by Michael Epstein

Page 8 of 22

PRC-STP-00011, Rev. 0
Attachment B1
MGP062609
June 26, 2009

Eq. 3-18 to 21:

$C_D = 0.7000$ $A_g = 0.1000$ $u_{inf} = 1.0000 \times 10^{-3}$ $K_c = 0.7500$

$Q_{suc} := 13 \cdot Gpm^{-1}$ $Q_{suc} = 8.2017 \times 10^{-4}$

$q := \dfrac{2 \cdot Q_{suc}}{C_D \cdot A_g \cdot u_{inf}}$ $q = 23.4335$ $x := \dfrac{q}{2} + \dfrac{K_c}{2 \cdot q}$ $x = 11.7328$

$C_D \cdot \dfrac{A_g}{2} \cdot u_{inf} \cdot x = 4.1065 \times 10^{-4}$ $C_D \cdot \dfrac{A_g}{2} \cdot u_{inf} \cdot \left(x^2 - K_c \right)^{0.5} = 4.0953 \times 10^{-4}$

$Q_{suc} := 1 \cdot Gpm^{-1}$ $Q_{suc} = 6.3090 \times 10^{-5}$

$q := \dfrac{2 \cdot Q_{suc}}{C_D \cdot A_g \cdot u_{inf}}$ $q = 1.8026$ $x := \dfrac{q}{2} + \dfrac{K_c}{2 \cdot q}$ $x = 1.1093$

$C_D \cdot \dfrac{A_g}{2} \cdot u_{inf} \cdot x = 3.8826 \times 10^{-5}$ $C_D \cdot \dfrac{A_g}{2} \cdot u_{inf} \cdot \left(x^2 - K_c \right)^{0.5} = 2.4264 \times 10^{-5}$

Eq. 3-25:

$\delta_{gap} = 0.0254$ $g = 9.8100$ $\beta = 2.0700 \times 10^{-4}$ $C_D = 0.7000$

$q_p := 4.13 \cdot 10^{-4}$ $\dfrac{9 \cdot q_p^2}{2 \cdot C_D^2 \cdot A_g^2 \cdot \delta_{gap} \cdot g \cdot \beta} = 3.0370$

$q_p := 2.61 \cdot 10^{-5}$ $\dfrac{9 \cdot q_p^2}{2 \cdot C_D^2 \cdot A_g^2 \cdot \delta_{gap} \cdot g \cdot \beta} = 0.0121$

Review of FAI/09-91 Portions
Authored by Michael Epstein

Page 9 of 22

PRC-STP-00011, Rev. 0
Attachment B1
MGP062609
June 26, 2009

4.0 Check of Section 4 Equations

Set up to check PSD equations

$d_{max} := 500 \cdot 10^{-6}$ 99.9% of particle volume below this value

Equations 4-28 and 4-29 are verified as correct, use as functions here:

$$fop(d_{med}) := \exp\left(\frac{5}{11 \cdot \sqrt{2}} \cdot \ln\left(\frac{d_{max}}{d_{med}}\right)\right) \qquad fvgp(d_{med}) := \begin{vmatrix} \sigma \leftarrow fop(d_{med}) \\ \frac{\pi}{6} \cdot d_{med}^3 \cdot \exp\left[-9 \cdot (\ln(\sigma))^2\right] \end{vmatrix}$$

Use values for the 10 micron median PSD:

$\sigma := fop\left(10^{-5}\right) \qquad \sigma = 3.5162 \qquad v_{gp} := fvgp\left(10^{-5}\right) \qquad v_{gp} = 3.4633 \times 10^{-22}$

Eq. 4-6:   Check that the distribution approaches 1.0 for large particles, and check that we can reproduce the 10 micron median volume. Note we use N = 1 since this does not matter.

$$fn(x, v_{gp}, \sigma) := \frac{1}{\sqrt{2 \cdot \pi} \cdot \ln(\sigma)} \cdot \exp\left[-\frac{\left(x - \frac{1}{3} \ln(v_{gp})\right)^2}{2 \cdot (\ln(\sigma))^2}\right]$$

$$x_{max} := \frac{1}{3} \cdot \ln\left(\frac{\pi}{6} \cdot d_{max}^3\right) \qquad \int_{-100}^{x_{max}} fn(x, v_{gp}, \sigma)\, dx = 1.0000$$

$$\text{Imax} := 300 \quad i := 0..\text{Imax} \qquad d_i := 10^{-8} \cdot \left(\frac{d_{max}}{10^{-8}}\right)^{\frac{i}{\text{Imax}}} \qquad x_i := \frac{1}{3} \cdot \ln\left[\frac{\pi}{6} \cdot (d_i)^3\right]$$

$$\text{Norm} := \int_{-100}^{x_{max}} e^{3 \cdot x} \cdot fn(x, v_{gp}, \sigma)\, dx \qquad c_i := \frac{1}{\text{Norm}} \cdot \int_{-100}^{x_i} e^{3 \cdot x} \cdot fn(x, v_{gp}, \sigma)\, dx$$

PRC-STP-00011, Rev. 0
Attachment B1
MGP062609
June 26, 2009

Review of FAI/09-91 Portions   Page 10 of 22
Authored by Michael Epstein

Plot of the cumulative volume distribution proves median at 50%
Due to the normalization up to dmax, the distribution below is 1.0 at dmax.

$d_{imax} = 5.0000 \times 10^{-4}$ $C_{imax} = 1.0000$

Eq. 4-9: $v_{gp} \cdot exp\left[\dfrac{9}{2} \cdot (ln(\sigma))^2\right] = 4.2584 \times 10^{-19}$

$$\int_{-100}^{x_{max}} e^{3 \cdot x} \cdot fn(x, v_{gp}, \sigma)\, dx = 4.2585 \times 10^{-19}$$

Review of FAI/09-91 Portions
Authored by Michael Epstein

Page 11 of 22

PRC-STP-00011, Rev. 0
Attachment B1
MGP062609
June 26, 2009

Eq. 4-10:

$$v_{gp}^2 \cdot \exp\left[18 \cdot (\ln(\sigma))^2\right] = 2.7416 \times 10^{-31} \qquad x_{max} = -7.8166$$

$$\int_{-1000}^{x_{max}} e^{6 \cdot x} \cdot fn(x, v_{gp}, \sigma) \, dx = 7.9775 \times 10^{-32}$$

The second moment integral is sensitive to the upper bound, expand into sections:

$$I1 := \int_{-\infty}^{-100} e^{6 \cdot x} \cdot fn(x, v_{gp}, \sigma) \, dx \qquad I2 := \int_{-100}^{-20} e^{6 \cdot x} \cdot fn(x, v_{gp}, \sigma) \, dx$$

$$I3 := \int_{-20}^{x_{max}} e^{6 \cdot x} \cdot fn(x, v_{gp}, \sigma) \, dx \qquad I4 := \int_{x_{max}}^{0} e^{6 \cdot x} \cdot fn(x, v_{gp}, \sigma) \, dx$$

$$I5 := \int_{0}^{100} e^{6 \cdot x} \cdot fn(x, v_{gp}, \sigma) \, dx$$

$$I1 = 0.0000 \qquad I2 = 5.8012 \times 10^{-56}$$

$$I3 = 6.9733 \times 10^{-32} \qquad I4 = 2.0442 \times 10^{-31} \qquad I5 = 3.8021 \times 10^{-39}$$

$$I3 + I4 = 2.7416 \times 10^{-31} \qquad \text{Agreement!}$$

Eq. 4-12 & 4-13:

Verify using N = 1 and assigning X0, X1, and X2 with Eq. 4-8 to 4-10.

$$X_0 := 1 \qquad X_1 := X_0 \cdot v_{gp} \cdot \exp\left[\frac{9}{2} \cdot (\ln(\sigma))^2\right] \qquad X_1 = 4.2584 \times 10^{-19}$$

$$X_2 := X_0 \cdot v_{gp}^2 \cdot \exp\left[18 \cdot (\ln(\sigma))^2\right] \qquad X_2 = 2.7416 \times 10^{-31}$$

$$v_{gp} = 3.4633 \times 10^{-22} \qquad \frac{X_1^2}{X_0^{\frac{2}{3}} \cdot X_2^{\frac{1}{2}}} = 3.4633 \times 10^{-22}$$

$$\ln(\sigma) = 1.2574 \qquad \frac{1}{3} \left(\ln\left(\frac{X_0 \cdot X_2}{X_1^2} \right) \right)^{\frac{1}{2}} = 1.2574$$

Review of FAI/09-91 Portions
Authored by Michael Epstein

Page 12 of 22

PRC-STP-00011, Rev. 0
Attachment B1
MGP062609
June 26, 2009

Eq. 4-20,
4-21, 4-22

Settling terms can be tested by comparing integrals with the formulas.

$g = 9.8100$ $\rho_p := 6000$ $\rho_f = 1.0000 \times 10^3$ $\mu_f = 1.0000 \times 10^{-3}$

$$B := \frac{2}{9} \cdot \left(\frac{3}{4 \cdot \pi}\right)^{\frac{2}{3}} \cdot \frac{g \cdot (\rho_p - \rho_f)}{\mu_f} \qquad B = 4.1947 \times 10^6 \qquad fu(v) := B \cdot v^{\frac{2}{3}}$$

$X_0 = 1.0000$ $X_1 = 4.2584 \times 10^{-19}$ $X_2 = 2.7416 \times 10^{-31}$

Eq. 4-20

$$B \cdot X_0 \cdot \left(\frac{X_1^8}{X_0^7 \cdot X_2}\right)^{\frac{1}{9}} = 4.8856 \times 10^{-7}$$

$$\int_{-100}^{x_{max}} B \cdot e^{2 \cdot x} \cdot fn(x, v_{gp}, \sigma) \, dx = 4.8501 \times 10^{-7}$$

Eq. 4-21

$$B \cdot X_0 \cdot \left(\frac{X_1 \cdot X_2}{X_0^2}\right)^{\frac{5}{9}} = 2.7405 \times 10^{-21}$$

$$I1 := \int_{-1000}^{-20} B \cdot e^{5 \cdot x} \cdot fn(x, v_{gp}, \sigma) \, dx \qquad I2 := \int_{-20}^{x_{max}} B \cdot e^{5 \cdot x} \cdot fn(x, v_{gp}, \sigma) \, dx$$

$$I3 := \int_{x_{max}}^{0} B \cdot e^{5 \cdot x} \cdot fn(x, v_{gp}, \sigma) \, dx \qquad I1 + I2 + I3 = 2.7405 \times 10^{-21}$$

Eq. 4-22

$$B \cdot X_0 \cdot \left(\frac{X_2^5}{X_0 \cdot X_1^4}\right)^{\frac{4}{9}} = 2.3242 \times 10^{-29}$$

$$I1 := \int_{-1000}^{-20} B \cdot e^{8 \cdot x} \cdot fn(x, v_{gp}, \sigma) \, dx \qquad I2 := \int_{-20}^{x_{max}} B \cdot e^{8 \cdot x} \cdot fn(x, v_{gp}, \sigma) \, dx$$

$$I3 := \int_{x_{max}}^{0} B \cdot e^{8 \cdot x} \cdot fn(x, v_{gp}, \sigma) \, dx \qquad I1 + I2 + I3 = 2.3214 \times 10^{-29}$$

PRC-STP-00011, Rev. 0
Attachment B1
MGP062609
June 26, 2009

Review of FAI/09-91 Portions   Page 13 of 22
Authored by Michael Epstein

Eq. 4-20,   Coagulation terms can be tested by comparing integrals with the formulas
& 4-22   B-10 should be the same as coagulation in 4-20
                   B-11 should be the same as coagulation in 4-22.
                   Again note N = 1

$$B = 4.1947 \times 10^6 \qquad \epsilon_0 := \frac{1}{3} \qquad BC := \frac{3 \cdot \pi}{4} \cdot \left(\frac{3}{4 \cdot \pi}\right)^{\frac{2}{3}} \cdot \epsilon_0 \cdot B \qquad BC = 1.2678 \times 10^6$$

$$v_{gp} = 3.4633 \times 10^{-22} \qquad \sigma = 3.5162$$

$$X_0 = 1.0000 \qquad X_1 = 4.2584 \times 10^{-19} \qquad X_2 = 2.7416 \times 10^{-31}$$

B-10:
$$BC \cdot v_{gp}^{\frac{4}{3}} \cdot \exp\left[4 \cdot (\ln(\sigma))^2\right] \cdot \left[1 - \exp\left[4 \cdot (\ln(\sigma))^2\right] \cdot \text{erfc}(2 \cdot \ln(\sigma))\right] = 1.3592 \times 10^{-20}$$

4-20:
$$BC \cdot X_0^2 \cdot \left(\frac{X_1^8}{X_0^7 \cdot X_2}\right)^{\frac{2}{9}} \cdot \left[1 - \left(\frac{X_0 \cdot X_2}{X_1^2}\right)^{\frac{4}{9}} \cdot \text{erfc}(2 \cdot \ln(\sigma))\right] = 1.3592 \times 10^{-20}$$

B-11:
$$2 \cdot BC \cdot v_{gp}^{\frac{10}{3}} \cdot \exp\left[25 \cdot (\ln(\sigma))^2\right] \cdot \left[1 - \exp\left[4 \cdot (\ln(\sigma))^2\right] \cdot \text{erfc}(2 \cdot \ln(\sigma))\right] = 8.5535 \times 10^{-49}$$

4-22:
$$2 \cdot BC \cdot X_0^2 \cdot \left(\frac{X_1^{\frac{10}{9}} \cdot X_2^{\frac{10}{9}}}{X_0^{\frac{20}{9}}}\right) \cdot \left[1 - \left(\frac{X_0 \cdot X_2}{X_1^2}\right)^{\frac{4}{9}} \cdot \text{erfc}(2 \cdot \ln(\sigma))\right] = 8.5535 \times 10^{-49}$$

Review of FAI/09-91 Portions
Authored by Michael Epstein

Page 14 of 22

PRC-STP-00011, Rev. 0
Attachment B1
MGP062609
June 26, 2009

Eq. 4-20,
& 4-22

Coagulation terms can be tested by comparing integrals with the formulas
The result of B-10 should agree with B-2 $\gamma=0$
The result of B-11 should agree with B-2 $\gamma=2$
First set up the coagulation function from 4-18, 4-19
We already know B-10 and 4-20 agree, and B-11 and 4-22 agree from above

$$\epsilon_o = 0.3333 \qquad \rho_p = 6.0000 \times 10^3 \qquad \rho_f = 1.0000 \times 10^3 \qquad \mu_f = 1.0000 \times 10^{-3} \qquad g = 9.8100$$

$$CK := \frac{\pi}{3} \cdot \left(\frac{3}{4\cdot\pi}\right)^{\frac{4}{3}} \cdot \frac{\epsilon_o \cdot (\rho_p - \rho_f) \cdot g}{\mu_f} \qquad CK = 2.5357 \times 10^6$$

$$K18(vb,v) := CK \cdot v^{\frac{2}{3}} \cdot \left(vb^{\frac{2}{3}} - v^{\frac{2}{3}}\right) \qquad K19(vb,v) := CK \cdot vb^{\frac{2}{3}} \cdot \left(v^{\frac{2}{3}} - vb^{\frac{2}{3}}\right)$$

B-2 $\gamma=0$:

$$I1 := \frac{1}{2} \cdot \int_{-100}^{x_{max}} \int_{-100}^{xb} K18\left(e^{3\cdot xb}, e^{3\cdot x}\right) \cdot fn(xb, v_{gp}, \sigma) \cdot fn(x, v_{gp}, \sigma) \, dx \, dxb$$

$$I2 := \frac{1}{2} \cdot \int_{-100}^{x_{max}} \int_{xb}^{x_{max}} K19\left(e^{3\cdot xb}, e^{3\cdot x}\right) \cdot fn(xb, v_{gp}, \sigma) \cdot fn(x, v_{gp}, \sigma) \, dx \, dxb$$

$$I1 = 7.0308 \times 10^{-21} \qquad I2 = 6.4855 \times 10^{-21} \qquad I1 + I2 = 1.3516 \times 10^{-20}$$

B-10:

$$BC \cdot v_{gp}^{\frac{4}{3}} \cdot \exp\left[4 \cdot (\ln(\sigma))^2\right] \cdot \left[1 - \exp\left[4 \cdot (\ln(\sigma))^2\right] \cdot erfc(2 \cdot \ln(\sigma))\right] = 1.3592 \times 10^{-20}$$

Review of FAI/09-91 Portions
Authored by Michael Epstein

Page 15 of 22

PRC-STP-00011, Rev. 0
Attachment B1
MGP062609
June 26, 2009

Eq. 4-20,
& 4-22

Coagulation terms can be tested by comparing integrals with the formulas
The result of B-10 should agree with B-2 $\gamma=0$
The result of B-11 should agree with B-2 $\gamma=2$
First set up the coagulation function from 4-18, 4-19
We already know B-10 and 4-20 agree, and B-11 and 4-22 agree from above

$$\epsilon_0 = 0.3333 \qquad \rho_p = 6.0000 \times 10^3 \qquad \rho_f = 1.0000 \times 10^3 \qquad \mu_f = 1.0000 \times 10^{-3} \qquad g = 9.8100$$

$$CK = 2.5357 \times 10^6$$

$$dv2(vb, v) := (vb + v)^2 - vb^2 - v^2$$

B-2 $\gamma=2$:

$$I1 := \frac{1}{2} \cdot \int_{-100}^{x_{max}} \int_{-100}^{xb} dv2\left(e^{3 \cdot xb}, e^{3 \cdot x}\right) \cdot K18\left(e^{3 \cdot xb}, e^{3 \cdot x}\right) \cdot fn\left(xb, v_{gp}, \sigma\right) \cdot fn\left(x, v_{gp}, \sigma\right) dx\, dxb$$

$$I2 := \frac{1}{2} \cdot \int_{-100}^{x_{max}} \int_{xb}^{x_{max}} dv2\left(e^{3 \cdot xb}, e^{3 \cdot x}\right) \cdot K19\left(e^{3 \cdot xb}, e^{3 \cdot x}\right) \cdot fn\left(xb, v_{gp}, \sigma\right) \cdot fn\left(x, v_{gp}, \sigma\right) dx\, dxb$$

$$I1 = 2.0248 \times 10^{-49} \qquad I2 = 2.0201 \times 10^{-49} \qquad I1 + I2 = 4.0449 \times 10^{-49}$$

Review of FAI/09-91 Portions
Authored by Michael Epstein

Page 16 of 22

PRC-STP-00011, Rev. 0
Attachment B1
MGP062609
June 26, 2009

B-11:

$$2 \cdot BC \cdot v_{gp}^{\frac{10}{3}} \cdot \exp\left[25 \cdot (\ln(\sigma))^2\right] \cdot \left[1 - \exp\left[4 \cdot (\ln(\sigma))^2\right] \cdot \text{erfc}(2 \cdot \ln(\sigma))\right] = 0.0000$$

$$I1A := \frac{1}{2} \cdot \int_{-100}^{-20} \int_{-100}^{xb} dv2\left(e^{3 \cdot xb}, e^{3 \cdot x}\right) \cdot K18\left(e^{3 \cdot xb}, e^{3 \cdot x}\right) \cdot fn\left(xb, v_{gp}, \sigma\right) \cdot fn\left(x, v_{gp}, \sigma\right) dx \, dxb$$

$$I1B := \frac{1}{2} \cdot \int_{-20}^{x_{max}} \int_{-100}^{xb} dv2\left(e^{3 \cdot xb}, e^{3 \cdot x}\right) \cdot K18\left(e^{3 \cdot xb}, e^{3 \cdot x}\right) \cdot fn\left(xb, v_{gp}, \sigma\right) \cdot fn\left(x, v_{gp}, \sigma\right) dx \, dxb$$

$$I1C := \frac{1}{2} \cdot \int_{x_{max}}^{0} \int_{-100}^{xb} dv2\left(e^{3 \cdot xb}, e^{3 \cdot x}\right) \cdot K18\left(e^{3 \cdot xb}, e^{3 \cdot x}\right) \cdot fn\left(xb, v_{gp}, \sigma\right) \cdot fn\left(x, v_{gp}, \sigma\right) dx \, dxb$$

$$I1 := I1A + I1B + I1C$$

$$I2A := \frac{1}{2} \cdot \int_{-100}^{-20} \int_{xb}^{0} dv2\left(e^{3 \cdot xb}, e^{3 \cdot x}\right) \cdot K19\left(e^{3 \cdot xb}, e^{3 \cdot x}\right) \cdot fn\left(xb, v_{gp}, \sigma\right) \cdot fn\left(x, v_{gp}, \sigma\right) dx \, dxb$$

$$I2B := \frac{1}{2} \cdot \int_{-20}^{x_{max}} \int_{xb}^{0} dv2\left(e^{3 \cdot xb}, e^{3 \cdot x}\right) \cdot K19\left(e^{3 \cdot xb}, e^{3 \cdot x}\right) \cdot fn\left(xb, v_{gp}, \sigma\right) \cdot fn\left(x, v_{gp}, \sigma\right) dx \, dxb$$

$$I2C := \frac{1}{2} \cdot \int_{x_{max}}^{0} \int_{xb}^{0} dv2\left(e^{3 \cdot xb}, e^{3 \cdot x}\right) \cdot K19\left(e^{3 \cdot xb}, e^{3 \cdot x}\right) \cdot fn\left(xb, v_{gp}, \sigma\right) \cdot fn\left(x, v_{gp}, \sigma\right) dx \, dxb$$

$$I2 := I2A + I2B + I2C$$

$$I1 = 4.2768 \times 10^{-49} \qquad I2 = 4.2768 \times 10^{-49} \qquad I1 + I2 = 8.5535 \times 10^{-49}$$

Review of FAI/09-91 Portions
Authored by Michael Epstein

Page 17 of 22

PRC-STP-00011, Rev. 0
Attachment B1
MGP062609
June 26, 2009

Eq. 4-20, & 4-22   Integrals of B-4 and B-6 should agree with B-10 and B-11 respectively

$$d_{min} := 10^{-9} \qquad v_{min} := \frac{\pi}{6} \cdot d_{min}^3 \qquad v_{min} = 5.2360 \times 10^{-28}$$

$$d_{med} := 10^{-5} \qquad v_{med} := \frac{\pi}{6} \cdot d_{med}^3 \qquad v_{med} = 5.2360 \times 10^{-16}$$

$$d_{max} = 5.0000 \times 10^{-4} \qquad v_{max} := \frac{\pi}{6} \cdot d_{max}^3 \qquad v_{max} = 6.5450 \times 10^{-11}$$

$$\xi_{min} := \frac{\frac{1}{3}\left(\ln(v_{min}) - \ln(v_{gp})\right)}{\sqrt{2} \cdot \ln(\sigma)} \qquad \xi_{min} = -2.5123$$

$$\xi_{med} := \frac{\frac{1}{3}\left(\ln(v_{med}) - \ln(v_{gp})\right)}{\sqrt{2} \cdot \ln(\sigma)} \qquad \xi_{med} = 2.6673$$

$$\xi_{max} := \frac{\frac{1}{3}\left(\ln(v_{max}) - \ln(v_{gp})\right)}{\sqrt{2} \cdot \ln(\sigma)} \qquad \xi_{max} = 4.8673$$

$$a := 2\sqrt{2} \cdot \ln(\sigma) \qquad a = 3.5564 \qquad B = 4.1947 \times 10^6 \qquad v_{gp} = 3.4633 \times 10^{-22}$$

$$C4 := \frac{3}{4} \cdot \left(\frac{3}{4 \cdot \pi}\right)^{\frac{2}{3}} \cdot \varepsilon_0 \cdot B \cdot v_{gp}^{\frac{4}{3}} \qquad C4 = 9.8151 \times 10^{-24}$$

$$b := 5\sqrt{2} \cdot \ln(\sigma) \qquad b = 8.8910 \qquad c := 3\sqrt{2} \cdot \ln(\sigma) \qquad c = 5.3346$$

$$d := 7\sqrt{2} \cdot \ln(\sigma) \qquad d = 12.4473$$

$$C6 := \frac{3}{2} \cdot \left(\frac{3}{4 \cdot \pi}\right)^{\frac{2}{3}} \cdot \varepsilon_0 \cdot B \cdot v_{gp}^{\frac{10}{3}} \qquad C6 = 2.3545 \times 10^{-66}$$

Review of FAI/09-91 Portions
Authored by Michael Epstein

Page 18 of 22

PRC-STP-00011, Rev. 0
Attachment B1
MGP062609
June 26, 2009

B-4

$$11A := C4 \cdot \int_{-10}^{\xi_{med}} e^{a \cdot x - x^2} \cdot \int_{-10}^{x} e^{a \cdot \xi - \xi^2} d\xi \, dx + C4 \cdot \int_{\xi_{med}}^{10} e^{a \cdot x - x^2} \cdot \int_{-10}^{x} e^{a \cdot \xi - \xi^2} d\xi \, dx$$

$$11B := C4 \cdot \int_{-10}^{\xi_{med}} e^{-x^2} \cdot \int_{-10}^{x} e^{2 \cdot a \cdot \xi - \xi^2} d\xi \, dx + C4 \cdot \int_{\xi_{med}}^{10} e^{-x^2} \cdot \int_{-10}^{x} e^{2 \cdot a \cdot \xi - \xi^2} d\xi \, dx$$

$$11 := 11A - 11B$$

$$12A := C4 \cdot \int_{-10}^{\xi_{med}} e^{a \cdot x - x^2} \cdot \int_{x}^{10} e^{a \cdot \xi - \xi^2} d\xi \, dx + C4 \cdot \int_{\xi_{med}}^{10} e^{a \cdot x - x^2} \cdot \int_{x}^{10} e^{a \cdot \xi - \xi^2} d\xi \, dx$$

$$12B := C4 \cdot \int_{-10}^{\xi_{med}} e^{2 \cdot a \cdot x - x^2} \cdot \int_{x}^{10} e^{-\xi^2} d\xi \, dx + C4 \cdot \int_{\xi_{med}}^{10} e^{2 \cdot a \cdot x - x^2} \cdot \int_{x}^{10} e^{-\xi^2} d\xi \, dx$$

$$12 := 12A - 12B$$

$$11 = 6.7959 \times 10^{-21} \qquad 12 = 6.7959 \times 10^{-21} \qquad 11 + 12 = 1.3592 \times 10^{-20}$$

B-10:

$$BC \cdot v_{gp}^{\frac{4}{3}} \cdot exp\left[4 \cdot (\ln(\sigma))^2\right] \cdot \left[1 - exp\left[4 \cdot (\ln(\sigma))^2\right] \cdot erfc(2 \cdot \ln(\sigma))\right] = 1.3592 \times 10^{-20}$$

Review of FAI/09-91 Portions   Page 19 of 22
Authored by Michael Epstein

PRC-STP-00011, Rev. 0
Attachment B1
MGP062609
June 26, 2009

$$b = 8.8910 \quad c = 5.3346 \quad d = 12.4473$$

B-6

$$I1A := C6 \cdot \int_{-10}^{\xi_{med}} e^{b \cdot x - x^2} \cdot \int_{-10}^{x} e^{b \cdot \xi - \xi^2} d\xi\, dx + C6 \cdot \int_{\xi_{med}}^{10} e^{b \cdot x - x^2} \cdot \int_{-10}^{x} e^{b \cdot \xi - \xi^2} d\xi\, dx$$

$$I1B := C6 \cdot \int_{-10}^{\xi_{med}} e^{c \cdot x - x^2} \cdot \int_{-10}^{x} e^{d \cdot \xi - \xi^2} d\xi\, dx + C6 \cdot \int_{\xi_{med}}^{10} e^{c \cdot x - x^2} \cdot \int_{-10}^{x} e^{d \cdot \xi - \xi^2} d\xi\, dx$$

$$I1 := I1A - I1B$$

$$I2A := C6 \cdot \int_{-10}^{\xi_{med}} e^{b \cdot x - x^2} \cdot \int_{x}^{10} e^{b \cdot \xi - \xi^2} d\xi\, dx + C6 \cdot \int_{\xi_{med}}^{10} e^{b \cdot x - x^2} \cdot \int_{x}^{10} e^{b \cdot \xi - \xi^2} d\xi\, dx$$

$$I2B := C6 \cdot \int_{-10}^{\xi_{med}} e^{d \cdot x - x^2} \cdot \int_{x}^{10} e^{c \cdot \xi - \xi^2} d\xi\, dx + C6 \cdot \int_{\xi_{med}}^{10} e^{d \cdot x - x^2} \cdot \int_{x}^{10} e^{c \cdot \xi - \xi^2} d\xi\, dx$$

$$I2 := I2A - I2B$$

$$I1 = 4.2768 \times 10^{-49} \qquad I2 = 4.2768 \times 10^{-49} \qquad I1 + I2 = 8.5535 \times 10^{-49}$$

B-11:

$$2 \cdot BC \cdot v_{gp}^{\frac{10}{3}} \cdot \exp\left[25 \cdot (\ln(\sigma))^2\right] \cdot \left[1 - \exp\left[4 \cdot (\ln(\sigma))^2\right] \cdot \mathrm{erfc}(2 \cdot \ln(\sigma))\right] = 8.5535 \times 10^{-49}$$

Review of FAI/09-91 Portions
Authored by Michael Epstein

Page 20 of 22

PRC-STP-00011, Rev. 0
Attachment B1
MGP062609
June 26, 2009

.

.

Eq. 4-20,
& 4-22

Supporting work in App. B
Evaluate integrals at median of distribution

$v_{med} = 5.2360 \times 10^{-16}$ $\quad$ $v_{gp} = 3.4633 \times 10^{-22}$ $\quad$ $\sigma = 3.5162$ $\quad$ $\xi_{med} = 2.6673$

$\xi := \xi_{med}$

B-7 $\quad$ $\int_{-\infty}^{\xi} e^{a \cdot \xi - \xi^2} d\xi = 37.4937$ $\qquad$ $\frac{\sqrt{\pi}}{2} \cdot e^{(0.5 \cdot a)^2} \cdot \left(1 + erf\left(\xi - \frac{a}{2}\right)\right) = 37.4937$

B-8 $\quad$ $\int_{\xi}^{\infty} e^{a \cdot \xi - \xi^2} d\xi = 4.3664$ $\qquad$ $\frac{\sqrt{\pi}}{2} \cdot e^{(0.5 \cdot a)^2} \cdot \left(1 - erf\left(\xi - \frac{a}{2}\right)\right) = 4.3664$

B-9 $\quad$ $\int_{-\infty}^{\infty} e^{-x^2} \cdot erf(x + a) \, dx = 1.7718$ $\qquad$ $\sqrt{\pi} \cdot erf\left(\frac{a}{\sqrt{2}}\right) = 1.7718$

$\int_{-\infty}^{\infty} e^{-x^2} dx = 1.7725$ $\qquad$ $\sqrt{\pi} = 1.7725$

Review of FAI/09-91 Portions
Authored by Michael Epstein

Page 21 of 22

PRC-STP-00011, Rev. 0
Attachment B1
MGP062609
June 26, 2009

5.0 Check of Appendix A Equations

A-5   Coefficient: $8.09 \cdot \sqrt{0.5} \cdot 0.25 = 1.4301$

A-7   Coefficient: $C_u := \left(\dfrac{\pi}{6} \cdot \dfrac{1}{1.43} \right)^{\frac{1}{3}}$ $C_u = 0.7154$

A-8 $\nu_f := 10^{-6}$ $\rho_p = 6.0000 \times 10^3$ $\rho_f = 1.0000 \times 10^3$ $f := 0.02$

$u_{sus} := \dfrac{C_u}{\sqrt{f}} \left[\dfrac{(\rho_p - \rho_f) \cdot g \cdot \nu_f}{\rho_f} \right]^{\frac{1}{3}}$ $u_{sus} = 0.1852$

A-9   Coefficient: $C_z := \dfrac{25}{48 \cdot \pi \cdot C_u^3}$ $C_z = 0.4528$

A-9 $Q_0 = 4.7318 \times 10^{-4}$ $\alpha_0 = 0.0200$ $E_0 = 0.1200$

$z_{sus} := \dfrac{C_z \cdot f^{1.5} \cdot \alpha_0 \cdot Q_0}{E_0^2 \cdot \nu_f}$ $z_{sus} = 0.8416$

A-17 $\pi \cdot \left(\dfrac{6}{5} \cdot E_0 \cdot z_{sus} \right)^2 = 0.0461$

Review of FAI/09-91 Portions
Authored by Michael Epstein

Page 22 of 22

PRC-STP-00011, Rev. 0
Attachment B1
MGP062609
June 26, 2009

5.0 Check of Appendix C Equations

C-4 $\quad v_{gp} = 3.4633 \times 10^{-22} \qquad d_{gp} := \left(\dfrac{6}{\pi} \cdot v_{gp} \right)^{\frac{1}{3}} \qquad d_{gp} = 8.7129 \times 10^{-8} \qquad \sigma = 3.5162$

$d_{med} = 1.0000 \times 10^{-5}$

$\dfrac{1}{2} \cdot \left(1 + erf\left(\dfrac{\ln(d_{med}) - \ln(d_{gp})}{\sqrt{2} \cdot \ln(\sigma)} - \dfrac{3 \cdot \ln(\sigma)}{\sqrt{2}} \right) \right) = 0.5000$

C-5 $\quad \ln(\sigma) = 1.2574 \qquad d_{max} = 5.0000 \times 10^{-4}$

$\dfrac{5}{11\sqrt{2}} \cdot \left(\ln(d_{max}) - \ln(d_{med}) \right) = 1.2574$

C-6 $\quad d_{gp} = 8.7129 \times 10^{-8} \qquad d_{med} \exp\left(-3 \cdot \ln(\sigma)^2 \right) = 8.7129 \times 10^{-8}$

C-3 $\quad \rho_p = 6.0000 \times 10^3 \qquad \rho_f = 1.0000 \times 10^3 \qquad \mu_f = 1.0000 \times 10^{-3} \qquad g = 9.8100$

$d_p := \left[\dfrac{18 \cdot \mu_f^2}{\rho_f (\rho_p - \rho_f) \cdot g} \right]^{\frac{1}{3}} \qquad d_p = 7.1594 \times 10^{-5}$
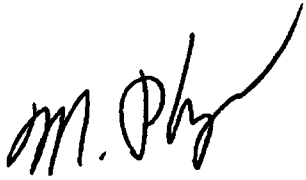
$\dfrac{1}{2} \cdot \left(1 + erf\left(\dfrac{\ln(d_p) - \ln(d_{gp})}{\sqrt{2} \cdot \ln(\sigma)} - \dfrac{3 \cdot \ln(\sigma)}{\sqrt{2}} \right) \right) = 0.9413$

Attachment B2

MGP062909A, *MathCAD Files for FAI/09-91*

FAUSKE
& ASSOCIATES, LLC

WORLD LEADER IN NUCLEAR AND CHEMICAL PROCESS SAFETY

MEMO: MGP062609

DATE: June 26, 2009

TO: QA File 5.35; M. Plys; J. Conzens; M. Epstein

FROM: Marty Plys; Desk 1-630-887-5207, Cell 1-312-953-7299, plys@fauske.com

SUBJECT: **Review of FAI/09-91 Portions Authored by Michael Epstein**

I have reviewed the sections of FAI/09-91 that were authored by Michael Epstein. In my review I checked the derivations of all equations and I checked all numerical answers provided. In the case of various terms in the lognormal differential equations, the derivation was checked by numerical evaluation of integrals for example values.

Two pages of markup to the report are attached. Also attached is the Mathcad file used to document checking of numerical answers and derivations.

Review of FAI/09-91 Portions
Authored by Michael Epstein

Page 2 of 22

PRC-STP-00011, Rev. 0
Attachment B2
MGP062609
June 26, 2009

3-5 8.20×10^{-4} $\underline{FAI/09-91\ markups}$

3-7 6.31×10^{-5} $\underline{per\ MGP\ review}$

3-8 4.06×10^{-4}

3-12 6.83×10^{-2}

3-13 $3.12 \times 10^{--}$

after 3-14: change 2.13×10^{-3}
           to 2.08×10^{-3}

p.3-6 : $8.22 \rightarrow 8.20$
          $6.45 \rightarrow 6.31$

change $q = 1.84$ to $q = 1.80$
       $x = 11.8$ to $x = 11.7$
       $n = 1.12$ to $n = 1.11$

3-22 $4.13 \rightarrow 4.11$

3-23 $3.92 \rightarrow 3.88$
        $2.61 \rightarrow 2.43$

3-25 C_b is denominator

4-1 $-$ sign before $\dfrac{n(v,t)\,u_{out}}{h\partial t}$

Review of FAI/09-91 Portions
Authored by Michael Epstein

Page 3 of 22

PRC-STP-00011, Rev. 0
Attachment B2
MGP062609
June 26, 2009

FAI/09-91 markup per MGP review (handwritten)

$$I_s(0) = -\frac{3}{4}\left(\frac{3}{4\pi}\right)^{\frac{2}{3}} \varepsilon_0 BN^2 v_s^{\frac{4}{3}} \int_{-\infty}^{\infty} \left\{ e^{(2\sqrt{2}\ln\sigma)\xi} \int_{-\infty}^{\xi} e^{(2\sqrt{2}\ln\sigma)\xi - \xi'} d\xi \right.$$

$$\left. + e^{(2\sqrt{2}\ln\sigma)\xi} \int_{\xi}^{\infty} e^{(2\sqrt{2}\ln\sigma)\xi - \xi'} d\xi - e^{(4\sqrt{2}\ln\sigma)\xi} \int_{\xi}^{\infty} e^{-\xi'} d\xi \right\} e^{-\xi'} d\overline{\xi} \quad (B-4)$$

(handwritten annotations at top right:)
$e^{+\sqrt{2}\ln\sigma\,\overline{\xi}} \int_{-\infty}^{\xi} e^{+\sqrt{2}\ln\sigma\,\xi - \xi^2} d\xi$

$-\int_{\xi}^{\infty} e^{+\sqrt{2}\ln\sigma\,\xi - \xi^2} d\xi$

$I_s(1) = 0 \qquad\qquad\qquad e^{-\alpha\xi - \xi^2} \qquad\qquad (B-5)$

$$I_s(2) = \frac{3}{2}\left(\frac{3}{4\pi}\right)^{\frac{2}{3}} \varepsilon_0 BN^2 v_s^{\frac{10}{3}} \int_{-\infty}^{\infty} \left\{ e^{(5\sqrt{2}\ln\sigma)\xi} \int_{-\infty}^{\xi} e^{(5\sqrt{2}\ln\sigma)\xi - \xi'} d\xi \right.$$

$$- e^{(3\sqrt{2}\ln\sigma)\xi} \int_{-\infty}^{\xi} e^{(7\sqrt{2}\ln\sigma)\xi - \xi'} d\xi + e^{(5\sqrt{2}\ln\sigma)\xi} \int_{\xi}^{\infty} e^{(5\sqrt{2}\ln\sigma)\xi - \xi'} d\xi \quad (B-6)$$

$$\left. - e^{(7\sqrt{2}\ln\sigma)\xi} \int_{\xi}^{\infty} e^{(3\sqrt{2}\ln\sigma)\xi - \xi'} d\xi \right\} e^{-\xi'} d\overline{\xi}$$

(handwritten check mark ✓)

The double integrals in Eqs. (B-4) and (B-6) are made considerably easier to evaluate with the knowledge that

$$\int_{-\infty}^{\xi} e^{a\xi - \xi'} d\xi = \frac{\sqrt{\pi}}{2} e^{\left(\frac{a}{2}\right)^2} \left[1 + \text{erf}\left(\overline{\xi} - \frac{a}{2}\right) \right] \quad (B-7)$$

$$\int_{\xi}^{\infty} e^{a\xi - \xi'} d\xi = \frac{\sqrt{\pi}}{2} e^{\left(\frac{a}{2}\right)^2} \left[1 - \text{erf}\left(\overline{\xi} - \frac{a}{2}\right) \right] \quad (B-8)$$

$$\int_{-\infty}^{\infty} e^{-x^2} \text{erf}(x + a)\, dx = \sqrt{\pi}\,\text{erf}\left(\frac{a}{\sqrt{2}}\right) \quad (B-9)$$

The definite integral in Eq. (B-9) could not be found in published tables of integrals available to the authors and was derived by the authors.

Review of FAI/09-91 Portions
Authored by Michael Epstein

Page 4 of 22

PRC-STP-00011, Rev. 0
Attachment B2
MGP062609
June 26, 2009

LOG-NORMAL WELL-MIXED SLUDGE IN SCS-CON-230

Calculate suspended sludge concentration, outflow to basin, outflow to filters.
FAI Report FAI/09-91, Sludge Particle Separation Efficiencies for the Rectangular
 SCS-CON-230 Container
Customer: CH2MHill Plateau Remediation, Richland WA
Contact: John Dearing, 509-372-1877, Jim Sloughter 509-373-0591
Authors: Michael Epstein derived the container pressure and log-normal equations.
   Marty Plys implemented and derived input values including PSD's.
   epstein@fauske.com, plys@fauske.com, 16W070 83rd Street, Burr Ridge, IL 60527

Note: No dimensions used because of Mathcad expects all vector elements to have the same
dimensions, which prohibits integration of quantities with different dimensions.

Equation Testing File:

This file is used to test Mike Epstein's equations In Sections 2, 3, and 4 of FAI/09-91.
This file also checks App. B against the log-normal equations of Section 4.
The first couple of pages are taken from SCS-CON-230-Model.mcd.

1.0 INPUTS - Generic

Conversion factors to be used here:

Inches to meters: $1 \cdot in = 0.025400 \, m$ C to K: $T_k := 273.15$

gpm to m^3/s: $1 \cdot gpm = 6.30902 \times 10^{-5} \, m^3 \cdot s^{-1}$ $Gpm := \left(6.30902 \times 10^{-5}\right)^{-1}$

Other properties and constants:

Water density, viscosity, and $\rho_f := 1000$ $\mu_f := 10^{-3}$ $\beta := 2.07 \cdot 10^{-4}$
thermal expansion coefficient
Water thermal conductivity, $k_f := 0.60$ $c_{pf} := 4184$ $\nu_f := \dfrac{\mu_f}{\rho_f}$ $\alpha_f := \dfrac{k_f}{\rho_f c_{pf}}$
spec. heat, and diffusivity

Acceleration of gravity $g := 9.81$ $\nu_f = 1.0000 \times 10^{-6}$ $\alpha_f = 1.4340 \times 10^{-7}$

Review of FAI/09-91 Portions
Authored by Michael Epstein

Page 5 of 22

PRC-STP-00011, Rev. 0
Attachment B2
MGP062609
June 26, 2009

SCS-CON-230 Dimensions that follow are converted from inches to meters.
L = length, W = width, H = height, V = volume, Ac = cross-sectional area, Awc = wall area

$L := 142 \cdot 0.0254$ $L = 3.6068$

$H := 128 \cdot 0.0254$ $H = 3.2512$ Height does not include eggcrate section on bottom

$W := 60 \cdot 0.0254$ $W = 1.5240$

$V_c := L \cdot W \cdot H$ $V_c = 17.8711$

$A_c := W \cdot L$ $A_c = 5.4968$

$A_{wc} := 2 \cdot H \cdot (L + W)$ $A_{wc} = 33.3625$

Egg crate volume $V_{egg} := 0.98$

Gap flow area: The perimeter is given as the same upstream and downstream, but use separate variables in case of changes. Outflow occurs at the downstream width, need the effective height which is container volume/outflow area.

Gap thickness: $\delta_{gap} := 1 \cdot 0.0254$ $\delta_{gap} = 0.0254$

Upstream gap: $A_{gu} := 0.0254 \cdot (60 + 9 + 9) \cdot \delta_{gap}$ $A_{gu} = 0.0503$

Downstream gap $A_{gd} := 0.0254 \cdot (60 + 9 + 9) \cdot \delta_{gap}$ $A_{gd} = 0.0503$

Assumed wall thickness and thermal cond. for heat loss $x_{wc} := 0.125 \cdot 0.0254$ $x_{wc} = 3.1750 \times 10^{-3}$

     $k_{wc} := 40$ Units W/m/K

Nominal inlet source is two distributors, with nominal solids fraction α:

Inlet flow, per source m**3/s $Q_o := 7.5 \cdot Gpm^{-1}$ $Q_o = 4.7318 \times 10^{-4}$

Solids frac, # Inlets $\alpha_o := 0.02$ $N_o := 2$

Filter flow $Q_{fl} := 7 \cdot Gpm^{-1}$ $Q_{fl} = 4.4163 \times 10^{-4}$

Backflush flow rate $Q_{bf} := 5 \cdot Gpm^{-1}$ $Q_{bf} = 3.1545 \times 10^{-4}$

Loss coefficient (well known) and container pressure loss coefficient (conservative):

Loss coefficient: $C_D := 0.7$

Container K: $K_c := 0.75$

Authored by Michael Epstein

2.0 Check of Section 2 Equations

Eq. 2-9:　　　$A_c = 5.4968$　　　$E_o := 0.12$　　　$H_d := 1.9$　　　$2 \cdot \pi \cdot \left(\frac{6}{5}\right)^2 \cdot \frac{E_o^2 \cdot H_d^2}{A_c} = 0.0856$

Eq. 2-12:　　　$\dfrac{9 \cdot \pi \cdot E_o \cdot H_d^2}{5 \cdot A_c} = 0.4457$

3.0 Check of Section 3 Equations

Eq. 3-5:　　　$Q_{fl} = 4.4163 \times 10^{-4}$　　　$Q_{fl} \cdot Gpm = 7.0000$　　　$Q_o = 4.7318 \times 10^{-4}$　　　$Q_o \cdot Gpm = 7.5000$

　　　　　　　$Q_{suc} := 4 \cdot Q_{fl} - 2 \cdot Q_o$　　　$Q_{suc} = 8.2017 \times 10^{-4}$　　　$Q_{suc} \cdot Gpm = 13.0000$

Eq. 3-6:　　　$A_{gu} + A_{gd} = 0.1006$　　　$\rho_f = 1.0000 \times 10^3$　　　$C_D = 0.7000$　　　$Q_{suc} = 8.2017 \times 10^{-4}$

　　　　　　　$A_g := 0.10$　　　　　　$\frac{1}{2} \cdot \rho_f \left(\frac{Q_{suc}}{C_D \cdot A_g}\right)^2 = 0.0686$

Eq. 3-7:　　　$Q_{bf} = 3.1545 \times 10^{-4}$　　　　　　$Q_{bf} \cdot Gpm = 5.0000$

　　　　　　　$Q_{suc} := 3 \cdot Q_{fl} - 2 \cdot Q_o - Q_{bf}$　　　$Q_{suc} \cdot Gpm = 1.0000$　　　$Q_{suc} = 6.3090 \times 10^{-5}$

Eq. 3-8:　　　$\frac{1}{2} \cdot \rho_f \left(\frac{Q_{suc}}{C_D \cdot A_g}\right)^2 = 4.0616 \times 10^{-4}$

Review of FAI/09-91 Portions
Authored by Michael Epstein

Page 7 of 22

PRC-STP-00011, Rev. 0
Attachment B2
MGP062609
June 26, 2009

Between Eq. 3-11 and Eq. 3-12:

In-basin cross-flow velocity rounded value 1 mm/s justified by 120 gpm over 30 feet width and 1 m depth because gap is 2.5 feet submerged:

$$\frac{120 \cdot \left(6.30902 \times 10^{-5}\right)}{1 \cdot (30 \cdot 12 \cdot 0.0254)} = 8.2796 \times 10^{-4} \qquad u_{inf} := 0.001$$

$$K_c = 0.7500 \qquad \rho_f = 1.0000 \times 10^3 \qquad \frac{K_c}{2} \cdot \rho_f \cdot u_{inf}^2 = 3.7500 \times 10^{-4}$$

$$C_D = 0.7000 \qquad A_g = 0.1000$$

Eq. 3-12: $\quad Q_{suc} := 13 \cdot Gpm^{-1} \qquad Q_{suc} = 8.2017 \times 10^{-4}$

$$\frac{1}{2} \cdot \rho_f \left(\frac{Q_{suc}}{C_D \cdot A_g}\right)^2 - \frac{K_c}{2} \cdot \rho_f \cdot u_{inf}^2 = 0.0683$$

Eq. 3-13: $\quad Q_{suc} := 1 \cdot Gpm^{-1} \qquad Q_{suc} = 6.3090 \times 10^{-5}$

$$\frac{1}{2} \cdot \rho_f \left(\frac{Q_{suc}}{C_D \cdot A_g}\right)^2 - \frac{K_c}{2} \cdot \rho_f \cdot u_{inf}^2 = 3.1161 \times 10^{-5}$$

Eq. 3-14: $\quad Q_{suc} := 13 \cdot Gpm^{-1} \qquad Q_{suc} = 8.2017 \times 10^{-4} \qquad \frac{1}{\sqrt{K_c}} \cdot \left(\frac{2 \cdot Q_{suc}}{C_D \cdot A_g}\right) = 0.0271$

$\qquad\qquad\quad Q_{suc} := 1 \cdot Gpm^{-1} \qquad Q_{suc} = 6.3090 \times 10^{-5} \qquad \frac{1}{\sqrt{K_c}} \cdot \left(\frac{2 \cdot Q_{suc}}{C_D \cdot A_g}\right) = 2.0814 \times 10^{-3}$

Review of FAI/09-91 Portions
Authored by Michael Epstein

Page 8 of 22

PRC-STP-00011, Rev. 0
Attachment B2
MGP062609
June 26, 2009

Eq. 3-18 to 21:

$$C_D = 0.7000 \qquad A_g = 0.1000 \qquad u_{inf} = 1.0000 \times 10^{-3} \qquad K_c = 0.7500$$

$$Q_{suc} := 13 \cdot Gpm^{-1} \qquad Q_{suc} = 8.2017 \times 10^{-4}$$

$$q := \frac{2 \cdot Q_{suc}}{C_D \cdot A_g \cdot u_{inf}} \qquad q = 23.4335 \qquad x := \frac{q}{2} + \frac{K_c}{2 \cdot q} \qquad x = 11.7328$$

$$C_D \cdot \frac{A_g}{2} \cdot u_{inf} \cdot x = 4.1065 \times 10^{-4} \qquad \qquad C_D \cdot \frac{A_g}{2} \cdot u_{inf} \cdot \left(x^2 - K_c\right)^{0.5} = 4.0953 \times 10^{-4}$$

$$Q_{suc} := 1 \cdot Gpm^{-1} \qquad Q_{suc} = 6.3090 \times 10^{-5}$$

$$q := \frac{2 \cdot Q_{suc}}{C_D \cdot A_g \cdot u_{inf}} \qquad q = 1.8026 \qquad x := \frac{q}{2} + \frac{K_c}{2 \cdot q} \qquad x = 1.1093$$

$$C_D \cdot \frac{A_g}{2} \cdot u_{inf} \cdot x = 3.8826 \times 10^{-5} \qquad \qquad C_D \cdot \frac{A_g}{2} \cdot u_{inf} \cdot \left(x^2 - K_c\right)^{0.5} = 2.4264 \times 10^{-5}$$

Eq. 3-25:

$$\delta_{gap} = 0.0254 \qquad g = 9.8100 \qquad \beta = 2.0700 \times 10^{-4} \qquad C_D = 0.7000$$

$$q_p := 4.13 \cdot 10^{-4} \qquad \frac{9 \cdot q_p^2}{2 \cdot C_D^2 \cdot A_g^2 \cdot \delta_{gap} \cdot g \cdot \beta} = 3.0370$$

$$q_p := 2.61 \cdot 10^{-5} \qquad \frac{9 \cdot q_p^2}{2 \cdot C_D^2 \cdot A_g^2 \cdot \delta_{gap} \cdot g \cdot \beta} = 0.0121$$

Review of FAI/09-91 Portions
Authored by Michael Epstein

Page 9 of 22

PRC-STP-00011, Rev. 0
Attachment B2
MGP062609
June 26, 2009

4.0 Check of Section 4 Equations

Set up to check PSD equations

$$d_{max} := 500 \cdot 10^{-6} \qquad \text{99.9\% of particle volume below this value}$$

Equations 4-28 and 4-29 are verified as correct, use as functions here:

$$f\sigma p(d_{med}) := \exp\left(\frac{5}{11 \cdot \sqrt{2}} \cdot \ln\left(\frac{d_{max}}{d_{med}}\right)\right) \qquad fvgp(d_{med}) := \left| \begin{array}{l} \sigma \leftarrow f\sigma p(d_{med}) \\ \frac{\pi}{6} \cdot d_{med}^{3} \cdot \exp\left[-9 \cdot (\ln(\sigma))^2\right] \end{array} \right.$$

Use values for the 10 micron median PSD:

$$\sigma := f\sigma p\left(10^{-5}\right) \qquad \sigma = 3.5162 \qquad v_{gp} := fvgp\left(10^{-5}\right) \qquad v_{gp} = 3.4633 \times 10^{-22}$$

Eq. 4-6: Check that the distribution approaches 1.0 for large particles, and check that we can reproduce the 10 micron median volume. Note we use N = 1 since this does not matter.

$$fn(x, v_{gp}, \sigma) := \frac{1}{\sqrt{2 \cdot \pi} \cdot \ln(\sigma)} \cdot \exp\left[-\frac{\left(x - \frac{1}{3} \ln(v_{gp})\right)^2}{2 \cdot (\ln(\sigma))^2}\right]$$

$$x_{max} := \frac{1}{3} \cdot \ln\left(\frac{\pi}{6} \cdot d_{max}^{3}\right) \qquad \int_{-100}^{x_{max}} fn(x, v_{gp}, \sigma) \, dx = 1.0000$$

$$\text{Imax} := 300 \qquad i := 0 .. \text{Imax} \qquad d_i := 10^{-8} \cdot \left(\frac{d_{max}}{10^{-8}}\right)^{\frac{i}{\text{Imax}}} \qquad x_i := \frac{1}{3} \cdot \ln\left[\frac{\pi}{6} \cdot (d_i)^3\right]$$

$$\text{Norm} := \int_{-100}^{x_{max}} e^{3 \cdot x} \cdot fn(x, v_{gp}, \sigma) \, dx \qquad C_i := \frac{1}{\text{Norm}} \cdot \int_{-100}^{x_i} e^{3 \cdot x} \cdot fn(x, v_{gp}, \sigma) \, dx$$

PRC-STP-00011, Rev. 0
Attachment B2
MGP062609
June 26, 2009

Review of FAI/09-91 Portions   Page 10 of 22
Authored by Michael Epstein

Plot of the cumulative volume distribution proves median at 50%
Due to the normalization up to dmax, the distribution below is 1.0 at dmax.

$$d_{Jmax} = 5.0000 \times 10^{-4} \qquad C_{Imax} = 1.0000$$

Eq. 4-9:

$$v_{gp} \cdot \exp\left[\frac{9}{2} \cdot (\ln(\sigma))^2\right] = 4.2584 \times 10^{-19}$$

$$\int_{-100}^{x_{max}} e^{3 \cdot x} \cdot fn(x, v_{gp}, \sigma) \, dx = 4.2585 \times 10^{-19}$$

Review of FAI/09-91 Portions
Authored by Michael Epstein

Page 11 of 22

PRC-STP-00011, Rev. 0
Attachment B2
MGP062609
June 26, 2009

Eq. 4-10:
$$v_{gp}^2 \cdot \exp\left[18 \cdot (\ln(\sigma))^2\right] = 2.7416 \times 10^{-31}$$

$$x_{max} = -7.8166$$

$$\int_{-1000}^{x_{max}} e^{6 \cdot x} \cdot fn(x, v_{gp}, \sigma) \, dx = 7.9775 \times 10^{-32}$$

The second moment integral
is sensitive to the upper bound,
expand into sections:

$$I1 := \int_{-\infty}^{-100} e^{6 \cdot x} \cdot fn(x, v_{gp}, \sigma) \, dx \qquad I2 := \int_{-100}^{-20} e^{6 \cdot x} \cdot fn(x, v_{gp}, \sigma) \, dx$$

$$I3 := \int_{-20}^{x_{max}} e^{6 \cdot x} \cdot fn(x, v_{gp}, \sigma) \, dx \qquad I4 := \int_{x_{max}}^{0} e^{6 \cdot x} \cdot fn(x, v_{gp}, \sigma) \, dx$$

$$I5 := \int_{0}^{100} e^{6 \cdot x} \cdot fn(x, v_{gp}, \sigma) \, dx$$

$$I1 = 0.0000 \qquad I2 = 5.8012 \times 10^{-56}$$

$$I3 = 6.9733 \times 10^{-32} \qquad I4 = 2.0442 \times 10^{-31} \qquad I5 = 3.8021 \times 10^{-39}$$

$$I3 + I4 = 2.7416 \times 10^{-31} \qquad \text{Agreement!}$$

Eq. 4-12
& 4-13:

Verify using N = 1 and assigning X0, X1, and X2 with Eq. 4-8 to 4-10.

$$X_0 := 1 \qquad X_1 := X_0 \cdot v_{gp} \cdot \exp\left[\frac{9}{2} \cdot (\ln(\sigma))^2\right] \qquad X_1 = 4.2584 \times 10^{-19}$$

$$X_2 := X_0 \cdot v_{gp}^2 \cdot \exp\left[18 \cdot (\ln(\sigma))^2\right] \qquad X_2 = 2.7416 \times 10^{-31}$$

$$v_{gp} = 3.4633 \times 10^{-22} \qquad \frac{X_1^2}{X_0^{\frac{2}{3}} \cdot X_2^{\frac{1}{2}}} = 3.4633 \times 10^{-22}$$

$$\ln(\sigma) = 1.2574 \qquad \frac{1}{3}\left(\ln\left(\frac{X_0 \cdot X_2}{X_1^2}\right)\right)^{\frac{1}{2}} = 1.2574$$

PRC-STP-00011, Rev. 0
Attachment B2
MGP062609
June 26, 2009

Review of FAI/09-91 Portions
Authored by Michael Epstein

Page 12 of 22

**Eq. 4-20,
4-21, 4-22**

Settling terms can be tested by comparing integrals with the formulas.

$$g = 9.8100 \qquad \rho_p := 6000 \qquad \rho_f = 1.0000 \times 10^3 \qquad \mu_f = 1.0000 \times 10^{-3}$$

$$B := \frac{2}{9} \cdot \left(\frac{3}{4 \cdot \pi}\right)^{\frac{2}{3}} \cdot \frac{g \cdot (\rho_p - \rho_f)}{\mu_f} \qquad B = 4.1947 \times 10^6 \qquad fu(v) := B \cdot v^{\frac{2}{3}}$$

$$X_0 = 1.0000 \qquad X_1 = 4.2584 \times 10^{-19} \qquad X_2 = 2.7416 \times 10^{-31}$$

Eq. 4-20

$$B \cdot X_0 \cdot \left(\frac{X_1^8}{X_0^7 \cdot X_2}\right)^{\frac{1}{9}} = 4.8856 \times 10^{-7}$$

$$\int_{-100}^{x_{max}} B \cdot e^{2 \cdot x} \cdot fn(x, v_{gp}, \sigma) \, dx = 4.8501 \times 10^{-7}$$

Eq. 4-21

$$B \cdot X_0 \cdot \left(\frac{X_1 \cdot X_2}{X_0^2}\right)^{\frac{5}{9}} = 2.7405 \times 10^{-21}$$

$$I1 := \int_{-1000}^{-20} B \cdot e^{5 \cdot x} \cdot fn(x, v_{gp}, \sigma) \, dx \qquad I2 := \int_{-20}^{x_{max}} B \cdot e^{5 \cdot x} \cdot fn(x, v_{gp}, \sigma) \, dx$$

$$I3 := \int_{x_{max}}^{0} B \cdot e^{5 \cdot x} \cdot fn(x, v_{gp}, \sigma) \, dx \qquad I1 + I2 + I3 = 2.7405 \times 10^{-21}$$

Eq. 4-22

$$B \cdot X_0 \cdot \left(\frac{X_2^5}{X_0 \cdot X_1^4}\right)^{\frac{4}{9}} = 2.3242 \times 10^{-29}$$

$$I1 := \int_{-1000}^{-20} B \cdot e^{8 \cdot x} \cdot fn(x, v_{gp}, \sigma) \, dx \qquad I2 := \int_{-20}^{x_{max}} B \cdot e^{8 \cdot x} \cdot fn(x, v_{gp}, \sigma) \, dx$$

$$I3 := \int_{x_{max}}^{0} B \cdot e^{8 \cdot x} \cdot fn(x, v_{gp}, \sigma) \, dx \qquad I1 + I2 + I3 = 2.3214 \times 10^{-29}$$

Eq. 4-20,   Coagulation terms can be tested by comparing integrals with the formulas
& 4-22   B-10 should be the same as coagulation in 4-20
                 B-11 should be the same as coagulation in 4-22.
                 Again note N = 1

$$B = 4.1947 \times 10^6 \qquad \epsilon_o := \frac{1}{3} \qquad BC := \frac{3 \cdot \pi}{4} \cdot \left(\frac{3}{4 \cdot \pi}\right)^{\frac{2}{3}} \cdot \epsilon_o \cdot B \qquad BC = 1.2678 \times 10^6$$

$$v_{gp} = 3.4633 \times 10^{-22} \qquad \sigma = 3.5162$$

$$X_0 = 1.0000 \qquad X_1 = 4.2584 \times 10^{-19} \qquad X_2 = 2.7416 \times 10^{-31}$$

B-10:
$$BC \cdot v_{gp}^{\frac{4}{3}} \cdot \exp\left[4 \cdot (\ln(\sigma))^2\right] \cdot \left[1 - \exp\left[4 \cdot (\ln(\sigma))^2\right] \cdot \text{erfc}(2 \cdot \ln(\sigma))\right] = 1.3592 \times 10^{-20}$$

4-20:
$$BC \cdot X_0^2 \cdot \left(\frac{X_1^8}{X_0^7 \cdot X_2}\right)^{\frac{2}{9}} \cdot \left[1 - \left(\frac{X_0 \cdot X_2}{X_1^2}\right)^{\frac{4}{9}} \cdot \text{erfc}(2 \cdot \ln(\sigma))\right] = 1.3592 \times 10^{-20}$$

B-11:
$$2 \cdot BC \cdot v_{gp}^{\frac{10}{3}} \cdot \exp\left[25 \cdot (\ln(\sigma))^2\right] \cdot \left[1 - \exp\left[4 \cdot (\ln(\sigma))^2\right] \cdot \text{erfc}(2 \cdot \ln(\sigma))\right] = 8.5535 \times 10^{-49}$$

4-22:
$$2 \cdot BC \cdot X_0^2 \cdot \left(\frac{X_1^{\frac{10}{9}} \cdot X_2^{\frac{10}{9}}}{X_0^{\frac{20}{9}}}\right) \cdot \left[1 - \left(\frac{X_0 \cdot X_2}{X_1^2}\right)^{\frac{4}{9}} \cdot \text{erfc}(2 \cdot \ln(\sigma))\right] = 8.5535 \times 10^{-49}$$

Review of FAI/09-91 Portions
Authored by Michael Epstein

Page 14 of 22

PRC-STP-00011, Rev. 0
Attachment B2
MGP062609
June 26, 2009

Eq. 4-20,
& 4-22

Coagulation terms can be tested by comparing integrals with the formulas
The result of B-10 should agree with B-2 $\gamma=0$
The result of B-11 should agree with B-2 $\gamma=2$
First set up the coagulation function from 4-18, 4-19
We already know B-10 and 4-20 agree, and B-11 and 4-22 agree from above

$$\epsilon_o = 0.3333 \qquad \rho_p = 6.0000 \times 10^3 \qquad \rho_f = 1.0000 \times 10^3 \qquad \mu_f = 1.0000 \times 10^{-3} \qquad g = 9.8100$$

$$CK := \frac{\pi}{3} \cdot \left(\frac{3}{4 \cdot \pi}\right)^{\frac{4}{3}} \cdot \frac{\epsilon_o \cdot (\rho_p - \rho_f) \cdot g}{\mu_f} \qquad CK = 2.5357 \times 10^6$$

$$K18(vb,v) := CK \cdot v^{\frac{2}{3}} \cdot \left(vb^{\frac{2}{3}} - v^{\frac{2}{3}}\right) \qquad K19(vb,v) := CK \cdot vb^{\frac{2}{3}} \cdot \left(v^{\frac{2}{3}} - vb^{\frac{2}{3}}\right)$$

B-2 $\gamma=0$:

$$I1 := \frac{1}{2} \cdot \int_{-100}^{x_{max}} \int_{-100}^{xb} K18\left(e^{3 \cdot xb}, e^{3 \cdot x}\right) \cdot fn\left(xb, v_{gp}, \sigma\right) \cdot fn\left(x, v_{gp}, \sigma\right) dx \, dxb$$

$$I2 := \frac{1}{2} \cdot \int_{-100}^{x_{max}} \int_{xb}^{x_{max}} K19\left(e^{3 \cdot xb}, e^{3 \cdot x}\right) \cdot fn\left(xb, v_{gp}, \sigma\right) \cdot fn\left(x, v_{gp}, \sigma\right) dx \, dxb$$

$$I1 = 7.0308 \times 10^{-21} \qquad I2 = 6.4855 \times 10^{-21} \qquad I1 + I2 = 1.3516 \times 10^{-20}$$

B-10:

$$BC \cdot v_{gp}^{\frac{4}{3}} \cdot \exp\left[4 \cdot (\ln(\sigma))^2\right] \cdot \left[1 - \exp\left[4 \cdot (\ln(\sigma))^2\right] \cdot erfc(2 \cdot \ln(\sigma))\right] = 1.3592 \times 10^{-20}$$

Review of FAI/09-91 Portions
Authored by Michael Epstein

Page 15 of 22

PRC-STP-00011, Rev. 0
Attachment B2
MGP062609
June 26, 2009

Eq. 4-20,
& 4-22

Coagulation terms can be tested by comparing integrals with the formulas
The result of B-10 should agree with B-2 γ=0
The result of B-11 should agree with B-2 γ=2
First set up the coagulation function from 4-18, 4-19
We already know B-10 and 4-20 agree, and B-11 and 4-22 agree from above

$$\epsilon_o = 0.3333 \qquad \rho_p = 6.0000 \times 10^3 \qquad \rho_f = 1.0000 \times 10^3 \qquad \mu_f = 1.0000 \times 10^{-3} \qquad g = 9.8100$$

$$CK = 2.5357 \times 10^6$$

$$dv2(vb,v) := (vb + v)^2 - vb^2 - v^2$$

B-2 γ=2:

$$I1 := \frac{1}{2} \cdot \int_{-100}^{x_{max}} \int_{-100}^{xb} dv2\left(e^{3 \cdot xb}, e^{3 \cdot x}\right) \cdot K18\left(e^{3 \cdot xb}, e^{3 \cdot x}\right) \cdot fn\left(xb, v_{gp}, \sigma\right) \cdot fn\left(x, v_{gp}, \sigma\right) dx\,dxb$$

$$I2 := \frac{1}{2} \cdot \int_{-100}^{x_{max}} \int_{xb}^{x_{max}} dv2\left(e^{3 \cdot xb}, e^{3 \cdot x}\right) \cdot K19\left(e^{3 \cdot xb}, e^{3 \cdot x}\right) \cdot fn\left(xb, v_{gp}, \sigma\right) \cdot fn\left(x, v_{gp}, \sigma\right) dx\,dxb$$

$$I1 = 2.0248 \times 10^{-49} \qquad I2 = 2.0201 \times 10^{-49} \qquad I1 + I2 = 4.0449 \times 10^{-49}$$

Review of FAI/09-91 Portions
Authored by Michael Epstein

Page 16 of 22

PRC-STP-00011, Rev. 0
Attachment B2
MGP062609
June 26, 2009

.

.

B-11:

$$2 \cdot BC \cdot v_{gp}^{\frac{10}{3}} \cdot \exp\left[25 \cdot (\ln(\sigma))^2\right] \cdot \left[1 - \exp\left[4 \cdot (\ln(\sigma))^2\right] \cdot \text{erfc}(2 \cdot \ln(\sigma))\right] = 0.0000$$

$$I1A := \frac{1}{2} \cdot \int_{-100}^{-20} \int_{-100}^{xb} dv2\left(e^{3 \cdot xb}, e^{3 \cdot x}\right) \cdot K18\left(e^{3 \cdot xb}, e^{3 \cdot x}\right) \cdot fn\left(xb, v_{gp}, \sigma\right) \cdot fn\left(x, v_{gp}, \sigma\right) dx \, dxb$$

$$I1B := \frac{1}{2} \cdot \int_{-20}^{x_{max}} \int_{-100}^{xb} dv2\left(e^{3 \cdot xb}, e^{3 \cdot x}\right) \cdot K18\left(e^{3 \cdot xb}, e^{3 \cdot x}\right) \cdot fn\left(xb, v_{gp}, \sigma\right) \cdot fn\left(x, v_{gp}, \sigma\right) dx \, dxb$$

$$I1C := \frac{1}{2} \cdot \int_{x_{max}}^{0} \int_{-100}^{xb} dv2\left(e^{3 \cdot xb}, e^{3 \cdot x}\right) \cdot K18\left(e^{3 \cdot xb}, e^{3 \cdot x}\right) \cdot fn\left(xb, v_{gp}, \sigma\right) \cdot fn\left(x, v_{gp}, \sigma\right) dx \, dxb$$

$$I1 := I1A + I1B + I1C$$

$$I2A := \frac{1}{2} \cdot \int_{-100}^{-20} \int_{xb}^{0} dv2\left(e^{3 \cdot xb}, e^{3 \cdot x}\right) \cdot K19\left(e^{3 \cdot xb}, e^{3 \cdot x}\right) \cdot fn\left(xb, v_{gp}, \sigma\right) \cdot fn\left(x, v_{gp}, \sigma\right) dx \, dxb$$

$$I2B := \frac{1}{2} \cdot \int_{-20}^{x_{max}} \int_{xb}^{0} dv2\left(e^{3 \cdot xb}, e^{3 \cdot x}\right) \cdot K19\left(e^{3 \cdot xb}, e^{3 \cdot x}\right) \cdot fn\left(xb, v_{gp}, \sigma\right) \cdot fn\left(x, v_{gp}, \sigma\right) dx \, dxb$$

$$I2C := \frac{1}{2} \cdot \int_{x_{max}}^{0} \int_{xb}^{0} dv2\left(e^{3 \cdot xb}, e^{3 \cdot x}\right) \cdot K19\left(e^{3 \cdot xb}, e^{3 \cdot x}\right) \cdot fn\left(xb, v_{gp}, \sigma\right) \cdot fn\left(x, v_{gp}, \sigma\right) dx \, dxb$$

$$I2 := I2A + I2B + I2C$$

$$I1 = 4.2768 \times 10^{-49} \qquad I2 = 4.2768 \times 10^{-49} \qquad I1 + I2 = 8.5535 \times 10^{-49}$$

Review of FAI/09-91 Portions
Authored by Michael Epstein

Page 17 of 22

PRC-STP-00011, Rev. 0
Attachment B2
MGP062609
June 26, 2009

Eq. 4-20,
& 4-22

Integrals of B-4 and B-6 should agree with B-10 and B-11 respectively

$d_{min} := 10^{-9}$ $\qquad$ $v_{min} := \frac{\pi}{6} \cdot d_{min}^{3}$ $\qquad$ $v_{min} = 5.2360 \times 10^{-28}$

$d_{med} := 10^{-5}$ $\qquad$ $v_{med} := \frac{\pi}{6} \cdot d_{med}^{3}$ $\qquad$ $v_{med} = 5.2360 \times 10^{-16}$

$d_{max} = 5.0000 \times 10^{-4}$ $\qquad$ $v_{max} := \frac{\pi}{6} \cdot d_{max}^{3}$ $\qquad$ $v_{max} = 6.5450 \times 10^{-11}$

$\xi_{min} := \dfrac{\frac{1}{3}\left(\ln(v_{min}) - \ln(v_{gp})\right)}{\sqrt{2} \cdot \ln(\sigma)}$ $\qquad$ $\xi_{min} = -2.5123$

$\xi_{med} := \dfrac{\frac{1}{3}\left(\ln(v_{med}) - \ln(v_{gp})\right)}{\sqrt{2} \cdot \ln(\sigma)}$ $\qquad$ $\xi_{med} = 2.6673$

$\xi_{max} := \dfrac{\frac{1}{3}\left(\ln(v_{max}) - \ln(v_{gp})\right)}{\sqrt{2} \cdot \ln(\sigma)}$ $\qquad$ $\xi_{max} = 4.8673$

$a := 2 \cdot \sqrt{2} \cdot \ln(\sigma)$ $\qquad$ $a = 3.5564$ $\qquad$ $B = 4.1947 \times 10^{6}$ $\qquad$ $v_{gp} = 3.4633 \times 10^{-22}$

$C4 := \frac{3}{4} \cdot \left(\frac{3}{4 \cdot \pi}\right)^{\frac{2}{3}} \cdot \varepsilon_o \cdot B \cdot v_{gp}^{\frac{4}{3}}$ $\qquad$ $C4 = 9.8151 \times 10^{-24}$

$b := 5 \cdot \sqrt{2} \cdot \ln(\sigma)$ $\qquad$ $b = 8.8910$ $\qquad$ $c := 3 \cdot \sqrt{2} \cdot \ln(\sigma)$ $\qquad$ $c = 5.3346$

$d := 7 \cdot \sqrt{2} \cdot \ln(\sigma)$ $\qquad$ $d = 12.4473$

$C6 := \frac{3}{2} \cdot \left(\frac{3}{4 \cdot \pi}\right)^{\frac{2}{3}} \cdot \varepsilon_o \cdot B \cdot v_{gp}^{\frac{10}{3}}$ $\qquad$ $C6 = 2.3545 \times 10^{-66}$

Review of FAI/09-91 Portions
Authored by Michael Epstein

Page 18 of 22

PRC-STP-00011, Rev. 0
Attachment B2
MGP062609
June 26, 2009

B-4

$$I1A := C4 \cdot \int_{-10}^{\xi_{med}} e^{a \cdot x - x^2} \cdot \int_{-10}^{x} e^{a \cdot \xi - \xi^2} d\xi \, dx + C4 \cdot \int_{\xi_{med}}^{10} e^{a \cdot x - x^2} \cdot \int_{-10}^{x} e^{a \cdot \xi - \xi^2} d\xi \, dx$$

$$I1B := C4 \cdot \int_{-10}^{\xi_{med}} e^{-x^2} \cdot \int_{-10}^{x} e^{2 \cdot a \cdot \xi - \xi^2} d\xi \, dx + C4 \cdot \int_{\xi_{med}}^{10} e^{-x^2} \cdot \int_{-10}^{x} e^{2 \cdot a \cdot \xi - \xi^2} d\xi \, dx$$

$$I1 := I1A - I1B$$

$$I2A := C4 \cdot \int_{-10}^{\xi_{med}} e^{a \cdot x - x^2} \cdot \int_{x}^{10} e^{a \cdot \xi - \xi^2} d\xi \, dx + C4 \cdot \int_{\xi_{med}}^{10} e^{a \cdot x - x^2} \cdot \int_{x}^{10} e^{a \cdot \xi - \xi^2} d\xi \, dx$$

$$I2B := C4 \cdot \int_{-10}^{\xi_{med}} e^{2 \cdot a \cdot x - x^2} \cdot \int_{x}^{10} e^{-\xi^2} d\xi \, dx + C4 \cdot \int_{\xi_{med}}^{10} e^{2 \cdot a \cdot x - x^2} \cdot \int_{x}^{10} e^{-\xi^2} d\xi \, dx$$

$$I2 := I2A - I2B$$

$$I1 = 6.7959 \times 10^{-21} \qquad I2 = 6.7959 \times 10^{-21} \qquad I1 + I2 = 1.3592 \times 10^{-20}$$

B-10:

$$BC \cdot v_{gp}^{\frac{4}{3}} \cdot \exp\left[4 \cdot (\ln(\sigma))^2\right] \cdot \left[1 - \exp\left[4 \cdot (\ln(\sigma))^2\right] \cdot erfc(2 \cdot \ln(\sigma))\right] = 1.3592 \times 10^{-20}$$

Review of FAI/09-91 Portions
Authored by Michael Epstein

Page 19 of 22

PRC-STP-00011, Rev. 0
Attachment B2
MGP062609
June 26, 2009

$$b = 8.8910 \qquad c = 5.3346 \qquad d = 12.4473$$

B-6

$$I1A := C6 \cdot \int_{-10}^{\xi_{med}} e^{b \cdot x - x^2} \cdot \int_{-10}^{x} e^{b \cdot \xi - \xi^2} \, d\xi \, dx + C6 \cdot \int_{\xi_{med}}^{10} e^{b \cdot x - x^2} \cdot \int_{-10}^{x} e^{b \cdot \xi - \xi^2} \, d\xi \, dx$$

$$I1B := C6 \cdot \int_{-10}^{\xi_{med}} e^{c \cdot x - x^2} \cdot \int_{-10}^{x} e^{d \cdot \xi - \xi^2} \, d\xi \, dx + C6 \cdot \int_{\xi_{med}}^{10} e^{c \cdot x - x^2} \cdot \int_{-10}^{x} e^{d \cdot \xi - \xi^2} \, d\xi \, dx$$

$$I1 := I1A - I1B$$

$$I2A := C6 \cdot \int_{-10}^{\xi_{med}} e^{b \cdot x - x^2} \cdot \int_{x}^{10} e^{b \cdot \xi - \xi^2} \, d\xi \, dx + C6 \cdot \int_{\xi_{med}}^{10} e^{b \cdot x - x^2} \cdot \int_{x}^{10} e^{b \cdot \xi - \xi^2} \, d\xi \, dx$$

$$I2B := C6 \cdot \int_{-10}^{\xi_{med}} e^{d \cdot x - x^2} \cdot \int_{x}^{10} e^{c \cdot \xi - \xi^2} \, d\xi \, dx + C6 \cdot \int_{\xi_{med}}^{10} e^{d \cdot x - x^2} \cdot \int_{x}^{10} e^{c \cdot \xi - \xi^2} \, d\xi \, dx$$

$$I2 := I2A - I2B$$

$$I1 = 4.2768 \times 10^{-49} \qquad I2 = 4.2768 \times 10^{-49} \qquad I1 + I2 = 8.5535 \times 10^{-49}$$

B-11:

$$2 \cdot BC \cdot v_{gp}^{\frac{10}{3}} \cdot \exp\left[25 \cdot (\ln(\sigma))^2\right] \cdot \left[1 - \exp\left[4 \cdot (\ln(\sigma))^2\right] \cdot \text{erfc}(2 \cdot \ln(\sigma))\right] = 8.5535 \times 10^{-49}$$

Review of FAI/09-91 Portions
Authored by Michael Epstein

Page 20 of 22

PRC-STP-00011, Rev. 0
Attachment B2
MGP062609
June 26, 2009

.

.

Eq. 4-20,
& 4-22

Supporting work in App. B
Evaluate integrals at median of distribution

$$v_{med} = 5.2360 \times 10^{-16} \qquad v_{gp} = 3.4633 \times 10^{-22} \qquad \sigma = 3.5162 \qquad \xi_{med} = 2.6673$$

$$\xi := \xi_{med}$$

B-7

$$\int_{-\infty}^{\xi} e^{a \cdot \xi - \xi^2} d\xi = 37.4937 \qquad \frac{\sqrt{\pi}}{2} \cdot e^{(0.5 \cdot a)^2} \cdot \left(1 + erf\left(\xi - \frac{a}{2}\right)\right) = 37.4937$$

B-8

$$\int_{\xi}^{\infty} e^{a \cdot \xi - \xi^2} d\xi = 4.3664 \qquad \frac{\sqrt{\pi}}{2} \cdot e^{(0.5 \cdot a)^2} \cdot \left(1 - erf\left(\xi - \frac{a}{2}\right)\right) = 4.3664$$

B-9

$$\int_{-\infty}^{\infty} e^{-x^2} \cdot erf(x + a) \, dx = 1.7718 \qquad \sqrt{\pi} \cdot erf\left(\frac{a}{\sqrt{2}}\right) = 1.7718$$

$$\int_{-\infty}^{\infty} e^{-x^2} dx = 1.7725 \qquad \sqrt{\pi} = 1.7725$$

Review of FAI/09-91 Portions
Authored by Michael Epstein

Page 21 of 22

PRC-STP-00011, Rev. 0
Attachment B2
MGP062609
June 26, 2009

5.0 Check of Appendix A Equations

A-5   Coefficient: $8.09 \cdot \sqrt{0.5} \cdot 0.25 = 1.4301$

A-7   Coefficient: $C_u := \left(\dfrac{\pi}{6} \cdot \dfrac{1}{1.43} \right)^{\frac{1}{3}}$ $C_u = 0.7154$

A-8 $\nu_f := 10^{-6}$ $\rho_p = 6.0000 \times 10^3$ $\rho_f = 1.0000 \times 10^3$ $f := 0.02$

$$u_{sus} := \dfrac{C_u}{\sqrt{f}} \cdot \left[\dfrac{(\rho_p - \rho_f) \cdot g \cdot \nu_f}{\rho_f} \right]^{\frac{1}{3}}$$ $u_{sus} = 0.1852$

A-9   Coefficient: $C_z := \dfrac{25}{48 \cdot \pi \cdot C_u^{\,3}}$ $C_z = 0.4528$

A-9 $Q_o = 4.7318 \times 10^{-4}$ $\alpha_o = 0.0200$ $E_o = 0.1200$

$$z_{sus} := \dfrac{C_z \cdot f^{1.5} \cdot \alpha_o \cdot Q_o}{E_o^{\,2} \cdot \nu_f}$$ $z_{sus} = 0.8416$

A-17 $\pi \cdot \left(\dfrac{6}{5} \cdot E_o \cdot z_{sus} \right)^2 = 0.0461$

Review of FAI/09-91 Portions
Authored by Michael Epstein

Page 22 of 22

PRC-STP-00011, Rev. 0
Attachment B2
MGP062609
June 26, 2009

5.0 Check of Appendix C Equations

C-4 $\quad v_{gp} = 3.4633 \times 10^{-22} \quad d_{gp} := \left(\frac{6}{\pi} \cdot v_{gp}\right)^{\frac{1}{3}} \quad d_{gp} = 8.7129 \times 10^{-8} \quad \sigma = 3.5162$

$d_{med} = 1.0000 \times 10^{-5}$

$\frac{1}{2} \cdot \left(1 + erf\left(\frac{\ln(d_{med}) - \ln(d_{gp})}{\sqrt{2} \cdot \ln(\sigma)} - \frac{3 \cdot \ln(\sigma)}{\sqrt{2}}\right)\right) = 0.5000$

C-5 $\quad \ln(\sigma) = 1.2574 \quad d_{max} = 5.0000 \times 10^{-4}$

$\frac{5}{11\sqrt{2}} \cdot (\ln(d_{max}) - \ln(d_{med})) = 1.2574$

C-6 $\quad d_{gp} = 8.7129 \times 10^{-8} \quad d_{med} \cdot exp\left(-3 \cdot \ln(\sigma)^2\right) = 8.7129 \times 10^{-8}$

C-3 $\quad \rho_p = 6.0000 \times 10^3 \quad \rho_f = 1.0000 \times 10^3 \quad \mu_f = 1.0000 \times 10^{-3} \quad g = 9.8100$

$d_p := \left[\frac{18 \cdot \mu_f^2}{\rho_f \cdot (\rho_p - \rho_f) \cdot g}\right]^{\frac{1}{3}} \quad d_p = 7.1594 \times 10^{-5}$

$\frac{1}{2} \cdot \left(1 + erf\left(\frac{\ln(d_p) - \ln(d_{gp})}{\sqrt{2} \cdot \ln(\sigma)} - \frac{3 \cdot \ln(\sigma)}{\sqrt{2}}\right)\right) = 0.9413$

Attachment B3

MGP062909A, *MathCAD Files for FAI/09-91*

FAI FAUSKE
& ASSOCIATES, LLC

MEMO: MGP062909A

DATE: June 29, 2009

TO: QA File 5.35; M. Plys; J. Conzens; M. Epstein

FROM: Marty Plys; Desk 1-630-887-5207, Cell 1-312-953-7299, plys@fauske.com

SUBJECT: MathCAD Files for FAI/09-91

Attached on CD are electronic copies of the MathCAD files used for FAI/09-91.

```
06/18/2009   09:32 AM          111,659  SCS-CON-230-Test-Development.mcd
06/18/2009   09:37 AM           70,346  SCS-CON-230-Case-Group-3.mcd
06/18/2009   09:37 AM          238,260  SCS-CON-230-Model.mcd
06/18/2009   10:00 AM           55,455  SCS-CON-230-Case-Group-2.mcd
06/18/2009   10:00 AM           69,916  SCS-CON-230-Case-Group-1.mcd
06/26/2009   09:30 AM          127,863  SCS-CON-230-Test-Equations.mcd
```

In addition the QA review memos and June 29 version of FAI/09-91 are included for convenience.

BX-2
3   *N.F*
7-16-09